Kinetic Roughening of Growing Surfaces *

Joachim Krug and Herbert Spohn

Theoretische Physik, Ludwig Maximilians Universität

Theresienstrasse 37, D-8000 München 2, Germany

Contents

1 Introduction

Solids form through growth processes which take place at the surface. Physically, there is a huge variety of growth mechanisms depending on the materials involved, their temperature, composition, phases, etc. In these notes we will discuss a very particular growth mechanism: We imagine an already formed nucleus to which further material sticks from the ambient atmosphere. The process of attachment is

- reaction limited,

(there is a good supply of material, but a permanent link to the nucleus is formed only after many attempts)

- far away from equilibrium

(we consider time scales, on which the surface has not yet relaxed through surface diffusion and not yet reached a state of local thermal equilibrium with the surrounding gas/fluid phase).

We follow the tradition of Statistical Mechanics in studying oversimplified models which nevertheless attempt to capture some of the essential physics. It will turn out that these models describe also other physical processes of interest. Some of them will be explained in Chapter 4. The idea behind the most basic model is to focus on the two properties just mentioned and to ignore all other details. We disregard the ambient atmosphere and assume that particles stick randomly at the surface of an already formed cluster. Once a particle sticks, it remains there forever. Such a model was first proposed by Murray Eden (1958) in a biological context. The Eden model is one of the simplest growth processes.

Let us make the effort to define the Eden model (better one version of it) more precisely. To simplify geometry we let the cluster grow on an underlying square lattice. (The generalization to higher dimensions will be obvious.) We start with a single seed at the origin. At each one of the four available perimeter sites we add an extra particle at a random time with an exponential distribution. We continue this process. At some time t we have a cluster of sites, A_t. (A_t is a random set because it depends on the particular growth history.) The sites adjacent to it are the growth sites. Each one of the growth sites is filled independently with a

S = 2.5 x 10^6

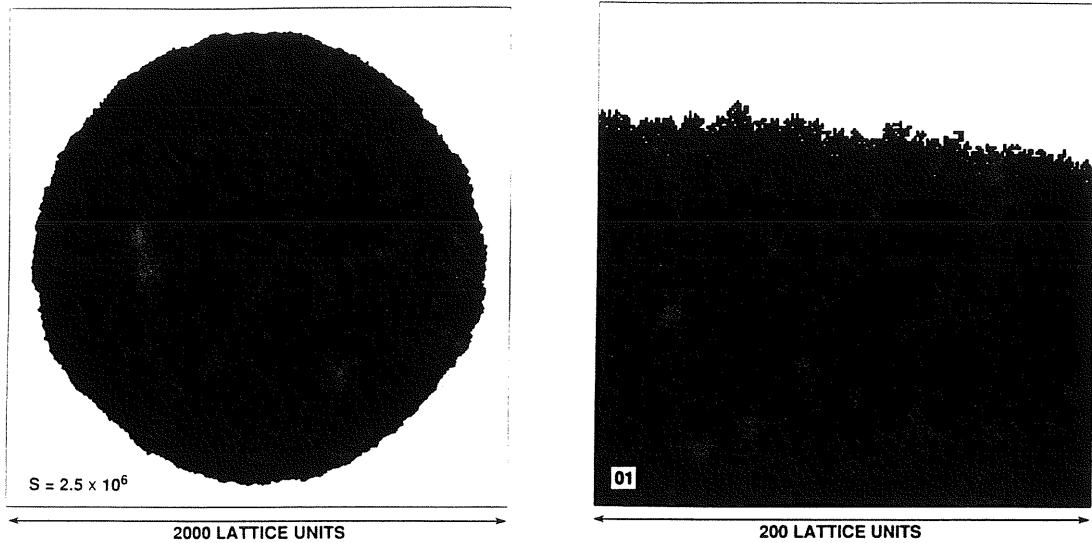2000 LATTICE UNITS   200 LATTICE UNITS

Figure 1: Eden cluster on a square lattice. The right hand figure shows the top part of the cluster enlarged by a factor of ten. Courtesy of P. Meakin.

particle after an exponentially distributed random time. In Figure 1 we show a cluster grown this way consisting of 2.5×10^6 particles. If we let the aggregation process run for a while, then the cluster will take a definite shape with some fuzziness – the shape fluctuations, compare with the enlargement in Figure 1.

What can be learned from such a model? Most basically we want to understand the interplay between the microscopic growth rule and the macroscopic shape. Under what conditions does the cluster form facets, edges, or corners, as observed for many real materials? From a statistical mechanics point of view the immediate question is how to understand the properties of the shape fluctuations. In fact, we will argue that they are universal, i.e. essentially independent of the particular growth rule. If so, this leads to the difficult problem of determining the universality classes and the general characteristics of the growth rules defining them.

For readers not familiar with critical phenomena an example may be useful here. For a diffusing particle the microscopic motion will differ from material to material. Still the mean square displacement is always proportional to t. In this sense diffusion is universal. The only condition needed is that the velocities of

the diffusing particle are statistically essentially independent when separated by a long time. This assumption breaks down e.g. in a turbulent fluid, where the mean square displacement grows as t^3 .

By definition universality means that the large scale properties of the fluctuations are independent of microscopic details (within the given class). Thus also real systems must have the same behavior. In this way the study of simplified models leads to predictions on real materials.

To give a guide through our undertaking: In Chapter 2 we consider a scale where fluctuations are negligible. We explain the link between the macroscopic shape and the inclination dependent growth velocity. In Chapter 3 our resolution is increased and we focus on a mesoscopic scale. On this scale there is still a well-defined and fairly smooth surface. Atomic roughness and overhangs are ignored. The scale is fine enough however to capture the stochastic nature of the growth process. We develop a scaling theory for shape fluctuations based on the notion of statistical self-similarity. Our discussion emphasizes generality. Up to then as the only guiding example of a concrete growth process we have the Eden model introduced above. This situation is rectified in Chapter 4 where we list and discuss a large variety of growth processes. The literature on the subject is rather ramified because of different interests and times. Since apparently not available we take the space to systematize somewhat. As additional bonus, so to speak by example, we border more sharply the physical domain of applicability of our theory.

At this point serious business has to start. Even if only approximately so, we want to compute on the basis of microscopic models the inclination dependence of the growth velocity, determine universality classes and their critical exponents, understand faceting transitions, etc. As far as one can go, these topics are covered in the remaining four chapters. In Chapter 5 we develop and analyse the continuum theory of Kardar, Parisi and Zhang (1986). In particular, we exploit the mapping to a directed polymer in a random medium, a model rather close to spin glasses. Thus methods from the theory of disordered systems come into play. Chapter 6 deals with two-dimensional models ($\hat{=}$ one-dimensional surface). They are closely related to one-dimensional lattice gases driven by an external

force. Probabilistically growth has been studied mostly through first passage percolation, Chapter 7. This approach leads, in particular, to a proof that the cluster takes a definite shape after a long time. In the final chapter we develop a simple theory for the average cluster shape by neglecting correlations. Such an approach cannot deal properly with surface fluctuations, but it is a useful tool for studying the macroscopic shape.

2 Macroscopic Shape

The shape of a cluster growing from a seed is related to the direction dependent growth velocity through a simple geometric construction that was known to crystallographers a long time ago (Wulff 1901, Gross 1918). Here we give a derivation based on an effective equation of motion for the cluster surface, and discuss some of the shapes which may occur.

2.1 Derivation

We fix a d-dimensional plane of reference which contains the seed at the origin and measure the height of the cluster surface at time t perpendicular to the plane by a function $h_t(\mathbf{x})$. $\mathbf{x}$ is a vector in the plane. To obtain the full cluster shape several coordinate systems may have to be glued together. We work on such a large scale that fluctuations in the height can be neglected. In spirit $h_t(\mathbf{x})$ is to be compared to the hydrodynamic fields of a fluid. $\mathbf{x}$ refers to a cell which is small on a macroscopic scale but contains so many lattice points that upon spatial averaging the surface has a well-defined non-fluctuating height. Our basic assumption is that the local growth velocity $v = \partial h_t(\mathbf{x})/\partial t$ in the h-direction is uniquely determined by the local surface gradient $\mathbf{u}_t = \nabla h_t$ through a known function,

$$\frac{\partial}{\partial t} h_t = v(\nabla h_t). \tag{2.1}$$

For an isotropic system (the cluster grows as a ball) we have $v(\mathbf{u}) = c\sqrt{1 + \mathbf{u}^2}$ because of our particular choice of the coordinate system with c the normal growth velocity. Due to anisotropies in the aggregation process, in general v has

a more complicated dependence on the surface gradient and as a consequence there will be more interesting macroscopic shapes. For a microscopic model $v(\mathbf{u})$ is determined by growing from a flat substrate orthogonal to $(\mathbf{u}, -1)$. After some transient time the surface will grow parallel to the substrate with normal velocity $v(\mathbf{u})/\sqrt{1 + \mathbf{u}^2}$.

To simplify our presentation we work in two dimensions, so $h_t(x)$ is a curve. For definiteness we take the underlying lattice to possess fourfold symmetry and choose the x–axis along one of the symmetry directions. Then $v(u)$ is even and needs to be specified only for $|u| \leq 1$, since the large u behavior is fixed by

$$v(u) = |u|v(1/u). \tag{2.2}$$

Starting from a seed the stationary growth shape is a solution to (2.1) which is of the scaling form

$$h_t(x) = tg(x/t). \tag{2.3}$$

Hence the shape function $g(y)$ satisfies

$$g(y) = yg'(y) + v(g'(y)). \tag{2.4}$$

Any solution of (2.4) has a definite curvature in the sense that either $g''(y) \geq 0$ or $g''(y) \leq 0$ everywhere. To see this, suppose that $g'(y_1) = g'(y_2)$ for some $y_1 < y_2$. It then follows from (2.4) that

$$g(y_2) - g(y_1) = \int_{y_1}^{y_2} g'(y)dy = g'(y_1)(y_2 - y_1). \tag{2.5}$$

This is possible only if either $g'(y) \equiv g'(y_1)$ on $[y_1, y_2]$, or if $g'(y_3) = g'(y_1)$ for some point $y_3 \in (y_1, y_2)$. In the latter case the argument is repeated for the interval $[y_1, y_3]$ to show that $g'(y)$ must be constant on $[y_1, y_2]$. Thus $g'(y)$ is monotone. Trivial solutions of (2.4) are the straight lines $g_u(y) = uy + v(u)$. The cluster shape is obtained from these through the following familiar construction: We draw the lines $g_u(y)$ for all possible slopes u, $-\infty < u < \infty$. (2.4) requires $g(y)$ for every y to be tangent to one of the $g_u(y)$'s. We conclude that $g(y)$ is the envelope of the family of lines $g_u(y)$, which may be written as

$$g(y) = \min_u [v(u) + uy]. \tag{2.6}$$

7

The cluster shape is the Legendre transform of the growth velocity. For convex $v(u), v''(u) > 0$, the minimum in (2.6) is unique and given by $v'(u) = -y$. The curvatures of v and g are related through

$$g''(y)v''(g'(y)) = -1. \qquad (2.7)$$

The physics behind (2.6) is clarified by considering a somewhat different growth geometry. Suppose that the initial condition for (2.1) is an infinitely extended corner, $h_0(x) = -u_0|x|$ for some $u_0 > 0$. Taken literally, the corner will propagate unchanged at velocity $v(u_0)$. However, physically we expect the initial corner to be rounded in some tiny neighborhood $-\epsilon \leq x \leq \epsilon$ of $x = 0$. If $v(u)$ is convex, we may as well use its Legendre transform (2.6) to model the rounded part, i.e. $h_0(x) = \frac{\epsilon}{y_0}(g(xy_0/\epsilon) - g(y_0)) - u_0\epsilon$ for $-\epsilon \leq x \leq \epsilon$ where $g'(y_0) = -u_0$. But then, by (2.3) the rounded part expands linearly under the growth, and the stationary growth shape of the corner is given by an expression similar to (2.6),

$$g(y) = \min_{|u| \leq u_0} [v(u) + uy]. \qquad (2.8)$$

The convexity of $v(u)$ implies that the inclinations $|u| \leq u_0$, which are initially present close to $x = 0$, propagate at a slower rate than $v(u_0)$. Hence they lag behind the 'ideal' corner solution $h_t(x) = -u_0|x| + v(u_0)t$ and thereby spread laterally along the x–axis. The surface inclination at fixed y is chosen by minimizing the local growth rate $v(u) + uy$ among the inclinations that were present initially. For cluster growth, the seed contains all possible inclinations and hence (2.8) reduces to (2.6).

A similar discussion applies to the related problem of a dissolving corner. Within the framework of (2.1) this is modeled by an initial condition $h_0(x) = u_0|x|$, for some $u_0 > 0$, and $v(u)$ is the inclination dependent dissolution velocity. In this case a rounding of the corner occurs if the inclinations $|u| \leq u_0$ propagate faster than $v(u_0)$, i.e. if $v''(u) < 0$. Then the shape function for dissolution is

$$g_{\text{diss}}(y) = \max_{|u| \leq u_0} [v(u) + uy]. \qquad (2.9)$$

For convex $v(u)$ the maximum in (2.9) is always attained at $u = \pm u_0$, which implies that the dissolving corner remains sharp.

2.2 Edges, facets and other singularities

Singularities in the growth velocity translate into corresponding non-analyticities in the growth shape. It is clear from (2.6) that the convex envelope $\hat{v}(u)$ of $v(u)$ determines the shape, rather than $v(u)$ itself. In particular, the extension of the cluster shape along the symmetry axes is given by $g(0) = \hat{v}(0)$, which also determines the domain of definition of $g(y)$ as $[-\hat{v}(0), \hat{v}(0)]$. $\hat{v}(u)$ is obtained from $v(u)$ by removing all nonconvex parts using the double tangent (Maxwell) construction. Unless $v(u)$ is convex, $\hat{v}(u)$ contains linear pieces where $\hat{v}''(u) \equiv 0$. We consider such a piece located between u_1 and u_2, $\hat{v}'(u) \equiv \hat{v}'(u_1) = \hat{v}'(u_2)$ for $u_1 \leq u \leq u_2$. As y in (2.6) passes through $y = -\hat{v}'(u_1)$, the inclination where the minimum is attained jumps discontinuously from u_1 to u_2. Thus $g(y)$ develops an edge at $y = -\hat{v}'(u_1)$ and the range of inclinations $u_1 < u < u_2$ disappears from the growth shape. This is quite analogous to two-phase coexistence in a fluid where a range of densities is thermodynamically unstable (Rottman and Wortis 1984).

While nonconvex parts of $v(u)$ are irrelevant to the growth shape, they may appear in the shape of a dissolving corner, cf. Equation (2.9), which is determined by the *concave* envelope of $v(u)$ in the range $|u| \leq u_0$. Figure 2 demonstrates the construction of growth and dissolution shapes for nonconvex $v(u)$. An example of a microscopic growth model where such a shape actually occurs will be given in Chapter 6.

Next we consider the case where $v(u)$ itself has a cusp at $u = 0$, say,

$$v(u) = v(0) + \lambda |u| + \mathcal{O}(|u|^\delta), \qquad (2.10)$$

where $\delta > 1$ and both λ and the next to leading term are positive. Inserting this into (2.6) we must minimize $\lambda |u| + uy$ with respect to u. For $-\lambda \leq y \leq \lambda$ the minimum is attained at $u = 0$ and hence $g(y) \equiv v(0)$ in this range. The growing cluster develops a facet of size $2\lambda t$. The next to leading term in (2.10) determines how the rounded part of the cluster shape joins the facet. Applying (2.6) yields

$$g(\lambda) - g(\lambda + \epsilon) \sim \epsilon^{\delta/(\delta-1)} \qquad (2.11)$$
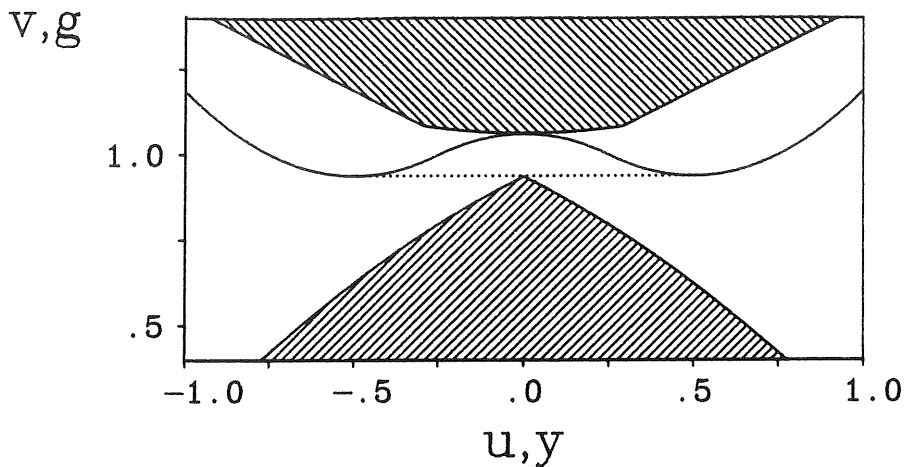
9

V,g

Figure 2: Growth shape $g(y)$ (bottom) and dissolution shape $g_{diss}(y)$ (top) for nonconvex growth velocity $v(u)$. The dotted line is the convex envelope $\hat{v}(u)$.

for $\epsilon \to 0$. Growing crystals are often faceted due to the slow (nucleation dominated) growth rate at singular faces (Chernov 1984). In Chapter 7 we will discuss a class of growth models which show a faceting transition.

The occurences of edges and facets in the growth shape are limiting cases of the curvature relation (2.7), provided $v(u)$ is replaced by $\hat{v}(u)$. Along linear pieces of $\hat{v}(u), \hat{v}''(u) = 0$ and thus $g''(y)$ is forced to diverge, whereas a cusp in $\hat{v}(u), \hat{v}''(u) = \infty$, leads to $g''(y) = 0$. For a general singularity of $v(u)$ of the form

$$v(u) \approx v(0) + \lambda |u|^{\alpha}, \quad \alpha \geq 1, \tag{2.12}$$

for $u \to 0$, (2.7) yields the singular growth shape

$$g(y) \approx v(0) - \lambda' |y|^{\alpha/(\alpha-1)}, \tag{2.13}$$
$$\lambda' = ((\alpha - 1)/\alpha)(\lambda \alpha)^{-1/(\alpha-1)},$$

for $y \to 0$. This kind of singularity occurs at the critical point of the faceting transition discussed in Chapter 7.

Finally we mention a type of singularity in $g(y)$ which is characteristic of the ballistic deposition models to be introduced below in Chapter 4. The deposition flux singles out one direction and hence fourfold symmetry, cf. Equation (2.2),

does not hold. One finds a convex growth velocity $v(u)$ with the asymptotic behavior (Krug and Meakin 1989)

$$v(u) \approx v_\perp(a + |u|), \quad u \to \pm\infty. \qquad (2.14)$$

Here $a > 0$ and $v_\perp$ denotes the growth velocity in the lateral direction (along the x–axis); in general $v_\perp < v(0)$. The shape function $g(y)$ is defined on $[-v_\perp, v_\perp]$. From (2.6) one gets $g(y) \to v_\perp a$ as $y \to \pm v_\perp$, i.e. $g(y)$ is discontinuous at the boundaries (since $g(\pm v_\perp) = 0$). The discontinuity is due to the nonlocal shadowing effects in these models, which produce fan-shaped clusters with an opening angle of $2\arctan(1/a)$ (cf. Chapter 4). The derivative $g'(v_\perp)$ can be finite or infinite depending on the corrections to (2.14).

2.3 The Wulff construction

Summarizing our main results, Equations (2.6), (2.8) and (2.9), we may conclude that a growing cluster (or crystal) attempts to minimize its total growth rate, while a dissolving cluster (crystal) maximizes the rate of dissolution. These general principles were stated by Wulff and Gross already at the beginning of the century. Wulff's geometric treatment of faceted growth was extended by Gross to include curved growth shapes and was given an analytic formulation by Chernov (1963) and Wolf (1987).

The celebrated Wulff construction in its textbook form determines the *equilibrium* shape of a crystal by minimizing the surface free energy at fixed volume. While such a general variational principle cannot be used as a starting point for a theory of growth shapes, we shall see below that the kinetically determined prescription (2.6) is completely equivalent to the Wulff construction with the direction dependent growth velocity replacing the surface free energy. Wulff (1901) originally assumed growth shapes and equilibrium shapes to be the same, and hence concluded that surface free energies could be derived from growth rate measurements. However, since growth rates are determined by kinetic as well as thermodynamic requirements, growth and equilibrium shapes of crystals are generally quite different (Métois et al. 1982).

11

In the context of equilibrium shapes it is well known (Andreev 1982, Rottman and Wortis 1984) that the Wulff construction can be recast in terms of Legendre transforms similar to (2.6), with the surface inclination u playing the role of a thermodynamic variable. To show the equivalence in the present case, we introduce the normal growth velocity $w(\vartheta)$ as a function of the angle ϑ formed by the growth direction with the vertical, $\vartheta = \arctan(-u)$, through

$$w(\vartheta) = v(-\tan\vartheta)\cos\vartheta. \qquad (2.15)$$

The growth shape is given in polar coordinates by a function $r(\varphi)$,

$$g(y) = r(\varphi)\cos\varphi, \; y = r(\varphi)\sin\varphi, \qquad (2.16)$$

where $-\pi/2 < \vartheta, \varphi < \pi/2$. Once the angle of inclination of the cluster surface at a given polar angle φ, $\vartheta(\varphi)$, is known, an elementary geometric construction gives

$$r(\varphi) = \frac{w(\vartheta(\varphi))}{\cos(\varphi - \vartheta(\varphi))}. \qquad (2.17)$$

The relation between φ and ϑ follows from (2.6). Since $\tan\varphi = y/g(y)$, we have

$$\tan\varphi = [u - \hat{v}(u)/\hat{v}'(u)]^{-1} \qquad (2.18)$$

which is rewritten using (2.15) as

$$\tan(\varphi - \vartheta(\varphi)) = \hat{w}'(\vartheta(\varphi))/\hat{w}(\vartheta(\varphi)) \qquad (2.19)$$

where $\hat{v}$ and $\hat{w}$ are the convex envelopes of v and w. Taking the derivative of (2.17) with respect to ϑ it follows that the angle determined by (2.19) is the one which minimizes (2.17), hence

$$r(\varphi) = \min_{\vartheta} \left(\frac{w(\vartheta)}{\cos(\varphi - \vartheta)} \right). \qquad (2.20)$$

This is the analytic representation of the Wulff construction: For each value of ϑ a line of inclination $-\tan\vartheta$ is drawn at a distance $w(\vartheta)$ from the origin. Then the growth shape is the inner envelope of all lines. An example of a $w(\vartheta)$–plot and the corresponding growth shape is shown in Figure 3.
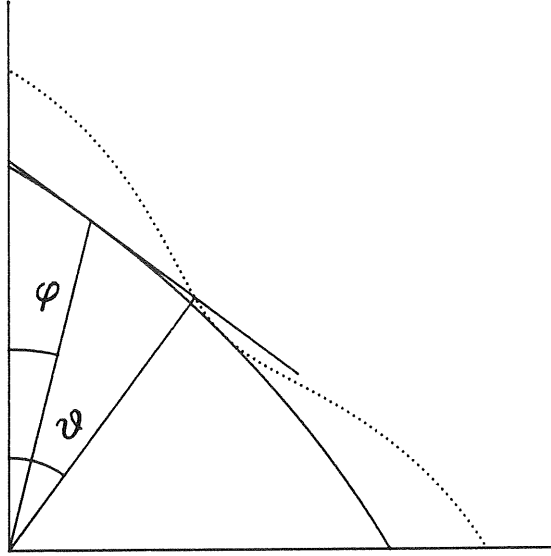
Figure 3: Wulff construction of one quadrant of the growth shape for the PNG model (see Section 4.2). The dotted line is the direction dependent growth velocity $w(\vartheta)$ and the full line is the growth shape $r(\varphi)$.

For future reference we record some general properties of the growth angle $\varphi(\vartheta)$ defined by (2.18). The convexity of $\hat{v}$ implies that φ is a monotonously increasing function of ϑ. Note however that the sign of $\varphi - \vartheta$ in (2.19) is not fixed, since convexity of $\hat{v}(u)$ only requires that $\hat{w}(\vartheta) + \hat{w}''(\vartheta) > 0$. A cusp in $v(u)$ (Equation (2.10)) leads to a discontinuity in $\varphi(\vartheta)$ and a general singularity of the form (2.12) yields

$$\varphi(\vartheta) \approx \frac{\lambda \alpha}{v(0)} \vartheta^{\alpha - 1}, \qquad \vartheta \to 0. \tag{2.21}$$

The asymptotically linear behaviour (2.14) implies that $\varphi \to \arctan(1/a)$ for $\vartheta \to \pi/2$.

Before closing this chapter we should note the intrinsic significance of $\varphi(\vartheta)$. In the context of the macroscopic evolution equation (2.1), $\varphi(\vartheta)$ determines the direction $\mathbf{m} = (\sin\varphi, \cos\varphi)$ in the (x,t)–plane along which a small surface segment with inclination $u = -\tan\vartheta$ translates locally. The trajectories in the (x,t)–plane of such segments of constant inclination form the *characteristics* of (2.1). A microscopic characterization of $\varphi(\vartheta)$ is obtained considering the growth of a planar

13

surface of fixed inclination $u = -\tan\vartheta$. The growing film is decomposed into clusters of connected particles which share the same ancestor substrate site (Meakin 1987b). For thick films the clusters are elongated in the direction determined by φ. While usually the clusters are hidden in the bulk of the film (Meakin 1987a), they become visible to the naked eye in the case of oblique incidence ballistic deposition, where they form the ubiquitous columnar microstructure (cf. Section 4.3).

3 Scaling Theory of Shape Fluctuations

Having determined (at least in principle) the macroscopic shape of the growing cluster, we may turn our attention to more refined aspects of the growth process. A striking feature already noted by Eden in his 1961 paper is the roughness of the cluster surface. We introduce and employ the notion of statistical scale invariance to characterize the roughness of growing surfaces. Statistical scale invariance is really at the heart of the more widely promoted concept of fractal geometry (Mandelbrot 1982) and shares with it certain limits of applicability to the real world of natural processes and computer simulations. We return to this further below, but start out with a discussion of 'ideal' kinetic roughness.

3.1 Statistical scale invariance

Since in general the average cluster shape is not explicitly known, it is impractical to study shape fluctuations in the cluster geometry (Zabolitzky and Stauffer 1986). We therefore use the substrate geometry instead and take the substrate to be an infinite, d-dimensional hyperplane in $(d+1)$-dimensional space. After some local coarse-graining the surface configuration at time t can be described by a single valued, continuous function $h_t(\mathbf{x})$ which measures the height of the surface perpendicular to the substrate above the substrate point $\mathbf{x}$. $h_t(\mathbf{x})$ should not be confused with the deterministic (macroscopic) surface profile discussed before in Chapter 2. Here we work on a 'mesoscopic' scale which is fine enough to capture the stochastic nature of the growth process, but sufficiently coarse for

14

allowing to ignore the discrete lattice structure, overhangs and other microscopic details (for a more detailed discussion of microscopic length scales see Section 3.2).

The initial condition is $h_0(\mathbf{x}) \equiv 0$. Being interested in fluctuations, we subtract the average height at time t. Hence $h_t(\mathbf{x})$ is a random function with zero mean. We call the growth process statistically scale invariant, if typical surface configurations can be made to 'look the same' by suitable simultaneous rescaling of space $(\mathbf{x})$, time (t), and height (h). More precisely, we require that for an arbitrary rescaling factor $b > 0$ the statistical properties of the rescaled process

$$h'_t(\mathbf{x}) = b^{-\zeta} h_{b^z t}(b\mathbf{x}) \tag{3.1}$$

coincide with those of $h_t(\mathbf{x})$. For a given growth process, this requirement fixes the scaling exponents ζ and z, which therefore carry the central information about the scaling properties of the surface fluctuations.

We illustrate the significance of ζ and z using as an example the height difference correlation function

$$G(|\mathbf{x} - \mathbf{x}'|, t) = \langle |h_t(\mathbf{x}) - h_t(\mathbf{x}')| \rangle. \tag{3.2}$$

For long times $(t \to \infty)$ we expect G to become stationary (time independent). (3.1) then implies

$$\xi_\perp(r) := \lim_{t \to \infty} G(r, t) = a r^\zeta \tag{3.3}$$

with $a > 0$ some constant. $\xi_\perp(r)$ measures the transverse 'wandering' of the surface over the horizontal distance r. This is why ζ has been termed the *wandering or roughness exponent* (Fisher M E 1986, Lipowsky 1988, 1989). Rough surfaces have $0 < \zeta < 1$. Marginal roughness with $\zeta = 0$ is characteristic of two dimensional surfaces in thermal equilibrium but also occurs in some nonequilibrium situations such as critical faceting (cf. Chapter 7) and diffusion-limited annihilation (Meakin and Deutch 1986). In these cases the power law (3.3) is replaced by $\xi_\perp(r) = a'(\log r)^{\zeta'}$. The opposite limit $\zeta = 1$ implies that the large scale surface orientation differs from the substrate orientation since $\xi_\perp(r)/r$ does not vanish for $r \to \infty$. Depending on the situation $\zeta = 1$ may be the signature of a fractal
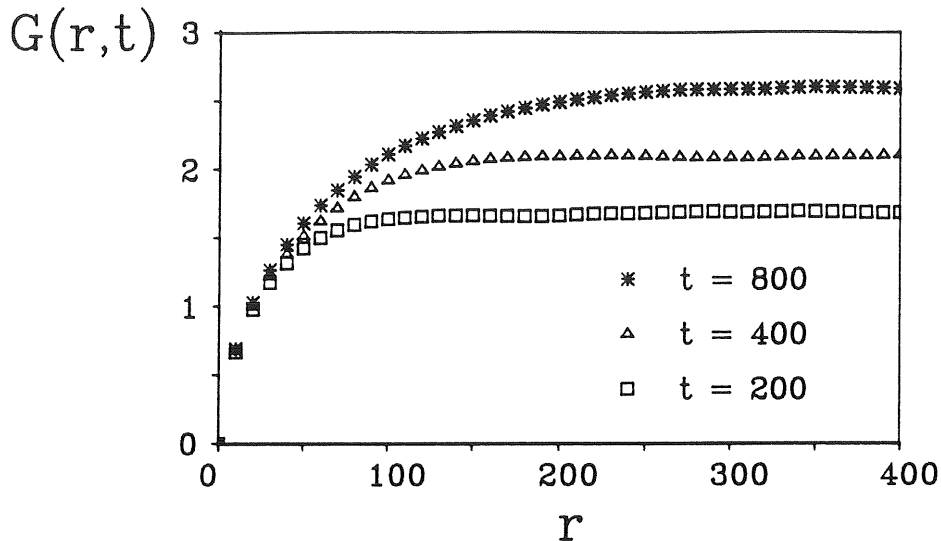
Figure 4: Height difference correlation function $G(r,t)$ for the one dimensional discrete time PNG model (the growth rule is defined in Section 4.2). Simulations were carried out on a lattice of size $L = 5000$ with a nucleation rate $p = 0.01$. The data are an average over 50 runs.

(Meakin and Jullien 1989, 1990), crumpled (Lipowsky 1988, 1989) or discontinuous (Krug and Meakin 1989) surface. For equilibrium models $\zeta = 1$ has been associated with the breakdown of two-phase coexistence at the lower critical dimensionality (Huse et al. 1985, Fisher M E 1986). Whatever happens in such cases, one must be prepared to abandon the picture of a single valued, continuous height function and look for other means of description.

Next we consider the approach of $G(r,t)$ to the stationary limit (3.3). Inserting (3.1) into (3.2), we obtain the homogeneity relation

$$G(r,t) = b^{-\zeta} G(br, b^z t). \tag{3.4}$$

Choosing $b = 1/r$ this may be rewritten as

$$G(r,t) = \xi_\perp(r) g(r/t^{1/z}). \tag{3.5}$$

with $g(0) = 1$ from (3.3). The interpretation of (3.5) is as follows: For finite t there exists a correlation length

$$\xi_{\parallel}(t) \sim t^{1/z} \tag{3.6}$$

16

such that on scales $r \ll \xi_\|(t)$ the surface is stationary and rough, whereas on scales $r \gg \xi_\|(t)$ the surface looks smooth in the sense that the transverse wandering does not further increase with r. Requiring that $G(r,t)$ becomes independent of r for $r \gg t^{1/z}$ implies that the scaling function in (3.5) vanishes as $g(x) \sim x^{-\zeta}$ for $x \gg 1$ and hence

$$G(r,t) \sim t^{\zeta/z} \sim \xi_\|^\zeta, \quad r \gg \xi_\|(t). \tag{3.7}$$

Thus the *dynamic exponent* z describes the temporal spread of surface fluctuations and, via (3.7), the increase of surface roughness in time. If the spread of fluctuations were purely diffusive, we would have $\xi_\|(t) = \sqrt{Dt}$ and $z = 2$. However, as we will demonstrate below, growth conditions usually lead to a superdiffusive $z < 2$. Figure 4 shows a numerical example of the correlation function $G(r,t)$. In this case $\zeta = 1/2$ and $z = 3/2$, compare with Chapter 5.

3.2   Corrections to scaling

In real systems and computer models, simple power laws like (3.3) are often obscured by the presence of additional length scales. Since experimental results in this field are scarce, we give a discussion appropriate for the standard type of computer simulation.

Let us first explore the consequences of taking (3.3) literally for all r, $0 < r < \infty$. The prefactor a then introduces a crossover scale r_c such that $\xi_\perp(r_c) = r_c$,

$$r_c = a^{1/(1-\zeta)}. \tag{3.8}$$

On scales $r \ll r_c$, $\xi_\perp(r)/r \gg 1$, and the surface is wildly agitated. In fact, in this regime it looks fractal. To understand this, we recall the definition of the fractal dimensionality D of a surface (Mandelbrot 1982). The height variables are averaged over horizontal patches of linear size ϵ. The area $A(\epsilon)$ of the averaged surface (the surface area 'on the scale ϵ') is measured and compared to the projected (substrate) area A_0. D is then defined through

$$A(\epsilon)/A_0 \sim \epsilon^{-(D-d)}, \tag{3.9}$$

where d denotes the substrate dimension. For a fractal surface $(D > d)$ $A(\epsilon)$ increases indefinitely as $\epsilon \to 0$. For a rough surface simple arguments show that

17

(Wong and Bray 1987, Burkhardt 1987)

$$A(\epsilon) = A_0(1 + \xi_\perp(\epsilon)/\epsilon) = A_0(1 + (\epsilon/r_c)^{-(1-\zeta)}). \qquad (3.10)$$

Comparing with (3.9) we find that the fractal dimension is scale dependent,

$$D = \begin{cases} d+1-\zeta & (\epsilon \ll r_c) \\ d & (\epsilon \gg r_c), \end{cases} \qquad (3.11)$$

so $D > d$ below the crossover scale r_c.

Mandelbrot (1986) has coined the term 'self-affine fractals' for geometrical objects with the property (3.11), 'affinity' replacing 'similarity' because such objects are (statistically) invariant under *anisotropic* rescaling of space. The standard example of a self-affine fractal (with $d = 1$ and $\zeta = 1/2$) is the record of a one dimensional Brownian motion (Wiener process). In this case the time axis plays the role of the spatial coordinate and the particle position corresponds to the surface height. The notion of self-affinity has become quite popular. It should be noted however that in contrast to the mathematically constructed Wiener process for physical surfaces the extrapolation to arbitrarily fine length scales implicit in (3.11) is impeded by various small-scale cutoffs, which we now discuss.

An obvious small-scale limit to scale invariance is the lattice constant r_0. More subtle corrections to scaling often arise from the local surface structure. Following Kertész and Wolf (1988) these are summarized in the intrinsic width ξ_i, which is the r–independent part of $\xi_\perp(r)$ and is introduced through

$$\xi_\perp(r)^2 = \xi_i^2 + a^2 r^{2\zeta}. \qquad (3.12)$$

The pure scaling form (3.3) is recovered only on length scales $r \gg r_i := (\xi_i/a)^{1/\zeta}$. The intrinsic width is built up from high steps (i.e. nearest neighbor height differences exceeding one lattice constant), overhangs and holes. Its significance is similar to that of the bulk correlation length in the theory of equilibrium interfaces between coexisting phases (Huse et al. 1985). In particular, any continuum description of the surface must start from a level of coarse-graining which is large compared to r_c. In computer simulations the intrinsic width can be reduced

18

either by using a modified growth algorithm (Kertész and Wolf 1988) or by restricting the set of admissible surface configurations to exclude holes, overhangs and high steps as in the solid-on-solid models, cf. Chapter 4. The crossover scale (3.8) usually turns out to be comparable to or smaller than r_i (or r_0), and hence the self-affine fractal regime $r \ll r_c$ in (3.11) does not exist.

The second severe limitation to the simple scaling form (3.5) is due to the finite size of the system. Once the correlation length $\xi_{\parallel}(t)$ becomes comparable to the linear size L of the system, i.e. after a time of order L^z, the growth turns stationary. This can be expressed through the finite size scaling form for the overall surface roughness

$$W(L,t) = [L^{-d} \int d^d x (h_t(\mathbf{x}) - \overline{h}_t(L))^2]^{1/2}, \tag{3.13}$$

where the integral runs over the substrate coordinates and $\overline{h}_t(L)$ is the spatial average

$$\overline{h}_t(L) = L^{-d} \int d^d x\, h_t(\mathbf{x}). \tag{3.14}$$

Note that since the ensemble average of $h_t(\mathbf{x})$ has already been subtracted, (3.14) is the difference between the spatial and the ensemble averages. The two coincide only in the limit $L \to \infty$. For long times the surface diffuses as a rigid object and one expects that $\langle \overline{h}_t(L)^2 \rangle \sim L^{-d} t$.

$W(L,t)$ should have a scaling form similar to $G(r,t)$ with $r = L$: It is a function of $L/\xi_{\parallel}(t)$ which saturates at a value proportional to L^ζ for $\xi_{\parallel}(t) \gg L$, and grows as $t^{\zeta/z}$, independent of L, for $\xi_{\parallel}(t) \ll L$, compare with Equations (3.3), (3.5) and (3.7). Thus we may write (Family and Vicsek 1985)

$$W(L,t) = L^\zeta f(t/L^z) \tag{3.15}$$

where $f(x \to \infty) = \text{const.}$ and $f(x \to 0) \sim x^{\zeta/z}$. This form has been used in many simulations to determine the exponents ζ and z.

3.3   Scaling relations

Static and dynamic surface fluctuations are coupled by the growth process itself. This leads to a scaling relation between ζ and z which has been derived in a

number of more or less formal ways (Huse and Henley 1985, Meakin et al. 1986b, Krug 1987, Kardar and Zhang 1987, Medina et al. 1989, Krug and Meakin 1989, Wolf and Kertész 1989). Here we show how it arises as a natural and immediate consequence of the general scaling picture.

Looking at the growing surface at time t, we observe bulges of all sizes up to the correlation length $\xi_{\parallel}(t)$. Let us focus our attention on one of the largest bulges and watch how it evolves in time. Its height is proportional to $\xi_{\perp}(\xi_{\parallel}(t))$ and its slopes have an inclination of the order $\xi_{\perp}(\xi_{\parallel}(t))/\xi_{\parallel}(t) \ll 1$. In default of any specific knowledge about the growth process, we may assume that everywhere the direction of growth is normal to the surface (Figure 5). Then the bulge widens at a rate proportional to the horizontal projection of the normal growth velocity of its slopes, i.e. proportional to the slope inclination. Thus

$$\frac{d}{dt}\xi_{\parallel} \sim \xi_{\perp}(\xi_{\parallel})/\xi_{\parallel} \sim \xi_{\parallel}^{\zeta-1} \tag{3.16}$$

and

$$\xi_{\parallel}(t) \sim t^{1/(2-\zeta)}. \tag{3.17}$$

Comparing (3.17) to the definition (3.6) of the dynamic exponent z, we conclude that

$$z = 2 - \zeta. \tag{3.18}$$

This scaling relation looks very universal: It is independent of both the surface dimension and the details of the growth process. Still there are some instances
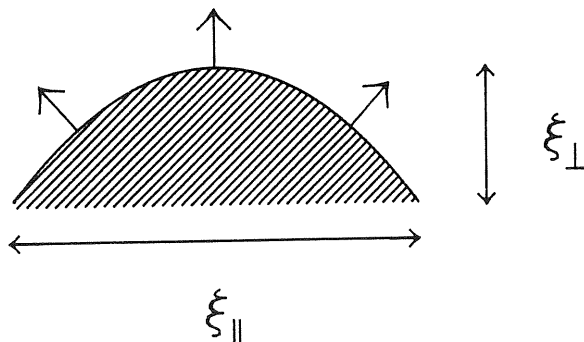

Figure 5: Widening of a surface fluctuation through normal growth.

where it fails. To explore its range of validity, we must scrutinize the suppositions inherent in the above argument. Treating the growth of the bulge as a deterministic process, we have in fact assumed that the macroscopic theory applies also at the mesoscopic level of (large-scale) fluctuations. But we know already that the direction of growth does not generally coincide with the surface normal. Using the expression (2.21) for the growth angle in the case of a general nonlinearity of the inclination dependent growth velocity, cf. Equation (2.10), we find that (3.16) generalizes to

$$\frac{d}{dt}\xi_{\parallel} \sim (\xi_{\perp}(\xi_{\parallel})/\xi_{\parallel})^{\alpha-1} \tag{3.19}$$

and hence $\xi_{\parallel}(t) \sim t^{1/z}$ with (Krug and Spohn 1988)

$$z = \alpha + \zeta(1-\alpha). \tag{3.20}$$

The relation between ζ and z is determined by the leading nonlinear term of $v(u)$ in the limit $u \to 0$. Terms linear in u only shift the bulge as a whole and do not contribute to its spreading. It should be noted however that even in the absence of nonlinearities the noise in the growth process causes the fluctuations to spread diffusively, $\xi_{\parallel} \sim t^{1/2}$. The nonlinearity is relevant only if it causes $\xi_{\parallel}(t)$ to grow *faster* than diffusively, i.e. if

$$\alpha < \frac{2-\zeta}{1-\zeta}. \tag{3.21}$$

4   Growth Models

At this point we have to provide some examples of the growth phenomena covered by our theory. The general physical setup we have in mind is that of two phases, one of them stable and the other unstable, separated by an interface. The stable phase grows at the expense of the unstable phase and the interface moves at a constant speed. The interface is sharp and globally flat on a macroscopic scale, and we are interested in its mesoscopic roughness. This explicitly excludes the kind of large-scale interfacial instabilities often encountered in solidification

processes, such as dendritic or cellular growth (Langer 1987). While in real systems the transition from stable to unstable growth (these terms referring now to the state of the interface) usually occurs upon changing the growth parameters rather than the underlying mechanism (Saito and Ueta 1989), the 'microscopic' models we shall consider are constructed to describe stable growth only. Clearly this limits their applicability to physical growth processes.

The basic stochastic model for *unstable* growth, which in fact triggered most of the present-day interest in growth processes, is the celebrated Witten-Sander model of diffusion-limited aggregation (DLA) (Witten and Sander 1981). The model is extremely easy to define: Given a cluster of N particles, the $N+1$'th particle is launched anywhere on the surface of a sphere enclosing the cluster and is allowed to diffuse until it touches the cluster and sticks to it. This procedure generates the intriguing, ramified patterns which now decorate the covers of countless conference proceedings. Despite considerable numerical and theoretical efforts a satisfactory understanding of DLA still eludes us (Meakin 1988a). The difficulty is due to the *nonlocal* nature of the diffusion field which governs most pattern forming interfacial instabilities. To determine the probability for the next particle to stick at some given point on the surface, one has to solve the stationary diffusion equation (Laplace equation) including the whole cluster surface as a zero-field boundary condition. In contrast, the growth models of interest here are *local* in the sense that the probability of adding a particle depends only on the local environment of the respective surface site. Physically, this implies that the transport mechanisms which carry new material to the growing surface and expel impurities or latent heat are, to a large extent, neglected, and the growth is assumed to be dominated by the aggregation kinetics.

Even within the restricted class of local models there is an abundance of varieties which can be (and have been) studied. Our aim here is to describe the major representatives and to discuss some of their features within the conceptual framework of the previous chapters. Before doing so, it may be useful to list a few general properties of local growth models in order to provide a first classification.

(i) *lattice-/off-lattice models:* For reasons of computational efficiency, simulations of growth processes are usually carried out on a discrete lattice of sites,

which are either vacant or occupied by a particle. Off-lattice models, in which the particles are represented by hard discs or spheres with real spatial coordinates, are more realistic but harder to program. While the macroscopic cluster shape obviously reflects the symmetry of the underlying lattice, the scaling properties of the shape fluctuations are generally expected to be insensitive to the lattice structure. A notable exception to this rule occurs for a class of deposition models to be described below.

(ii) *fully/partly irreversible models:* Although of course any growth process is irreversible, we may distinguish between fully irreversible models which only allow the addition of particles to the aggregate, and partly irreversible models which also include disaggregation, albeit at a smaller rate. In high spatial dimensionalities ($d \geq 3$) there is the possibility of a surface roughening transition as the degree of irreversibility is varied (cf. Chapter 5).

(iii) *flux-limited/reaction-limited models* (Krug 1989a): This distinction is best illustrated by two idealized physical situations. For the flux-limited case, consider vapor deposition onto a cold substrate. A dilute flux of particles impinges on the surface and the particles stick irreversibly where they hit. Reaction-limited growth is typified by molecular-beam epitaxy on vicinal faces of a crystalline semiconductor. In this case there is a constant density of atoms on the terraces which diffuse along the steps, looking for a growth site (e.g. a kink site) where they can be incorporated in the crystal. Although, as noted above, local growth models treat transport in a very summary fashion, they can still be distinguished according to whether the rate of growth is limited by the supply of new material (flux-limited) or by the availability of growth sites (reaction-limited). Among the models to be discussed in the following, the Eden- and SOS-models are reaction-limited, while the deposition models are flux-limited. It should be noted that the reaction-limited case appears quite naturally in the context of biological applications, in which the Eden-type models were first formulated: If the growth proceeds through cell division, there is no need to transport new material (new cells) to the cluster surface.

(iv) *sequential/synchronous models:* In most simulations particles are added to the aggregate sequentially, i.e. one by one, and 'time' is counted in terms of the

aggregate mass. This procedure can be shown to generate the same ensemble of configurations as the following continuous time random process: In an infinitesimal time interval dt, growth occurs independently at every growth site (site at which a particle can be added) with probability Γdt, where Γ is a rate constant. In contrast, in a synchronous (discrete time) process a randomly chosen finite fraction or possibly all of the growth sites are simultaneously updated in a single time step. One characteristic feature of synchronous models is the occurence of a faceting phase transition, cf. Chapters 7 and 8.

4.1   Eden models

The basic lattice model for cluster growth was devised by Murray Eden in 1956 as a minimal description of biological morphogenesis (Eden 1958). It is so simple that it hardly needs an explanation: Given a cluster of N particles, the $N+1$'th particle is added at a randomly chosen perimeter site of the cluster. A perimeter site is a vacant lattice site which has at least one occupied neighbor. The occupied neighbors of the perimeter sites will be referred to as surface sites. Jullien and Botet (1985) noted three different, equally natural ways of choosing among the perimeter sites: Either the perimeter sites themselves (version A), or the bonds connecting perimeter and surface sites (version B), or the surface sites (version C) may be assigned equal probabilities. In version C, an additional random choice is necessary if the chosen surface site is adjacent to several perimeter sites. Eden originally studied version B on the two dimensional square lattice. Our introductory model (Chapter 1) is the continuous time process corresponding to version A.

Large Eden clusters contain growth (perimeter) sites only in a thin surface layer which occupies a negligible fraction of the cluster volume as $N \to \infty$. This implies that clusters attain a well-defined macroscopic shape as was proved by Richardson (1973).

On the basis of simulations up to $N = 2^{15}$ Eden (1961) noted that the clusters are 'essentially circular in outline' (Figure 1). It was necessary to increase the cluster sizes by more than three orders of magnitude to firmly establish a slight
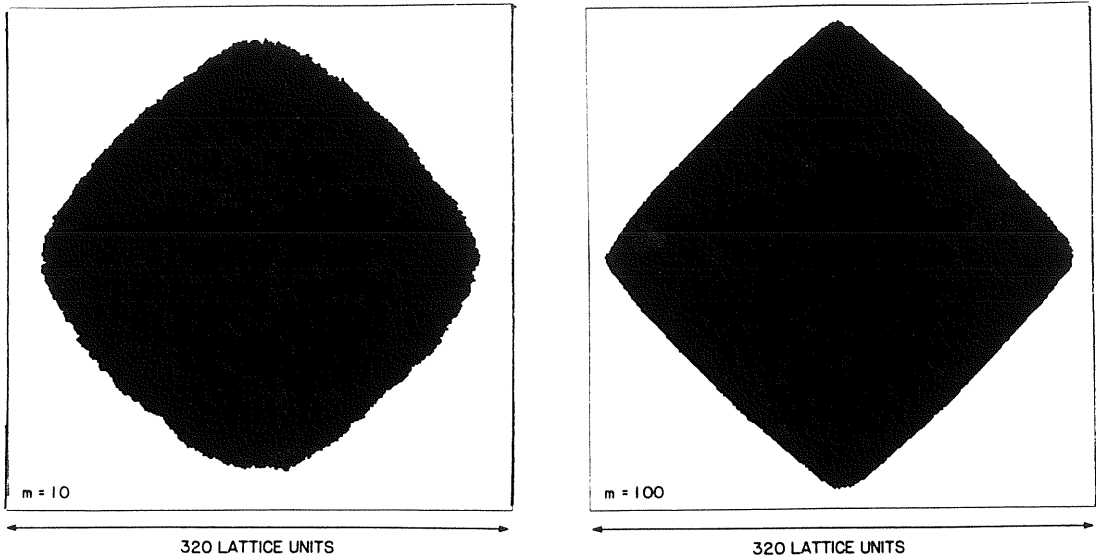
Figure 6: Eden clusters on a square lattice grown with noise reduction parameters $m = 10$ and $m = 100$. Courtesy of P. Meakin.

deviation from the circular shape (Freche et al. 1985), corresponding to a weak angular dependence of the normal growth velocity $w(\vartheta)$ (cf. Chapter 2). Keeping in mind the corresponding continuous-time process, it is easily seen that $w(\vartheta)$ is proportional to the number of perimeter sites (version A), the number of open bonds (version B) or the number of surface sites (version C) per unit area of the tilted substrate. These quantities were measured for versions A (Hirsch and Wolf 1986) and C (Meakin et al. 1986a), and the growth was found to be slower by about 2 % along the lattice diagonal, as compared to the lattice axes. The anisotropy is expected to become more pronounced in higher dimesions, since rigorous bounds show that the growth velocity along the lattice axes is of the order $d/\log(d)$ while along the space diagonal it is only $\mathcal{O}(\sqrt{d})$ (Kesten 1986).

Eden also observed that the cluster perimeter, defined as the number of open bonds, is larger than that of a perfect circle by a factor of 1.8. The 'excess perimeter' reflects the local crinkliness of the cluster surface (Mollison 1972). It consists of holes, overhangs and high steps, and constitutes the major contribution to the intrinsic surface width ξ_i introduced in (3.12) (Kertész and Wolf 1988). The excess perimeter is sensitive to the local growth rule: Going from

25

version A to version C it decreases by a factor of 6 (Jullien and Botet 1985). The *noise reduction* algorithm originally developed for DLA (Szép et al. 1985) allows to systematically reduce the excess perimeter, and thereby ξ_i. This algorithm introduces an integer valued noise reduction parameter m and requires a perimeter site (for version A) to be selected m times before it is occupied. As a consequence of this local averaging, the excess perimeter density and the intrinsic width both decrease as $1/m$ (Kertész and Wolf 1988).

In the limiting case $m = \infty$ all growth sites are occupied simultaneously and the growth becomes deterministic (no noise) (Krug and Spohn 1988). The resulting growth shape is a diamond. Since the shape would be expected to depend continuously on m there must be a transition toward the diamond shape with increasing m (Figure 6). Noise reduction enforces the lattice anisotropy. The surprising (and unexplained) feature is that without noise reduction ($m = 1$), the noise *almost* succeeds in turning the diamond into a circle. Clusters which are even less anisotropic can be generated by extending the definition of growth (perimeter) sites to include the next nearest neighbors of a surface site. Since the deterministic ($m = \infty$) shape is a square, the growth is now expected to be *faster* along the diagonal. This was confirmed and the anisotropy (for $m = 1$) was found to be only 1.2 % (Garmer 1989).

A similar shape transition occurs in the synchronous (discrete time) Eden model introduced by Richardson (1973). In one time step $t \to t + 1$, all perimeter sites of the cluster are filled simultaneously and independently with probability p. Again, the growth is deterministic for $p = 1$ and in the limit $p \to 0$, combined with a rescaling of time, the original Eden model is recovered. However the sequence of shapes which interpolate between (almost) circular and diamond are qualitatively different. While, in the case of noise reduction, the cluster edges remain slightly curved even for large m (Meakin 1988b), the Richardson model shows a faceting transition at some critical value $0 < p_c < 1$. For $p > p_c$ the cluster shape coincides with the diamond close to the diagonal, cf. Chapters 7 and 8. Synchronous models in which a finite lifetime is attributed to the growth sites have also been considered (Savit and Ziff 1985). In these cases there is a second (bulk percolation) threshold $p_c^b < p_c$, such that for $p < p_c^b$ clusters die out

eventually. At p_c^b the clusters (conditioned on survival) are fractal.

In an attempt to describe tumor induction, Williams and Bjerknes (1972) introduced a partly reversible variant of the Eden model which has motivated much of the subsequent mathematical work on growth models. The basic idea is that the rate of division of cancer cells exceeds that of normal cells by some factor $k > 1$ (the 'carcinogenic advantage'). Each time a cell (normal or cancer) divides, the daughter cell displaces one of the neighbors of the mother cell. Clearly the configuration changes only along the perimeter of the tumor. (Initially, there is a single cancer cell at the origin.) For $k \to \infty$ one recovers the (B-version of) the Eden model. Note that due to partial reversibility there is a finite probability $(= 1/k)$ for the cluster to ultimately disappear from the lattice.

Based on their computer simulations Williams and Bjerknes originally conjectured the cluster surface to be fractal, which would correspond to an infinite excess perimeter density. This was disproved by Mollison (1972) who showed that the excess perimeter density has a limit which is bounded from above by $(6k + 1)/(k - 1)$. Using results from the equivalent biased voter model, Bramson and Griffeath (1980, 1981) later proved that for $k > 1$ the cluster (provided it survives) attains a well-defined macroscopic shape. Mollison's bound suggests (as do computer simulations) that the excess perimeter density, and thereby the intrinsic surface width, increases without limit as $k \to 1$. The most striking mechanism which contributes to this intrinsic roughening is the creation of islands separate from the original cluster (Williams and Bjerknes 1972). Nothing appears to be known about the way the surface dissolves in the limit $k \to 1$.

All kinds of modified Eden models, including e.g. anisotropic growth rules (Sawada et al. 1982), directed lattices (Chernoutsan and Milošević 1985, Botet 1986) and an off-lattice version (Meakin 1988c) have been introduced in the literature (for a survey see Meakin 1986). As they do not add much to the general picture, we refrain from discussing them here. Likewise we do not consider other theoretical approaches to Eden growth, such as $1/d$ expansions (Parisi and Zhang 1984, Friedberg 1986), Cayley trees (Vannimenus et al. 1984) and field theory (Parisi and Zhang 1985, Cardy 1983), since these methods focus on bulk properties rather than surface fluctuations of clusters.

4.2 SOS models

The major contributions to the intrinsic width in (3.12) – holes, overhangs and high steps – can be eliminated from the outset by using a solid-on-solid (SOS) model with a restriction on the nearest-neighbor height differences. The prototype model in this class is the single step model (Meakin et al. 1986b, Plischke et al. 1987), which we explain here for the one-dimensional case (the two-dimensional model is discussed in Chapter 6).

By definition, SOS-models require the substrate geometry. The surface position at time t above site i of the one dimensional substrate lattice is given by an integer valued height variable $h_t(i)$ which is subject to the single step constraint $|h_t(i+1) - h_t(i)| = 1$. This is satisfied by choosing odd (even) values for $h_t(i)$ on odd (even) sites i. Initially $h_0(i) = 1(0)$ on odd (even) sites. In order to stay within the prescribed set of configurations, growth / evaporation events $h_t(i) \rightarrow h_t(i) + 2$ / $h_t(i) \rightarrow h_t(i) - 2$ occur only at local minima $(h_t(i+1) - 2h_t(i) + h_t(i-1) = 2)$ / local maxima $(h_t(i+1) - 2h_t(i) + h_t(i-1) = -2)$ of the surface. In the continuous time setting we assign the rate $\Gamma_+(\Gamma_-)$ to a growth (evaporation) event. As for the Eden models the growth velocity v is determined by the density of growth sites, i.e. the process is reaction-limited. More precisely, $v = \Gamma_+ \times$(density of local minima) $- \Gamma_- \times$(density of local maxima). Due to a symmetry particular to one dimensional surfaces, the number of local minima is equal to the number of local maxima in every configuration. Using the lattice gas representation to be introduced in Chapter 6 for a general class of SOS-models, one easily finds the growth velocity for a surface of average inclination u,

$$v(u) = \frac{1}{4}(\Gamma_+ - \Gamma_-)(1 - u^2), \quad |u| \leq 1. \tag{4.1}$$

Inclinations $|u| > 1$ clearly cannot occur in a single step configuration. Hence growth shapes can only be discussed in the corner geometry of Chapter 2. Since $v''(u) < 0$, we conclude from Equations (2.8) and (2.9) that a growing corner remains sharp, while a dissolving corner attains a rounded (parabolic) shape (Rost 1981, Marchand and Martin 1986).

A synchronous version of the single step model (with $\Gamma_- = 0$) is obtained

by filling all local surface minima simultaneously (Krug and Spohn 1988). The growth is deterministic and a flat surface remains flat. However the relaxation of an initially rough surface shows interesting scaling properties which will be discussed below in Section 5.4.

Our next example is the polynuclear growth (PNG) model, a classic in the theory of crystal growth (Frank 1974, Gilmer 1980, Goldenfeld 1984). It is a continuous time, off-lattice model which contains both random and deterministic events. Starting from a flat surface, monolayer islands nucleate, at a rate Γ per unit area, at random times and random positions. Once created, an island spreads laterally with constant speed c in all directions until it merges with another island in the same layer. Thus the basic constituents of the PNG model are layers rather than individual particles. Dimensional arguments show that the growth velocity of a d-dimensional horizontal ($u = 0$) surface is (van Saarloos and Gilmer 1986)

$$v(0) \sim (\Gamma c^d)^{1/(d+1)}. \tag{4.2}$$

For comparison with real crystal growth rates the dependence of Γ and c on temperature and chemical potential must be known. Since growth is limited by the density of surface steps (= edges of islands), tilting the surface increases the growth rate, so $v''(u) > 0$. This is confirmed by the exact calculation of $v(u)$ for $d = 1$ in Chapter 6.

A synchronous lattice version of the one dimensional PNG model is obtained as follows (Krug and Spohn 1989). In one unit of time ($t \rightarrow t + 1$) up/down surface steps are shifted one lattice unit to the left/right, and nucleation centers (pairs of up-down steps) are created with probability p at each site. The dynamics of the integer valued height variables $h_t(i)$ can be written as

$$h_{t+1}(i) = \max\{h_t(i-1), h_t(i), h_t(i+1)\} + \delta_t(i), \tag{4.3}$$

where $\delta_t(i) = 1$ resp. 0 with probability p resp. $1 - p$. For small p (4.3) mimics the continuous time model with $\Gamma = p, c = 1$. At $p = p_c = 0.539$ there is a faceting transition analogous to that of the Richardson model (Kertész and Wolf 1989). The transition is supressed if nucleation events which create steps of more than

unit height are discarded. For $p = 0$ (4.3) reduces to a deterministic growth model which is equivalent to the synchronous single step model, cf. Section 5.4.

As our final example we mention the restricted solid-on-solid (RSOS) model (Kim and Kosterlitz 1989). This is a sequential lattice model. A site $\mathbf{x}$ of the d-dimensional substrate lattice is chosen at random and a particle is added $(h_{t+1}(\mathbf{x}) = h_t(\mathbf{x}) + 1)$ *provided* this does not generate nearest neighbor height differences of more than one lattice constant; otherwise no growth takes place and a new site is selected. This simple procedure is surprisingly effective in suppressing corrections to scaling, cf. Section 5.3.

4.3 Ballistic deposition models

The first simulations of ballistic deposition were concerned with the structural properties of random packings of hard spheres. In 1959, Marjorie Vold introduced a model for the sedimentation of moist glass spheres in a nonpolar solvent. Spheres are dropped sequentially above randomly chosen positions of the horizontal substrate, move towards the surface along linear (ballistic) trajectories and stick permanently at the point of first contact with a previously deposited sphere (or the substrate). This procedure generates a chainlike structure of very low density (0.128 volume fraction from a simulation of 155 spheres). Having in mind stacks of ball bearings, Visscher and Bolsterli (1972) simulated a related model in which the dropped sphere is allowed to roll downhill, in contact with previously deposited spheres, until it reaches a three sphere contact which is stable under gravity. The density obtained this way is much higher than for the Vold model (0.58 volume fraction), but significantly lower than the close packed h.c.p. density (0.74 volume fraction). A sequential off-lattice model intermediate between these two was employed by Henderson et al. (1974) in their study of structural anisotropy and void formation in vapor deposited thin films. In this model, a deposited sphere comes to rest at its first three sphere contact, irrespective of whether it is stable or not. Large-scale simulations of all three models have been performed recently by Jullien and Meakin (1987).

The reader will have inferred from our description that ballistic deposition is

not strictly local, since protruding parts of the surface can shadow others from the incoming flux. Nevertheless the *accessible (active)* surface of the deposit has a local dynamics. To see this we consider a two dimensional square lattice version of the Vold model (Family and Vicsek 1985, Meakin et al. 1986b). The one dimensional substrate is oriented along the x-axis of the lattice and particles move in the y-direction along randomly chosen lattice columns, sticking permanently at the first perimeter site (as defined above in the context of Eden models) they encounter. Denoting by $h_t(i)$ the maximum y-coordinate for any of the occupied sites in column i, this height variable evolves upon deposition in column i according to the local rule

$$h_{t+1}(i) = \max\{h_t(i-1), h_t(i)+1, h_t(i+1)\}. \qquad (4.4)$$

A detailed numerical investigation of the surface configurations generated by (4.4) shows that the nearest neighbor height differences have an exponential distribution with mean $\langle|h_t(i+1) - h_t(i)|\rangle \simeq 1.136$ for $t \to \infty$ (Meakin et al. 1986b). Hence, although the bulk of the deposit is highly porous (Figure 7), with a density $\rho_0 \simeq 0.4684$, the accessible surface is well defined and has a rather small intrinsic width. The *internal* surface (the set of all perimeter sites) is much larger and scales like the deposit mass.

In the lattice model (4.4) there is always exactly one growth site per lattice column. Unlike the reaction-limited models discussed above, the density of growth sites is independent of surface inclination. To see how the inclination dependent growth velocity $v(u)$ arises in this case, we consider a general ballistic deposition process and fix the coordinate system such that the particles fall along the vertical (negative h-) direction. The deposit mass per horizontally projected substrate area increases at a constant rate J which is equal to the mass flux through a unit area perpendicular to the particle trajectories. The deposit thickness is related to its mass through the density ρ, hence

$$v(u) = J/\rho(u). \qquad (4.5)$$

Any variation of the growth velocity with surface inclination is therefore due to a corresponding variation of the deposit density (Krug 1989a). In general,

500 LATTICE UNITS
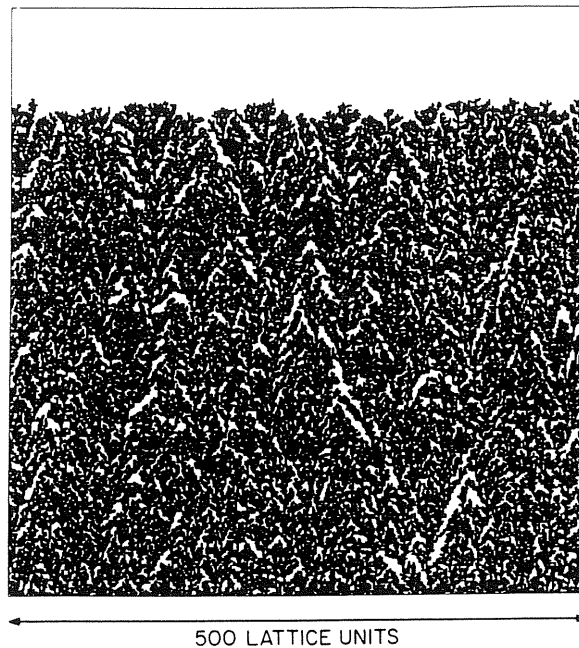
Figure 7: Square lattice simulation of ballistic deposition at normal incidence. Courtesy of P. Meakin.

depostion onto an inclined substrate (or equivalently depostion at oblique particle incidence) increases the porosity and lowers the density of the deposit, thereby leading to a (quadratic) minimum in $v(u)$ at $u = 0$. Clearly this effect is absent in models which presuppose an ordered (crystalline) deposit structure and thus, do not allow for voids and defects. In such cases (4.5) implies that v is independent of u. An example is the surface diffusion model studied by Family (1986) and by Liu and Plischke (1988).

These considerations shed some light on recent simulations of a lattice version of the Visscher-Bolsterli model (Meakin and Jullien 1987, Jullien and Meakin 1987). Since an exact implementation of the deposition rules for this model leads to a regular close packed deposit structure, one might think that the introduction of a lattice makes no difference. However, in off-lattice simulations or experiments the regular packing is never realized, because any amount of fluctuations leads to a defective structure of lower density which presumably shows a nontrivial $\rho(u)$ dependence (Figure 8). As the nonlinearity of $v(u)$ determines the scaling properties of the shape fluctuations (cf. Chapter 5), it follows that these are

100 DIAMETERS
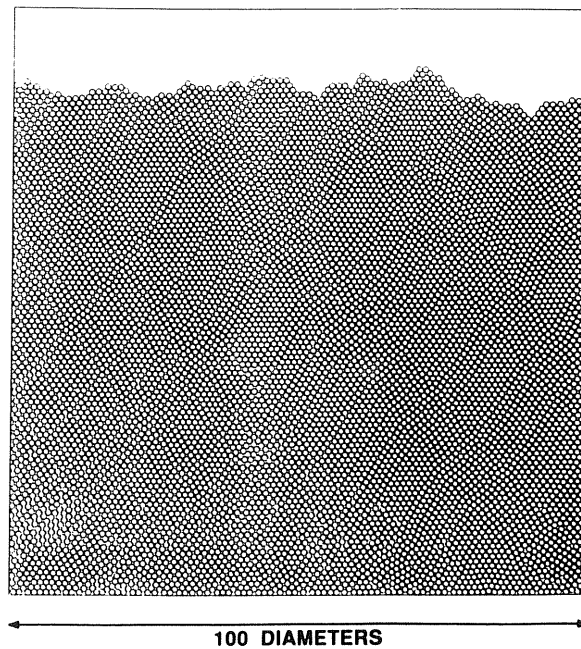
Figure 8: Off-lattice ballistic deposition with relaxation in two dimensions. Discs are dropped at random. From its first point of contact a disc rolls downhill until it reaches a position locally stable under gravity. Courtesy of P. Meakin.

different for the lattice- and off-lattice versions of the Visscher-Bolsterli model, the reason being a difference in the *bulk* structure (Krug 1989a).

For the Vold model and its variants the deposit density $\rho(u)$ vanishes in the limit of grazing particle incidence, $u \to \infty$ (Meakin and Jullien 1987, Jullien and Meakin 1987, Krug and Meakin 1989). This is due to the formation of a macroscopic network of voids which separate the columns of the 'columnar' deposit microstructure (Figure 9). As a consequence the accessible deposit surface acquires macroscopic discontinuities which can be viewed as a divergent contribution to the intrinsic surface width.

While the scaling properties of the columnar microstructure have only recently been elucidated (Krug and Meakin 1989, Meakin and Krug 1990), its structural features have received much attention both from the experimental and the theoretical side (Leamy et al. 1980). Looking at Figure 9, an immediate question concerns the relationship between the column orientation and the angle of particle incidence. In our geometry the orientation of the columns and of the

33

$\theta = 87.5°$

2000 LATTICE UNITS
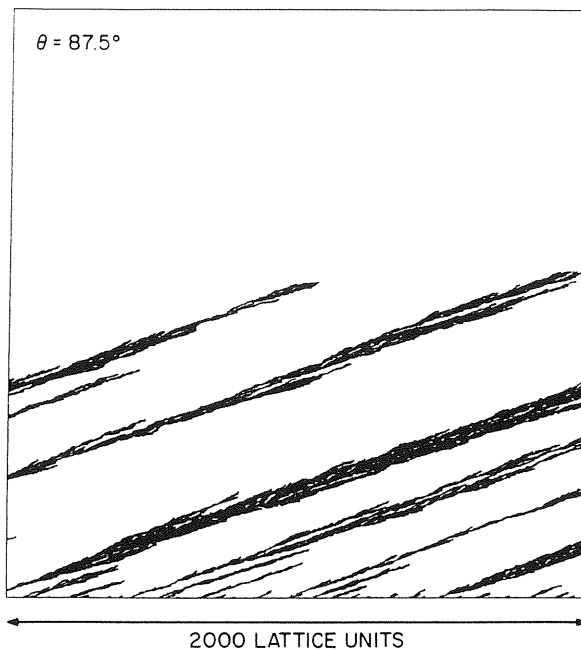
Figure 9: Off-lattice ballistic deposition at near-grazing incidence in two dimensions. The substrate is horizontal. Particles enter from the right along randomly chosen linear trajectories which form an angle $\theta = 87.5°$ with the substrate normal. Courtesy of P. Meakin.

substrate normal relative to the direction of incidence are measured by the angles ϑ and φ, respectively, which were introduced in Chapter 2. For some time φ and ϑ were believed to be related by the empirical 'tangent rule' (Nieuwenhuizen and Haanstra 1966)

$$\tan(\vartheta - \varphi) = \frac{1}{2}\tan\vartheta. \tag{4.6}$$

This is ruled out however by the general considerations of Chapter 2, since it would imply a nonmonotonic dependence of φ on ϑ. Indeed (4.6) has been refuted by large scale simulations of various deposition models (Meakin et al. 1986b, Meakin 1988d). One finds instead a monotonic increase of $\varphi(\vartheta)$ which appears to saturate at a constant value $\varphi_{\max}$ for $\vartheta \to \pi/2$ (near-grazing incidence). This is expected to be characteristic of columnar growth, since simple arguments show that the growth velocity of a column structure is a *linear* function of inclination, as in (2.14), with $a = \cotan\varphi$ and $v_\perp = 1$ (1/2) for the lattice (off-lattice) version

34

OFF-LATTICE
$S = 2.5 \times 10^5$

← 1400 DIAMETERS →
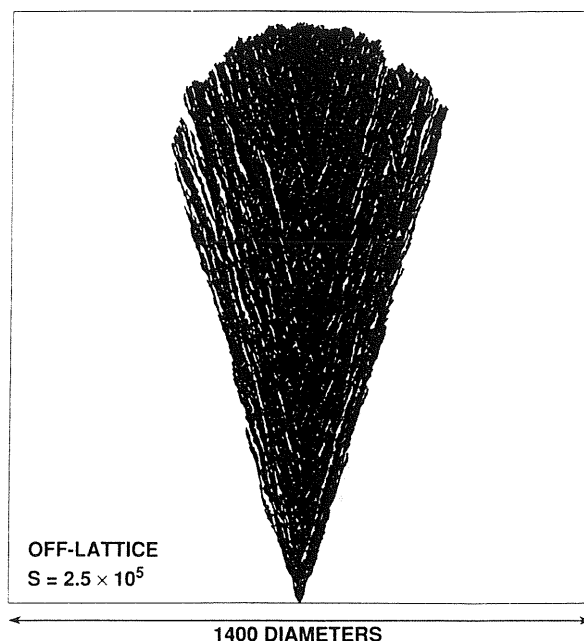
Figure 10: Cluster grown by off-lattice ballistic deposition onto a point seed. Particles rain down vertically. Courtesy of P. Meakin.

of the two dimensional Vold model (Krug and Meakin 1989, Limaye and Amritkar 1986). The theory of Chapter 2 then predicts that $\varphi = \varphi_{max}$ independent of ϑ.

Clusters can be grown through ballistic deposition by exposing a point seed to the unidirectional particle flux (Bensimon et al. 1984a, Liang and Kadanoff 1985). (Note that this is different from the ballistic aggregation model also due to Vold (1963), in which the particle trajectories have *random* orientations.) The shadowing effects lead to a fan-shaped cluster with a domed upper surface (Figure 10). The upper surface is related to the nonlinear part of $v(u)$, while the opening angle is determined by the asymptotically linear behavior (2.14), cf. Chapter 2. The opening angle is $2\varphi_{max}$ as would be expected intuitively.

An interesting shape transition occurs in the synchronous version of the Vold lattice model, in which the growth rule (4.4) is applied simultaneously to a finite fraction p of sites (Baiod et al. 1988). At the threshold value p_c ($p_c \simeq 0.7058$ in two dimensions) facets appear at the corners of the fan and spread towards the top as $p \to 1$. At the same time the opening angle of the fan increases according to $\varphi_{max}(p) = \arctan[p/(1-p)]$ (Krug and Meakin 1990). The origin of the transition

is the same as for the other synchronous models discussed previously, and will be explained in Chapter 7.

Several modifications of ballistic deposition have been introduced, including e.g. spatial correlations in the particle flux (Meakin and Jullien 1989,1990), particle diffusion superimposing the ballistic motion (Meakin 1983, Jullien et al. 1984, Nadal et al. 1984), and a finite density of depositing particles (Jullien and Meakin 1989). Long range correlations in the particle flux modify the surface scaling properties in a highly nontrivial way (Medina et al. 1989). A ballistic deposition model on the Cayley can be solved exactly (Bradley and Strenski 1985, Krug 1988). One finds surface fluctuations of order unity, i.e. $\zeta = 0$.

4.4   Low temperature Ising dynamics

The growth processes of interest here describe also the interface dynamics of a low temperature Ising model without conservation law. We consider a square lattice (extension to higher dimensions is obvious) with a spin $\sigma_\mathbf{x} = \pm 1$ at each lattice site $\mathbf{x} = (i,j)$. The spins interact through a ferromagnetic nearest neighbor coupling $J > 0$ and are subject to an external field $\mu > 0$ which prefers the $+$ phase. The energy of a configuration $\sigma = \{\sigma_\mathbf{x} \mid \mathbf{x} \in \mathbb{Z}^2\}$ is

$$H(\sigma) = -J \sum_{\langle \mathbf{xy} \rangle} \sigma_\mathbf{x} \sigma_\mathbf{y} - \mu \sum_\mathbf{x} \sigma_\mathbf{x} \tag{4.7}$$

where the first sum is over pairs $\langle \mathbf{xy} \rangle$ of nearest neighbors. The configurations evolve through single spin flips which occur according to the Metropolis rates,

$$\Gamma(\sigma \to \sigma^{(\mathbf{x})}) = \Gamma_0 \phi(\beta(H(\sigma^{(\mathbf{x})}) - H(\sigma))), \tag{4.8}$$
$$\phi(\lambda) = \min(1, e^{-\lambda}),$$

where $\sigma^{(\mathbf{x})}$ denotes the configuration σ with the spin at site $\mathbf{x}$ flipped, and $\beta = 1/k_B T$ is the inverse temperature. We choose a temperature below the critical temperature and prepare an initial configuration with a flat interface.

The Ising dynamics differs from other growth dynamics in one important respect. By random events deep inside the bulk of the unstable $-$ phase $+$ droplets of sufficient size may nucleate and start to grow themselves. Once there

36

is a finite density of such droplets, the interface looses its geometrical meaning. These considerations determine the time scale over which our theory is applicable to Ising interfaces. It depends strongly on the temperature and the external field.

To understand the equivalence with growth processes we orient the initial configuration with an interface along the $(1, -1)$ direction, i.e. $\sigma_{ij} = 1$ for $i + j \leq 1$ and $\sigma_{ij} = -1$ for $i + j > 1$. In the limit of zero temperature $(\beta \to \infty)$ and if the field is not too strong $(0 < \mu < 2J)$ the only allowed processes are those in which a $-$ spin with two $-$ and two $+$ neighbors flips at rate Γ_0. The interface advances into the unstable phase while remaining single valued with respect to the line $i + j = 0$, and on average parallel to the $(1, -1)$ direction. We introduce a coordinate system relative to the lines $i + j = 0$ and $i - j = 0$, $(k, m) = (i - j, i + j)$, and define the position $h(k)$ of the interface above point k by

$$h(k) = \max_{(i,j)}\{i + j \mid \sigma_{ij} = 1, i - j = k\}. \tag{4.9}$$

Then by construction $|h(k+1) - h(k)| = 1$ and when the spin at $(i, j) = \frac{1}{2}(h(k) + k, h(k) - k)$ flips, $h(k)$ increases by 2. The interface evolves according to the growth rule of the single step model with $\Gamma_+ = \Gamma_0$ and $\Gamma_- = 0$ (Marchand and Martin 1986). A partly reversible dynamics $(\Gamma_- > 0)$ is obtained by letting $\mu \to 0$ as $\beta \to \infty$ such that $\beta\mu = \text{const.} > 0$. The reversible case $(\mu = 0)$ is discussed by Kandel and Domany (1990).

Similar considerations apply to an interface initially oriented along the $(1, 0)$ direction. In order to have anything at all happening at zero temperature, we must choose the field $\mu > 2J$. On the other hand the suppression of droplet formation in the $-$ phase requires $\mu < 4J$. Taking $2J < \mu < 4J$ and $\beta \to \infty$ the only allowed spin flips are those of a $-$ spin which has at least one $+$ neighbor. Since all allowed processes occur at equal rate Γ_0, we recover the continuous time (version A) Eden model.

Although the exact equivalence holds only in the limiting cases discussed, we expect that the interface fluctuations of a kinetic Ising model are governed by our theory, provided $\mu \neq 0$ and times are so short that droplet formation in the bulk can be neglected.

5 Continuum Theory

5.1 The Kardar-Parisi-Zhang equation

Our starting point is the time evolution of the macroscopic height profile as governed by

$$\frac{\partial}{\partial t} h_t = v(\nabla h_t), \tag{5.1}$$

compare with Chapter 2. v is the growth velocity in the h-direction. We assume that v depends smoothly on ∇h_t. In fact, this assumption may be violated. (An example will be given in Section 7.2.) But in general this will happen only at isolated values in parameter space.

In the spirit of the scaling theory developed in Chapter 3 we assume now that (5.1) remains valid even on finer scales. On a finer scale we will see more details, in particular random increases in the surface height and local smoothening. Using a conventional description of both processes we obtain the equation

$$\frac{\partial}{\partial t} h_t = v(\nabla h_t) + \nu \Delta h_t + \zeta_t. \tag{5.2}$$

Since growth events occur independently when separated in space-time, the noise ζ_t is chosen to be Gaussian white noise with mean zero and covariance

$$\langle \zeta_t(\mathbf{x}) \zeta_{t'}(\mathbf{x}') \rangle = \gamma \delta(t - t') \delta(\mathbf{x} - \mathbf{x}'). \tag{5.3}$$

Note that we really have defined a *new* growth model. ν can be thought of as an effective surface tension. Physically the relaxation term $\nu \Delta h_t$ may arise through evaporation-condensation processes (Mullins 1959) or as a consequence of gravity induced restructuring (Edwards and Wilkinson 1982). On the basis of Equation (5.2), at least in principle, an effective inclination dependent growth velocity, $v_{\text{eff}}(\nabla h)$, may be computed which determines then the macroscopic shape according to the rules explained in Chapter 2. Of course, because of noise, in general v_{eff} will be different from the 'bare' growth velocity v.

We expect that the large scale behavior of the growth model (5.2) is again governed by our scaling theory. If the large scale properties of growing surfaces are universal, then we may as well rely for their prediction on Equation (5.2). As a

common experience in statistical physics, for continuum models more and better developed techniques are available. Thus a continuum growth model may be of advantage. We loose thereby the precise specification of the microscopic processes of adhesion and relaxation. But the real physics is anyhow more complicated than our simplified microscopic models. If only for this reason, we have to concentrate on those properties which are independent of microscopic details (of course within the class of local growth rules).

From our remarks it is clear that it makes no sense to 'derive' (5.2) from a microscopic model. It would not add to the credibility of this equation. A notable exception is the Ginzburg-Landau model A at low temperatures. In this case h_t is the position of the interface between the $+$ and $-$ phase. Its surface free energy is

$$H_0 = \sigma \int d^d x (1 + (\nabla h_t)^2)^{1/2} \tag{5.4}$$

with σ an effective surface tension (Buff et al. 1965, Diehl et al. 1980). As usual, H_0 acts as a potential for the dynamics. Keeping in mind our particular choice of the coordinate system we obtain

$$\frac{\partial}{\partial t} h_t = -L_0 (1 + (\nabla h_t)^2)^{1/2} (\delta H_0 / \delta h_t) + L_0^{1/2} (1 + (\nabla h_t)^2)^{1/4} \zeta_t, \tag{5.5}$$

where L_0 is a kinetic coefficient and the noise strength follows from detailed balance (Bausch et al. 1981, Kawasaki and Ohta 1982). Now under an applied external field μ, the system can gain energy by translating the interface into the unstable phase. Then H_0 is changed to the total energy

$$H = H_0 - \mu \int d^d x h_t(\mathbf{x}) \tag{5.6}$$

and the equation of motion becomes

$$\begin{aligned}
\frac{\partial}{\partial t} h_t &= L_0 \sigma \Delta h_t - L_0 \sigma (1 + (\nabla h_t)^2)^{-1} \sum_{i,j=1}^{d} (\partial h_t / \partial x_i)(\partial^2 h_t / \partial x_i \partial x_j)(\partial h_t / \partial x_j) \\
&\quad + L_0 \mu (1 + (\nabla h_t)^2)^{1/2} + L_0^{1/2} (1 + (\nabla h_t)^2)^{1/4} \zeta_t, \tag{5.7}
\end{aligned}$$

which is of the form (5.2) with $v(\nabla h) = L_0 \mu \sqrt{1 + (\nabla h)^2}$ corresponding to isotropic growth.

39

We proceed with the analysis of Equation (5.2) in order to see what it can teach us about growth. We are interested in shape fluctuations around a surface which is flat on the average. The surface gradients are then small and it is natural to expand $v(\nabla h_t)$. As we will show below terms of third and higher order are irrelevant for the large scale behavior. Therefore it suffices to consider

$$\frac{\partial}{\partial t} h_t = v(\mathbf{0}) + \nabla v'(\mathbf{0}) \cdot \nabla h_t + \frac{1}{2} \nabla h_t \cdot \nabla \nabla v(\mathbf{0}) \cdot \nabla h_t + \nu \Delta h_t + \zeta_t. \qquad (5.8)$$

$v(\mathbf{0})$ and $\nabla v(\mathbf{0})$ can be absorbed through the Galilei transformation

$$\tilde{h}_t(\mathbf{x}) = h_t(\mathbf{x} - \nabla v(\mathbf{0})t) - v(\mathbf{0})t. \qquad (5.9)$$

For simplicity we assume isotropy in the sense that $\partial^2 v / \partial u_i \partial u_j = \lambda \delta_{ij}$. Denoting $\tilde{h}_t$ again by h_t we arrive at the KPZ equation (Kardar, Parisi and Zhang 1986)

$$\frac{\partial}{\partial t} h_t = \frac{1}{2} \lambda (\nabla h_t)^2 + \nu \Delta h_t + \zeta_t. \qquad (5.10)$$

The equation has the three parameters λ, ν and γ. λ is the strength of the nonlinearity. We record that

$$\lambda = \frac{1}{d} \Delta v(\mathbf{0}). \qquad (5.11)$$

5.1.1 Linear theory

In some of the microscopic models discussed in Chapter 4 v is independent of ∇h_t and therefore $\lambda = 0$. Thus the linear theory will govern the large scale behavior. Since linear, the details are worked out easily. Of particular interest is the stationary two-point function. For $d = 1, 2$ only the height differences become stationary with the result

$$\langle (h_t(\mathbf{x}) - h_t(\mathbf{x}'))(h_s(\mathbf{x}) - h_s(\mathbf{x}')) \rangle = (2\pi)^{-d} \int d^d k (1 - e^{i \mathbf{k} \cdot (\mathbf{x} - \mathbf{x}')}) \frac{\gamma}{2\nu} \frac{1}{k^2} e^{-\nu k^2 |t-s|}. \qquad (5.12)$$

For $d \geq 3$ the surface is smooth with correlations

$$\langle h_t(\mathbf{x}) h_s(\mathbf{x}') \rangle = (2\pi)^{-d} \int d^d k \, e^{i \mathbf{k} \cdot (\mathbf{x} - \mathbf{x}')} \frac{\gamma}{2\nu} \frac{1}{k^2} e^{-\nu k^2 |t-s|}. \qquad (5.13)$$

Independent of dimension the dynamical exponent is

$$z = 2. \qquad (5.14)$$

40

For $d=1$ $h_t(x)$ is a random walk with respect to x, i.e. $\langle(h_t(x)-h_t(x'))^2\rangle = \frac{\gamma}{2\nu}|x-x'|$. For $d=2$ there are logarithmic fluctuations, whereas for $d \geq 3$ the static correlations decay as $\langle h_t(\mathbf{x})h_t(\mathbf{x}')\rangle \sim |\mathbf{x}-\mathbf{x}'|^{-(d-2)}$. We summarize this behavior by the wandering exponent

$$\zeta = (2-d)/2. \tag{5.15}$$

5.1.2 Scaling

Henceforth we assume $\lambda > 0$ (if $\lambda < 0$, then we change h_t to $-h_t$). We look for a statistically self-similar solution to (5.10). Therefore we define the rescaled surface

$$\tilde{h}_t(\mathbf{x}) = b^{-\zeta}h_{b^z t}(b\mathbf{x}), \tag{5.16}$$

b large, and insert in (5.10) to obtain the following equation for $\tilde{h}_t$,

$$\frac{\partial}{\partial t}\tilde{h}_t = b^{(\zeta+z-2)}\frac{1}{2}\lambda(\nabla\tilde{h}_t)^2 + b^{(z-2)}\nu\Delta\tilde{h}_t + b^{(z-2\zeta-d)/2}\zeta_t. \tag{5.17}$$

Here we used the scale invariance

$$\zeta_{b^z t}(b\mathbf{x}) = b^{-(z+d)/2}\zeta_t(\mathbf{x}) \tag{5.18}$$

which follows from (5.3).

If $\zeta > 0$, then the first term dominates as $b \to \infty$. To ensure scale invariance we have to set

$$\zeta + z = 2. \tag{5.19}$$

Thus we recovered the scaling relation (3.18). Note that higher orders in the expansion of $v(\nabla h_t)$, like $(\nabla h_t)^3$, are irrelevant compared to the second order term. For $b \to \infty$ the diffusion and noise term vanish. Nevertheless they are needed to single out the invariant distribution of physical relevance.

If $\zeta < 0$ the nonlinearity is irrelevant. z and ζ are then given by the linear theory, cf. Equations (5.14) and (5.15). At this point we have no tool for computing ζ. Taking the ζ of the linear theory suggests that in dimensions $d > 2$, at least for small λ, the nonlinearity is of no importance.

41

5.1.3 1+1 dimensions, noisy Burgers equation

In $1 + 1$ dimensions the height differences, $h_t(x') - h_t(x)$, become stationary as $t \to \infty$. Writing them as $\int_x^{x'} dy \frac{\partial}{\partial y} h_t(y)$ we may as well consider the surface slope $u_t = \partial h_t / \partial x$. If h_t is governed by the KPZ equation, then u_t satisfies

$$\frac{\partial}{\partial t} u_t = \frac{\partial}{\partial x} [\frac{1}{2} \lambda u_t^2 + \zeta_t + \nu \frac{\partial}{\partial x} u_t], \tag{5.20}$$

which is the noise driven Burgers equation (Burgers 1974). (Burgers equation has $\lambda = -1$, which can be achieved through substituting u_t by $-\frac{1}{\lambda} \tilde{u}_t$.) For Burgers u_t is the velocity field of a one dimensional fluid. Equation (5.20) is then the Navier-Stokes equation with random forcing. Burgers investigated in great detail the deterministic equation ($\zeta_t \equiv 0$) with random initial data (cf. Section 5.4).

Since u_t is locally conserved we are free to still fix its average value, which is taken $\langle u_t \rangle = 0$ by our choice of initial data. Noise and diffusion alone (i.e. Equation (5.20) with $\lambda = 0$) determine then a unique invariant distribution. It is the Gaussian white noise with covariance

$$\langle u_t(x) u_t(x') \rangle = (\gamma / 2\nu) \delta(x - x'). \tag{5.21}$$

It so happens that this measure is also invariant under the flow generated by the solutions of

$$\partial u_t / \partial t = (\lambda / 2) \partial u_t^2 / \partial x. \tag{5.22}$$

(Forster et al. 1977, Huse et al. 1985). To prove it we consider an interval of length L with periodic boundary conditions. Formally, the right side of Equation (5.22) is divergence free, since

$$\int_0^L dx \frac{\partial}{\partial x} u_t(x) = 0 \tag{5.23}$$

because of periodic boundary conditions. Therefore we only have to check the time invariance of the density

$$\exp \left[-\frac{\nu}{\gamma} \int_0^L dx u_t(x)^2 \right]. \tag{5.24}$$

Differentiating in time yields

$$- (\lambda \nu / 2\gamma) \left[\int_0^L dx u_t(x) \frac{\partial}{\partial x} u_t(x)^2 \right] \exp \left[-\frac{\nu}{\gamma} \int_0^L dx u_t(x)^2 \right]. \tag{5.25}$$

By partial integration the prefactor vanishes. Note that in higher dimensions the prefactor is $\int d^d x \mathbf{u}_t(\mathbf{x})(\mathbf{u}_t(\mathbf{x}) \cdot \nabla)\mathbf{u}_t(\mathbf{x})$ which does not vanish, in general.

The stationarity of white noise is a little bit of a surprise because a profile $u_t(x)$ which is smooth initially converges as $t \to \infty$ to a constant profile. Profiles typical for white noise are fairly rough and may not settle down as $t \to \infty$. These considerations provoke the question of how well defined Equation (5.20) is mathematically. Of course, physically a short distance cutoff should be introduced. If one discretizes Equation (5.20) as

$$
\begin{aligned}
\frac{d}{dt}u_t(j) = {} & (\lambda/6)(u_t(j+1)(u_t(j)+u_t(j+1)) - u_t(j-1)(u_t(j-1)+u_t(j))) \\
& + \nu(u_t(j+1) - 2u_t(j) + u_t(j-1)) + \zeta_t(j),
\end{aligned} \tag{5.26}
$$

then in the steady state the $u_t(j)$'s are distributed as independent Gaussians with variance $\gamma/2\nu$ (Nieuwenhuizen 1989). Also, as will be discussed in Chapter 6, for several lattice growth models the stationary distribution can be computed explicitly. For it the slopes are independent at large separation. These results strengthen our trust in (5.21).

We conclude that for the stationary growth process

$$
\langle (h_t(x) - h_t(x'))^2 \rangle = (\gamma/2\nu)|x - x'|. \tag{5.27}
$$

Therefore

$$
\zeta = 1/2 \text{ and } z = 3/2. \tag{5.28}
$$

Our argument gives no handle on the scaling function. Renormalization (Janssen and Schmittmann 1986) shows that there is a universal function, g, such that

$$
\int dx\, e^{ikx} \langle u_t(x)u_0(0)\rangle = \frac{\gamma}{2\nu}g((\lambda^2\gamma/2\nu)^{1/3}k|t|^{2/3}) \tag{5.29}
$$

for small k and large t, average in the stationary measure (5.21). The scaling function g is not known explicitly. By symmetry $g(x) = g(-x)$ and $g'(0) = 0$. Janssen and Schmittmann (1986) have computed $g(x)$ for small x and find $g''(0) \simeq -4.5$. Approximations suggest that g decays as $\exp(-c|x|^{3/2})$ for large x (van Beijeren et al. 1985, Yakhot and She 1988, Zaleski 1989). The crucial point in (5.29) is that only macroscopic parameters of the growth model appear: λ

43

is determined by the growth velocity, compare with (5.11), and $\gamma/2\nu$ measures the strength of the static fluctuations. The scaling form (5.29) governs the large scale behavior of any two dimensional growth process (provided the growth rules are sufficiently local and $\lambda \neq 0$, cf. Equation (5.11)).

Since with some luck we have guessed the stationary measure, the effective growth velocity $v_{\text{eff}}(\nabla h)$ can be computed (we refer to the discussion below Equation (5.3)). Actually, the Gaussian (5.24) is the steady state for any bare growth velocity $v(\nabla h)$. Then, on the basis of (5.20) with $(\lambda/2)u_t^2$ replaced by $v(u_t)$, the effective growth velocity is given by

$$v_{\text{eff}}(\nabla h) = \int du (\nu/\pi\gamma)^{1/2} e^{-\nu u^2/\gamma} v(\nabla h + u). \tag{5.30}$$

5.1.4 Renormalization

The method of dynamic renormalization has been applied to the noise driven Burgers equation by Forster, Nelson and Stephen (1977). Without alteration their results carry over to the KPZ equation (see Kardar et al. 1986, Medina et al. 1989). We rewrite this equation in terms of the height Fourier coefficients. They satisfy the integral equation

$$\hat{h}_t(\mathbf{k}) = e^{-\nu k^2 t}\hat{h}_0(\mathbf{k}) + \int_0^t ds\, e^{-\nu k^2(t-s)}$$
$$\left[\hat{\zeta}_s(\mathbf{k}) - \frac{\lambda}{2}(2\pi)^{-d} \int d^d q\ \mathbf{q}\cdot(\mathbf{k}-\mathbf{q})\hat{h}_s(\mathbf{k}-\mathbf{q})\hat{h}_s(\mathbf{q})\right]. \tag{5.31}$$

Equation (5.31) is solved perturbatively. The first terms in the perturbation expansion for $\langle \hat{h}_t(\mathbf{k})\hat{h}_t(-\mathbf{k})\rangle$ diverge for $d < 2$. The perturbation series is then reorganized into a renormalization by integrating out only the modes in the shell $e^{-l}\Lambda \leq |\mathbf{k}| \leq \Lambda$. Wave vector and time are rescaled as $\mathbf{k}' = e^l \mathbf{k}, t' = e^{zl}t$ and the remaining height modes as $\hat{h}'_{t'}(\mathbf{k}') = e^{-(d+\zeta)l}\hat{h}_t(\mathbf{k})$. The rescaled Fourier coefficients obey then, in approximation, again (5.31) provided the coefficients ν, λ and γ are adjusted according to the flow equations

$$\frac{d}{dl}\nu = [z - 2 + A_d \frac{2-d}{4d}\bar{\lambda}^2]\nu,$$

44

$$\frac{d}{dl}\gamma = [z - d - 2\zeta + A_d \frac{\overline{\lambda}^2}{4}]\gamma, \tag{5.32}$$

$$\frac{d}{dl}\lambda = [z + \zeta - 2]\lambda$$

with $A_d = (2^{d-1}\pi^{d/2}\Gamma(d/2))^{-1}$ and $\overline{\lambda}^2 = \lambda^2\gamma/2\nu^3$. For $A_d = 0$ (5.32) just expresses the scaling already found in (5.17). The terms proportional to A_d are the result of a first order expansion in $\overline{\lambda}$.

To discuss the renormalization group flow (5.32) z and ζ are adjusted such that $d\nu/dl = 0 = d\gamma/dl$. The effective coupling constant evolves then according to

$$\frac{d}{dl}\overline{\lambda} = \frac{2-d}{2}\overline{\lambda} + A_d\frac{2d-3}{4d}\overline{\lambda}^3. \tag{5.33}$$

Since obtained in an expansion around $\overline{\lambda} = 0$, we can trust (5.33) only for small $\overline{\lambda}$. For $d < 2$ the fixed point $\overline{\lambda} = 0$ is repulsive. Thus the large scale behavior is governed by the nonlinearity $(\nabla h_t)^2$ and $\overline{\lambda}$ should flow to a strong coupling fixed point. On the other hand for $d > 2$ $\overline{\lambda} = 0$ is an attractive fixed point. There is a weak coupling regime where the nonlinearity is irrelevant. The large scale behavior is governed by the linear theory.

These findings agree with the scaling analysis in (5.17). Equation (5.33) has a strong coupling fixed point but only for $0 < d < 3/2$. It predicts $z = (8 - 4d - d^2)/2(3-2d)$ and $\zeta = (d-2)^2/2(3-2d)$ satisfying $z + \zeta = 2$. ζ increases for $d > 1$ and ζ becomes even larger than one for $d > 1.415$, both unphysical results. For dimension one the exact exponents $\zeta = 1/2$, $z = 3/2$ are reproduced. Dimension $d = 0$ corresponds to a single growing column. Its height fluctuations increase as $\sqrt{t}$, i.e. $\zeta/z = 1/2$ and $\zeta = 2/3$, $z = 4/3$. This is also reproduced correctly by (5.33). For $d > 2$ a separatrix emerges. Above it $\overline{\lambda}$ flows to infinity, below to zero. This suggests that for $d > 2$ there is a weak and strong coupling regime. In the strong coupling regime the nonlinearity dominates. At this stage we cannot understand the mechanism causing the transition. We will return to this point once we achieved the mapping to the directed polymer. The harvest from the renormalization is fairly meager. In particular no tool is offered which would allow the computation of either the dynamic or the static exponent.

45

5.2 Directed polymer representation

Hopf (1950) and Cole (1951) observed that the Burgers equation can be mapped to a linear diffusion equation. The Hopf-Cole transformation extends to the KPZ equation in arbitrary dimension. The price to be paid is that additive noise is turned into multiplicative noise. We gain however a rather different perspective. Surprisingly enough the physics of disordered systems in thermal equilibrium enter the play.

We define

$$Z_t(\mathbf{x}) = \exp\left[-\frac{\lambda}{2\nu}h_t(\mathbf{x})\right]. \tag{5.34}$$

Then $Z_t(\mathbf{x})$ is governed by the 'diffusion' equation

$$\frac{\partial}{\partial t}Z_t = -(-\nu\Delta + \frac{\lambda}{2\nu}\zeta_t)Z_t. \tag{5.35}$$

(Note that $\int d^d x\, Z_t(\mathbf{x})$ is not conserved.) We may think of (5.35) also as an imaginary time Schrödinger equation. $\zeta_t(\mathbf{x})$ is then a space-time random potential. Through the Feynman-Kac formula the solution to (5.35) can be written in the form of the path integral

$$Z_t(\mathbf{x}) = \int_{\substack{\mathbf{y}(0)=\mathbf{0}\\ \mathbf{y}(t)=\mathbf{x}}} \mathcal{D}\mathbf{y}(\cdot)\exp\left[-\frac{1}{2\nu}\int_0^t ds\frac{1}{2}\dot{\mathbf{y}}(s)^2\right]\exp\left[-\frac{1}{2\nu}\int_0^t ds\lambda\zeta_s(\mathbf{y}(s))\right]. \tag{5.36}$$

We have split up the path integral into two factors. The first one is the 'free' (unperturbed) part. It is Brownian motion starting at the origin ending at $\mathbf{x}$ at time t, normalized to one when being integrated over all final points. A Brownian path, $\mathbf{y}(t)$, is then weighted with the exponential of an 'energy', which is given simply by summing the 'potential' $\zeta_t(\mathbf{x})$ along the path. Note that $Z_t(\mathbf{x})$ is random, because $\zeta_t(\mathbf{x})$ is.

The following physical interpretation is suggestive: $Z_t(\mathbf{x})$ is the partition function of a polymer chain in $d+1$ dimensions with length t and constrained endpoints. The chain is directed (no U–turn in time) and sits in an external random potential. 2ν plays the role of temperature. By (5.34) the height is the free energy, in particular the average height is

$$\langle h_t(\mathbf{x})\rangle = -\frac{2\nu}{\lambda}\langle \log Z_t(\mathbf{x})\rangle. \tag{5.37}$$

Thus our interest is quenched disorder (as in spin glasses).

The statistical mechanics problem (5.36) can be posed also in discrete form. To illustrate the method we present one example for simplicity in $1 + 1$ dimension. We choose the square lattice $\mathbb{Z}^2$ and label the horizontal axis by $t = 0, 1, \ldots$ and the vertical axis by $x = 0, \pm 1, \ldots$ A walk (polymer) is a sequence of connected bonds in $\mathbb{Z}^2$. Admissible walks are directed and make at most one step, i.e. $y(t+1) - y(t) = 0, \pm 1$. (These walks are just the restricted SOS interface configurations of a two dimensional Ising model at low temperatures.) To each bond of the lattice we associate a potential energy. The vertical bonds have the energy V_0. The horizontal bonds, b, have a random energy V_b. The V_b's are independent and have identical distribution. To each walk we assign the energy $E(y(\cdot)) = \sum$ energies along the walk $y(s), 0 \leq s \leq t$.

Our discrete version of (5.36) reads then

$$Z_t(x) = \sum_{\substack{\text{admissible} y(\cdot) \\ y(0)=0, y(t)=x}} e^{-\beta E(y(\cdot))} \tag{5.38}$$

with β the inverse temperature, $\beta > 0$. We have to distinguish now between the thermal average corresponding to (5.38), denoted by $\mathbb{E}$ (expectation), and the disorder average, denoted by $\langle \cdot \rangle$ as before. There are two control parameters. βV_0 regulates the diffusion coefficient of the free walk: for $V_b \equiv 0$ one has

$$\mathbb{E}(y(t)^2) = \sum_x x^2 Z_t(x) / \sum_x Z_t(x) = (\frac{1}{2} e^{\beta V_0} + 1)^{-1} t. \tag{5.39}$$

β controls the strength of the random potential. For large β a walk tries to minimize its energy by taking advantage of deep potential minima. This is counteracted by the entropic term which wants to maintain a mean square displacement as in (5.39). As for other problems in statistical mechanics there is a fight between energy and entropy. In fact our previous analysis shows that for $d = 1$ energy always wins, disorder dominates, whereas for $d \geq 3$ entropy wins for small disorder and energy for large disorder.

At this stage the reader may worry that we have lost completely the touch with growing surfaces. This is not the case. $Z_t(x)$ satisfies the recursion relation

$$Z_{t+1}(x) \quad = \quad Z_t(x-1) \exp[-\beta(V_0 + V_{(t,x-1)})]$$

$$+Z_t(x)\exp[-\beta V_{(t,x)}]$$
$$+Z_t(x+1)\exp[-\beta(V_0+V_{(t,x+1)})], \tag{5.40}$$

where in the random potential we indicated only the left endpoint of the bond. Following (5.34) we define

$$h_t(x) = -\frac{1}{\beta}\log Z_t(x). \tag{5.41}$$

Then

$$
\begin{aligned}
h_{t+1}(x) \;=\; & -\frac{1}{\beta}\log\Big\{\exp[-\beta(h_t(x-1)+V_0+V_{(t,x-1)})] \\
& +\exp[-\beta(h_t(x)+V_{(t,x)})] \\
& +\exp[-\beta(h_t(x+1)+V_0+V_{(t,x+1)})]\Big\}.
\end{aligned} \tag{5.42}
$$

For $\beta \to \infty$ the iteration becomes

$$
\begin{aligned}
h_{t+1}(x) \;=\; & \min\{h_t(x-1)+V_0+V_{(t,x-1)}, h_t(x)+V_{(t,x)}, \\
& h_t(x+1)+V_0+V_{(t,x+1)}\}.
\end{aligned} \tag{5.43}
$$

The iterations (5.42), (5.43) combine two steps: First to the current height configuration, $h_t(x)$, one adds independently at each site a random amount V_b. This corresponds to the noise term of the KPZ equation. In the second step one chooses at each site the minimum of the heights at the site itself and its two neighbors. The neighbors receive a penalty V_0. (For finite β the minimum rule is washed out somewhat.) This operation is a discrete version of $\nu\Delta h_t + \frac{1}{2}\lambda(\nabla h_t)^2$, i.e. a combination of lateral spreading and smoothening of the height profile. Note the similarity between (5.43) and the PNG growth rule (4.3).

Before entering into a more detailed analysis of the partition function (5.36) we should translate the objects of interest into the language of directed polymers. From (5.37) we conclude that the growth velocity in the h-direction is just the quenched free energy/length of the polymer. There are two obvious fluctuation quantities: (1) the fluctuations in the free energy and (2) the end-to-end distance (mean square displacement).

ad (1): The free energy is the height of the surface. If starting from a flat surface, the height at $\mathbf{x}$ at time t corresponds to summing over all walks with

48

endpoint x and arbitrary starting point. We may as well sum over all endpoints of walks starting at the origin. Thus if we define

$$Z_t = \int d^d x\, Z_t(\mathbf{x}),$$ (5.44)

then from the scaling theory of the growing surface

$$\langle (-\frac{1}{\beta}\log Z_t - \langle -\frac{1}{\beta}\log Z_t\rangle)^2\rangle^{1/2} \sim t^{\zeta/z}$$ (5.45)

for large t. One expects the same behaviour with both endpoints fixed.

ad (2): The mean square displacement is defined by

$$
\begin{aligned}
\langle \mathbb{E}((\mathbf{y}(t) - \mathbb{E}(\mathbf{y}(t)))^2)\rangle &= \langle \int d^d x\, \mathbf{x}^2 Z_t(\mathbf{x})/\int d^d x\, Z_t(\mathbf{x})\rangle \\
&\quad -\langle (\int d^d x\, \mathbf{x} Z_t(\mathbf{x})/\int d^d x\, Z_t(\mathbf{x}))^2\rangle.
\end{aligned}
$$ (5.46)

Using the statistical self-similarity of the height profile, one obtains

$$\langle (\mathbb{E}(\mathbf{y}(t)^2) - \mathbb{E}(\mathbf{y}(t))^2)^{1/2}\rangle \sim t^{1/z}$$ (5.47)

for large t. If $z < 2$, the walk is superdiffusive. The disorder roughens the walk. It makes larger excursions than an ordinary random walk.

5.2.1 Weak coupling

To estimate the importance of disorder a standard criterion is to consider the ratio

$$\langle Z_t^2\rangle/\langle Z_t\rangle^2.$$ (5.48)

If the ratio remains bounded for large t, then $Z_t \simeq \langle Z_t\rangle$ and the quenched and annealed free energy are equal. Disorder is irrelevant. The t-dependence of (5.48) is grasped most easily for the continuum directed polymer. To have a well defined path integral we have to allow for spatial correlations in the noise (white noise is too rough). Thus ζ_t is taken to be Gaussian with covariance

$$\langle \zeta_t(\mathbf{x})\zeta_{t'}(\mathbf{x}')\rangle = \delta(t-t')V(\mathbf{x}-\mathbf{x}'),$$ (5.49)

where V has a good decay at infinity. Performing the Gaussian average we obtain

$$\langle Z_t\rangle = \int_{\mathbf{y}(0)=0} \mathcal{D}\mathbf{y}(\cdot)\exp\left[-\frac{1}{2\nu}\int_0^t ds\left(\frac{1}{2}\dot{\mathbf{y}}(s)^2 - (\lambda^2/4\nu)V(0)\right)\right]$$ (5.50)

and

$$\langle Z_t^2 \rangle = \int_{\mathbf{y}_1(0)=\mathbf{0}} \mathcal{D}\mathbf{y}_1(\cdot) \int_{\mathbf{y}_2(0)=\mathbf{0}} \mathcal{D}\mathbf{y}_2(\cdot) \exp\left[-\frac{1}{2\nu} \int_0^t ds \{ \frac{1}{2}\dot{\mathbf{y}}_1(s)^2 + \frac{1}{2}\dot{\mathbf{y}}_2(s)^2 \right.$$

$$\left. -(\lambda^2/2\nu)V(0) - (\lambda^2/2\nu)V(\mathbf{y}_1(s)-\mathbf{y}_2(s))\} \right].\tag{5.51}$$

In order to translate back to a Schrödinger equation we define

$$H_1 = -\nu\Delta_1,$$
$$H_{12} = -\nu\Delta_1 - \nu\Delta_2 - \frac{1}{2}(\lambda/2\nu)^2 V(\mathbf{x}_1 - \mathbf{x}_2).\tag{5.52}$$

Then, writing the operator e^{-tH} as a kernel in position space,

$$\langle Z_t^2 \rangle / \langle Z_t \rangle^2 = \int d^d x_1 \int d^d x_2 e^{-tH_{12}}(\mathbf{0},\mathbf{0}\,|\,\mathbf{x}_1,\mathbf{x}_2)/(\int d^d x\, e^{-tH_1}(\mathbf{0}\,|\,\mathbf{x}))^2.\tag{5.53}$$

H_{12} has zero as the continuum edge. Therefore the ratio of partition functions remains bounded provided H_{12} has no bound state. Now in one and two dimensions a Schrödinger equation with a short range attractive potential always binds, whereas in three and more dimensions it binds only if λ is sufficiently large. (Note that, because of (5.49), $\hat{V}(\mathbf{k}) \geq 0$ and $V(0) = (2\pi)^{-d/2}\int d^d k \hat{V}(\mathbf{k}) < \infty$. The binding / no binding property is a theorem of Simon (1976).) Thus for $d > 2$ the directed polymer has a weak coupling regime. The same conclusion holds for lattice versions. In this case there are even rigorous proofs (Imbrie and Spencer 1988, Bolthausen 1989) guaranteeing that the free energy equals with probability one the annealed free energy and that the large scale behavior of the walk agrees with the free walk.

Our result provides a lower bound on the critical coupling for $d > 2$. To show that there must be a transition to a disordered phase we use an argument familiar from spin glasses. It applies only to the lattice version. One notes that the entropy is always positive. For small coupling the free energy agrees with the annealed free energy. We compute the entropy through the Legendre transform of the annealed free energy. It becomes negative at sufficiently large β. Thus there must be a transition.

To work out numbers one has to solve the lattice analogue of the two particle Schrödinger equation (5.52). This has been carried out for the Gaussian site case

(Cook and Derrida 1989a). The random potential, $V_{\mathbf{x}}$, is assigned to each site of a $d+1$ dimensional hypercubic lattice. The $V_{\mathbf{x}}$'s are independent Gaussians with variance one. A walk jumps forward in the one-direction (= time direction) and to one of the nearest neighbors in the remaining coordinates. Following the strategy explained one obtains

$$
\begin{aligned}
\beta_c &\leq 1.67 \text{ for } d = 2, \\
1.03 \leq \beta_c &\leq 1.90 \text{ for } d = 3, \\
(\log 2d)^{1/2} \leq \beta_c &\leq (2\log 2d)^{1/2} \text{ for } d \to \infty.
\end{aligned}
\tag{5.54}
$$

For $d = 2$ our arguments do not exclude a strictly positive β_c. The leading large d behavior is expected to coincide with the upper bound.

5.2.2 Replica

Computing the n-th moment of the partition function leads, as in (5.51), to the n-particle Schrödinger operator

$$
H_n = -\nu \sum_{j=1}^{n} \Delta_j - (\lambda/2\nu)^2 \sum_{i,j=1}^{n} V(\mathbf{x}_i - \mathbf{x}_j).
\tag{5.55}
$$

Let E_n be the ground state energy of H_n. Then

$$
\langle Z_t^n \rangle \approx e^{-E_n t}
\tag{5.56}
$$

for large t. The replica trick consists in the hope to obtain

$$
\langle \log Z_t \rangle = \lim_{n \to 0} \frac{1}{n} (\langle Z_t^n \rangle - 1).
\tag{5.57}
$$

For the Sherrington-Kirkpatrick model of spin glasses, E_n corresponds to the free energy of the n-replicated system. It is defined through a variational problem. The famous Parisi ansatz chooses a solution which breaks the symmetry in replica space. No direct analogue of this phenomenon is expected here (Derrida 1990).

If in $d = 1$ we replace $-V(x)$ by an attractive δ-potential, $-\delta(x)$, and ignore the self-interactions (Kardar and Zhang 1987), then the ground state wave function of H_n is

$$
\psi = Z^{-1} \exp\left[-\kappa \frac{1}{2} \sum_{i \neq j = 1}^{n} |x_i - x_j| \right]
\tag{5.58}
$$

51

with $\kappa = \lambda^2/16\nu^3$. It has the energy

$$E_n = -\frac{1}{3}\nu\kappa^2 n(n^2-1) \tag{5.59}$$

(Lieb and Liniger 1963, Kardar 1987). The cumulant expansion for $\langle Z_t^n \rangle$ is given by

$$\langle Z_t^n \rangle = \exp\left[\sum_{j=1}^{\infty}\frac{n^j}{j!}C_j(\log Z_t)\right], \tag{5.60}$$

where C_j is the j-th cumulant of $\log Z_t$ ($C_1 = \langle \log Z_t \rangle$, $C_2 = \langle(\log Z_t)^2\rangle - \langle \log Z_t \rangle^2$, etc.). Using (5.56) and taking the limit $n \to 0$ in (5.59) yields then (Kardar 1987)

$$\lim_{t\to\infty}\frac{1}{t}C_1 = \frac{1}{3}\nu\kappa^2, \quad \lim_{t\to\infty}\frac{1}{t}C_2 = 0, \quad \lim_{t\to\infty}\frac{1}{t}C_3 = -\frac{1}{18}\nu\kappa^2. \tag{5.61}$$

Thus we recover again $\zeta/z = 1/3$, compare with (5.45).

The argument is slightly more subtle than it appears. If we take the Hamiltonian (5.55), then for large n particles pile on top of each other and $E_n \sim -n^2$. We expect then an intermediate regime where (5.59) holds and which determines the behavior near $n = 0$. This discussion signals the difficulties for $d \geq 2$. Even for model potentials the exact E_n's are not known. The large n asymptotics, $\sim -n^2$, does not reflect the limit $n \to 0$. Furthermore a non-rational exponent ζ/z is hard to accomodate (McKane and Moore 1988, Zhang 1989).

5.2.3 Functional renormalization

Halpin-Healy (1989a) proposed a renormalization which follows the flow of the spatial part of the disorder under rescaling and integrating out large fluctuations. As in (5.49) he chooses a general covariance

$$\langle \zeta_t(\mathbf{x})\zeta_{t'}(\mathbf{x}')\rangle = \delta(t-t')R(|\mathbf{x}-\mathbf{x}'|). \tag{5.62}$$

He computes the effective action to one loop order followed by differential time $t \to (1 + z\delta l)t$ and length $\mathbf{x} \to (1 + \delta l)\mathbf{x}$ rescalings. The covariance R is then approximately governed by (Halpin-Healy 1990b)

$$\begin{aligned}
\frac{\partial}{\partial l}R &= (3-\frac{4}{z})R + \frac{r}{z}R' + \frac{1}{2}(R'')^2 - R''R''(0) \\
&\quad + \frac{(d-1)}{2}(\frac{R'}{r})^2 - (d-1)\frac{R'}{r}R''(0),
\end{aligned} \tag{5.63}$$

where $'$ denotes differentiation with respect to the radial coordinate, r. We search for fixed points of Equation (5.63). For large r the nonlinearities can be neglected. The linear equation has two independent solutions: the short range fixed point $R^*_{SR}(r) \approx r^{(3z-4-d)} \exp[-r^2/2zR''(0)]$ and the Flory fixed point $R^*_F(r) \approx r^{(4-3z)}$ for large r. Equating the algebraic decays yields (Nattermann 1989, Halpin-Healy 1990a)

$$z = (8 + d)/6. \tag{5.64}$$

(5.64) reproduces the known exponent for $d = 1$ and gives $z = 5/3$ for $d = 2$ close to numerical results (cf. Section 5.3). However for large d, z diverges in contradiction to the known asymptotic value $z = 2$. Halpin-Healy (1990b) argues that this implies an upper critical dimension $d_u = 4$ above which $z = 2$ in the strong and weak coupling phase. Even if (5.63) is a reasonable approximation, the difficulty remains how to extract from it the exponent relevant for short range disorder. The matching rule alluded to above is ad hoc and a better understanding of the flow generated by (5.63) is needed.

There is one further point of interest: Halpin-Healy (1989a) attempts to view the directed polymer in a disordered medium and interface fluctuations in a system with bond disorder (Fisher D S 1986) in a unified framework. (5.36) is generalized in the obvious way to the case where $\mathbf{y}(t)$ is an n-component vector field over a d'-dimensional base space. The directed polymer is then the particular case of $n = d$ and $d' = 1$ whereas the interface between the $+$ and $-$ phases of a bond-disordered d-dimensional ferromagnet corresponds to the case $n = 1$ and $d' = d - 1$.

5.2.4 Real space renormalization, hierarchical lattices

For spin systems in thermal equilibrium the Migdal-Kadanoff real space renormalization scheme becomes exact for hierarchical lattices (Berker and Ostlund 1979, Griffiths and Kaufman 1982, Kaufman and Griffiths 1984). We follow these ideas and define the directed polymer on a disordered hierarchical lattice (Derrida and Griffiths 1989, Cook and Derrida 1989a, Derrida 1990). For the construction of the lattice we refer to Figure 11. At generation $n + 1$ each bond of generation
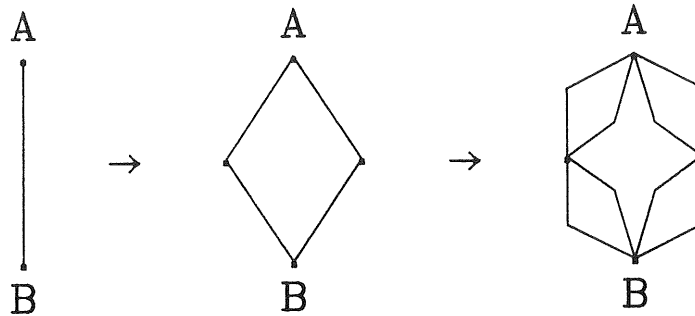
Figure 11: Construction of a hierarchical lattice with branching ratio $b = 2$.

n is substituted by the starting motif. As an analogue for dimension the starting motif has b branches. In the n-th generation lattice we assign to each bond independently a random energy V_b. A walk, w, is directed from A to B. It has the energy

$$E(w) = \sum_{b \in w} V_b. \tag{5.65}$$

The partition function is then given by

$$Z_t = \sum_w e^{-\beta E(w)}, \tag{5.66}$$

where the sum is over all walks from A to B in the nth generation lattice and $t = 2^n$. We have lost the spatial structure. But through the fluctuations in the free energy we can still identify the exponent ζ/z, compare with Equation (5.45).

Without modification the method developed in Section 5.2.1 can be applied to the b-branch hierarchical lattice. If V_b has a Gaussian distribution of width one, then one obtains the bounds

$$(\log(b-1))^{1/2} \leq \beta_c(b) \leq (2 \log b)^{1/2}. \tag{5.67}$$

Although not a consequence of (5.67) it is suggestive to set the lower critical branching at $b = 2$.

Next we note that for branching $b = 1$ a one-dimensional lattice is generated. This is the $d = 0$ directed polymer. There is only one walk and the free energy is a sum of independent random variables. Therefore its fluctuations increase

as $\sqrt{t}$ and $\zeta/z = 1/2$. Together with the scaling relation (3.18) we obtain $\zeta = 2/3$, $z = 4/3$. It is natural to try an expansion around $b = 1$. This is not at all straightforward but has been accomplished to second order (Cook and Derrida 1989a). As to be expected ζ/z is decreasing in b.

It may be of interest to understand why the directed polymer on a hierarchical lattice is difficult to attack analytically. If only interested in the strong coupling ζ/z it suffices to consider the ground state energy (the minimal energy walk). Let E_n be the ground state energy for the nth generation. Because of the hierarchical structure

$$E_{n+1} = \min\{E_n^{(1)} + E_n^{(2)}, \ldots, E_n^{(2b-1)} + E_n^{(2b)}\}, \tag{5.68}$$

where the $E_n^{(i)}$'s are the ground state energies of the sublattices corresponding to generation n. As these are independent random variables, (5.68) implies the following recursion relation for the probability distribution P_n of E_n:

$$
\begin{aligned}
Q_n(E) &= \int dE' P_n(E - E') P_n(E'), \\
P_{n+1}(E) &= b Q_n(E) \left[\int_E^\infty dE' Q_n(E') \right]^{b-1}.
\end{aligned}
\tag{5.69}
$$

Clearly (5.69) is meaningful also for noninteger b. To obtain ζ/z one has to follow how the distribution P_n scales for large n. The branching ratio plays the role of dimension. For spin models the usual identification is $b = 2^d$ (Melrose 1983). This relation overestimates b. E.g. the exact $d = 1$ exponent $\zeta/z = 1/3$ would be reached at $b = 2$ whereas it occurs in fact already at $b = 1.65$. Also the large d behavior is not reproduced, compare Equations (5.54) and (5.67). We have only a qualitative link between b and d.

The recursion relation (5.69) has been iterated numerically up to $b = 12$ (Halpin-Healy 1989b). One finds a continuous decrease of ζ/z. There is no indication of an upper critical dimension. Extrapolating beyond the known, a rather simple picture is suggested. There is a weak and strong coupling regime. In the strong coupling regime ζ shows a steady decrease from $\zeta = 2/3$ at $b = 1$ to $\zeta = 0$ at $b = \infty$. Correspondingly z increases from $4/3$ to 2. The nature of the transition has not been explored yet.

5.2.5 1/d-expansion, trees

Many problems of statistical mechanics simplify in large dimensions. For a directed polymer the limit $d \to \infty$ leads to a disordered tree. Again we assign to each bond of the tree independently a random potential V_b. A walk is directed branching outwards. The energy of a walk is as in (5.65) and the partition function is given by (5.66), where the sum is over all walks of length t (b^t walks for a tree of branching ratio b). Using an analogy with traveling fronts, the directed polymer on a tree can be solved fairly explicitly (Derrida and Spohn 1988), even for complicated branching structures. The main point to us here is that there is a transition from a high temperature phase to a low temperature 'spin glass' phase. The transition is not drastic. The fluctuations in the free energy are always of order one. They increase with increasing β and freeze into a β-independent distribution above the critical point β_c. Thus $\zeta = 0$ in both phases. Cook and Derrida (1989b, 1990) develop a 1/d-expansion which is based on a sequence of approximations consisting of more and more complicated trees. In particular, they compute the mean square displacement for large d and find it to be proportional to t, i.e. $z = 2$ in (5.47). If not an artifact of the method, this result indicates an upper critical dimension d_u. The picture implied is that in the strong coupling phase $\zeta = 0$ and $z = 2$ for $d > d_u$. The prefactor of the mean square displacement (the 'diffusion coefficient') diverges as $d \to d_u$. Below d_u the walk is superdiffusive, $z < 2$.

5.3   Numerical results for the KPZ exponents

To illustrate the present state of affairs regarding the values of the KPZ (strong coupling) scaling exponents, Tables 1, 2 and 3 give an up-to-date summary of simulation results obtained from a variety of growth models (see Chapter 4) as well as from the directed polymer. In the simulations various combinations of ζ and z are actually measured. We have chosen to express all results in terms of ζ and z, using the known scaling relations when necessary. In cases where two exponents were determined independently, this provides a check of the relation $\zeta + z = 2$, cf. Equation (3.18), which is shown then in the corresponding column

of the Tables. We refrain from citing error bars, as the different assessment of systematic errors by different authors renders a comparison difficult.

The results for $1 + 1$ dimensional growth have been included mainly to demonstrate the difficulty to obtain reliable results even in this now theoretically well understood case. Convincing agreement with the theoretical prediction $\zeta = 1/2$, $z = 3/2$ was achieved only using algorithms (Wolf and Kertész 1987a) and models (Meakin et al. 1986b, Krug and Spohn 1989, Kim and Kosterlitz 1989) specifically devised to suppress corrections to scaling.

As discussed in the preceding sections of this chapter, no exact results are available in higher dimensions ($d \geq 2$). Based on their simulations of the noise reduced Eden model, Wolf and Kertész (1987b) conjectured the following dimension dependence of the scaling exponents,

$$\zeta_d = 1/(d+1), \ z_d = (2d+1)/(d+1) \tag{5.70}$$

which gives the exact result for $d = 1$ (but not for $d = 0$). In contrast to the prediction (5.64), Equation (5.70) does not contain a finite upper critical dimension, i. e. $\zeta_d \to 0$ and $z_d \to 2$ only asymptotically for $d \to \infty$.

Later work by Kim and Kosterlitz (1989) on a restricted solid-on-solid model (see Section 4.2) led the authors to conjecture

$$\zeta_d = 2/(d+3), \ z_d = 2(d+2)/(d+3) \tag{5.71}$$

which is exact for $d = 1$ and $d = 0$, and also predicts no upper critical dimension. We note that both (5.70) and (5.71) give integer values for z_d/ζ_d in all dimensions, a suggestive prospect in the framework of the replica approach outlined in Section 5.2.2 (Mc Kane and Moore 1988, Zhang 1989). However both conjectures (5.70) and (5.71) have been questioned by the very recent results of Forrest and Tang (1990). Using a variant of the single step model and exceptionally large lattices (11520×11520 sites in $d = 2$), they find $\zeta_2/z_2 = 0.240 \pm 0.001$, slightly but significantly less than the simple fraction $1/4$.

Renz (1990) has performed simulations of the $T = 0$ directed polymer up to dimension $d = 5$. He finds $\zeta_4 = 0.26$, $z_4 = 1.75$ and $\zeta_5 = 0.21$, $z_5 = 1.79$. In particular the results in $d = 5$ seem to rule out the upper critical dimension $d_u = 4$ conjectured by Halpin-Healy (1990b), cf. Section 5.2.3.

Model	ζ	z	$\zeta + z$	Reference
polymer, $T = 0$	0.50	1.52	2.02	Huse and Henley (1985)
polymer, $T = 0$	0.41	1.59	-	Kardar (1985)
polymer, $T > 0$	0.51	1.49	-	Kardar (1985)
polymer, $T > 0$	0.42	1.58	-	Bovier et al. (1986)
polymer, $T = 0$	0.50	1.50	2.00	Nattermann and Renz (1988)
ballistic	0.42	1.40	1.82	Family and Vicsek (1985)
Eden	0.45	1.55	-	Plischke and Rácz (1985)
Eden	0.50	1.70	2.20	Jullien and Botet (1985)
Eden	0.50	1.67	2.17	Meakin et al. (1986a)
Eden	0.51	1.57	2.08	Zabolitzky and Stauffer (1986)
ballistic	0.48	1.54	2.02	Meakin et al. (1986b)
single step	0.50	1.51	2.01	Meakin et al. (1986b)
single step	0.57	1.43	-	Plischke et al. (1987)
Eden	0.50	1.50	-	Wolf and Kertész (1987a)
Eden	0.50	1.50	-	Meakin (1987b)
ballistic	0.50	1.50	-	Meakin (1987b)
PNG	0.50	1.50	-	Krug and Spohn (1989)
restricted SOS	0.50	1.50	2.00	Kim and Kosterlitz (1989)

Table 1: Numerical results for the strong coupling KPZ exponents in $d = 1$.

Model	ζ	z	$\zeta + z$	Reference
polymer, $T=0$	0.53	1.61	2.14	Kardar and Zhang (1987)
polymer, $T=0$	0.37	1.63	2.00	Renz (1990)
Eden	0.20	1.80	-	Jullien and Botet (1985)
ballistic	0.33	1.39	1.72	Meakin et al. (1986b)
single step	0.36	1.58	1.94	Meakin et al. (1986b)
Eden	0.33	1.50	1.83	Wolf and Kertész (1987b)
Eden	0.28	1.72	-	Meakin (1987b)
ballistic	0.41	1.59	-	Meakin (1987b)
single step	0.38	1.63	2.01	Liu and Plischke (1988)
ballistic	0.36	1.64	-	Baiod et al. (1988)
restricted SOS	0.40	1.60	2.00	Kim and Kosterlitz (1989)
Eden	0.40	1.60	-	Devillard and Stanley (1989)
single step	0.39	1.60	1.99	Forrest and Tang (1990)
KPZ equation	0.18	1.80	1.98	Chakrabarti and Toral (1989)
KPZ equation	0.24	1.85	2.09	Guo et al. (1990)
KPZ equation	0.38	1.58	1.96	Amar and Family (1990b)
ballistic	0.35	1.67	2.02	Family (1990)

Table 2: Numerical results for the strong coupling KPZ exponents in $d=2$.

Model	ζ	z	$\zeta + z$	Reference
polymer, $T=0$	0.64	1.56	2.20	Kardar and Zhang (1987)
polymer, $T=0$	0.28	1.71	1.99	Renz (1990)
Eden	0.08	1.92	-	Jullien and Botet (1985)
Eden	0.24	1.64	1.88	Wolf and Kertész (1987b)
restricted SOS	0.33	1.67	2.00	Kim and Kosterlitz (1989)
Eden	0.33	1.67	-	Devillard and Stanley (1989)
single step	0.30	1.67	1.97	Forrest and Tang (1990)

Table 3: Numerical results for the strong coupling KPZ exponents in $d=3$.

5.4 KPZ type equations without noise

On an abstract level we may regard the KPZ equation (5.10) as a nonlinear mechanism which transforms the correlations of the noise ζ_t into those of the field h_t. An alternative way to gain insight into this mechanism is to investigate the deterministic equation ($\zeta_t \equiv 0$) subject to noisy initial data. This approach has been pursued in the hydrodynamic context of Burgers' equation (Burgers 1974, Kida 1979 and references therein). For surface growth, the physical picture behind the statistical initial value problem is the flattening of an initially rough surface due to growth. We show here that such processes can be described by a scaling theory quite similar to that presented in Chapter 3 for the stochastic case. A more detailed account can be found in Krug and Spohn (1988).

5.4.1 The Kuramoto–Sivashinsky equation

Before turning to surface growth we briefly discuss a close cousin of the deterministic KPZ equation, the Kuramoto-Sivashinsky equation of chemical turbulence (Kuramoto and Yamada 1976)

$$\frac{\partial}{\partial t}\theta(\mathbf{x},t) = \omega_0 + \nu\Delta\theta + \mu(\nabla\theta)^2 - \lambda\Delta^2\theta. \tag{5.72}$$

Here $\theta(\mathbf{x},t)$ is the phase of a complex Ginzburg-Landau type order parameter $w(\mathbf{x},t)$. Physically, $w = a + ib$ where a and b are local concentrations of two reacting species in an autocatalytic reaction. ω_0 is the local oscillation frequency in the absence of spatial coupling. Equations similar to (5.72) arise in combustion theory, with $\theta(\mathbf{x},t)$ describing the position of a flame front moving at average velocity ω_0 (Sivashinsky 1977).

The coefficients of the gradient terms depend on the system parameters. Clearly for $\nu > 0$ the fourth order derivative is irrelevant and (5.72) reduces to the deterministic KPZ equation. In contrast for $\nu < 0$ the system becomes linearly unstable for small wave numbers $k^2 < -\nu/\lambda$, and a turbulent stationary state evolves. Using a momentum shell renormalization Yakhot (1981) argues that the short wave length components of θ in the turbulent state effectively generate a stochastic force with short range correlations. Moreover the viscosity ν acquires

a correction which is positive in $d = 1$. Hence the turbulent state appears to be described by the *stochastic* KPZ equation. From the exact results of KPZ for $d = 1$ one expects then the stationary power spectrum to scale as $\langle |\hat{\theta}(k)|^2 \rangle \sim k^{-2}$ for small k. This has been confirmed by numerical integration of (5.72) (Yamada and Kuramoto 1976). The verification of the dynamic exponent $z = 3/2$ is hampered by strong crossover effects (Hyman et al. 1986, Zaleski 1989, and references therein).

5.4.2 General nonlinearity

For the KPZ equation there is no linear instability, so all reasonable initial profiles flatten in the course of time. We consider deterministic growth with a general nonlinearity $v(\mathbf{u}) \approx v(\mathbf{0}) + \lambda |\mathbf{u}|^\alpha$ in the inclination dependent growth velocity,

$$\frac{\partial}{\partial t} h_t(\mathbf{x}) = \nu \Delta h_t + \lambda |\nabla h_t|^\alpha \tag{5.73}$$

where a small 'viscosity' $\nu > 0$ has been added to suppress unphysical solutions. The ensemble of random initial profiles $h_0(\mathbf{x})$ is characterized by $\langle h_0(\mathbf{x}) \rangle = 0$ and the covariance

$$\langle (h_0(\mathbf{x}) - h_0(\mathbf{x}'))^2 \rangle \approx A_0 |\mathbf{x} - \mathbf{x}'|^{2\zeta} \tag{5.74}$$

for $|\mathbf{x} - \mathbf{x}'| \gg 1$, $\zeta > 0$, compare with Equation (3.3). Here a crucial difference appears between the stochastic evolution (5.10) and its deterministic counterpart: While in the former case the static roughening exponent ζ is fixed by the steady state of the dynamics, for the deterministic problem it is an input parameter which is introduced through the initial condition (5.74). Since the dynamics (5.73) is purely relaxational, it does not generate a proper steady state but merely transforms the static scaling properties of the initial data into a dynamically scale invariant process.

Having initialized the deterministic growth at time $t = 0$, we follow the evolution of dynamic correlation functions of the type introduced in Section 3.1. Consider in particular the height-height correlation function

$$G(|\mathbf{x} - \mathbf{x}'|, t) = \langle (h_t(\mathbf{x}) - h_t(\mathbf{x}'))^2 \rangle. \tag{5.75}$$

Assuming statistical scale invariance for the relaxation process, as in Equation (3.1), this may be written

$$G(r,t) = A(r/\xi_{\|}(t))r^{2\zeta} \qquad (5.76)$$

just as in the stochastic case. However, the amplitude scaling function A is expected to have a different form: At $t = 0$ the surface is rough on all scales, so $A(y) \to A_0$ for $y \to \infty$. For $t > 0$ the surface is smoothened on scales $r \ll \xi_{\|}(t)$, hence $A(y) \to 0$ for $y \to 0$.

As in the stochastic case the growth of the correlation length $\xi_{\|}(t) \sim t^{1/z}$ defines a dynamic exponent z. Since here both the nonlinearity exponent α and the roughness exponent ζ can be fixed at will, z is uniquely determined by the scaling relation

$$z = \alpha + \zeta(1 - \alpha) \qquad (5.77)$$

cf. Equation (3.20). For $\alpha > (2 - \zeta)/(1 - \zeta)$ the nonlinearity is irrelevant and $z = 2$.

At our present level of generality not much is known about the amplitude scaling function. Burgers (1974) investigates the particular case of dimension $d = 1$, $\alpha = 2$ and $\zeta = 1/2$. Since he regards $u_t(x) = -2\lambda \partial h_t / \partial x$ as the velocity field of a one dimensional fluid, $\zeta = 1/2$ means that the initial velocity field has short range correlations. Using the Hopf-Cole transformation (5.34), Burgers shows that the asymptotic $(t \to \infty, \nu \to 0)$ velocity profile consists of linear pieces separated by shock discontinuities with an average distance $l \sim t^{2/3}$. The corresponding surface profile $h_t(x)$ is then composed of parabolic arcs of typical extension l, so l can be identified with $\xi_{\|}$ and $z = 3/2$ as expected from the scaling relation (5.77). He also calculates the short distance behavior of A. The full amplitude scaling function is determined numerically by Kida (1979).

In the context of turbulence one would also like to know how the mean kinetic energy decays in the course of time. In the surface picture this corresponds to a typical slope squared, which we estimate as

$$\langle u_t^2 \rangle \sim G(\xi_{\|}(t), t)/\xi_{\|}(t)^2 \sim t^{-2(1-\zeta)/z}. \qquad (5.78)$$

Indeed Burgers obtains a $t^{-2/3}$ decay of the kinetic energy.

The case $\alpha = 1$ (still retaining $d = 1$, $\zeta = 1/2$) is more tractable (Krug and Spohn 1988). Details will be given in the following Section.

As explained already, the deterministic KPZ equation ($\alpha = 2$) is an approximation to isotropic growth,

$$\frac{\partial}{\partial t} h_t = \lambda \sqrt{1 + (\nabla h_t)^2},\qquad (5.79)$$

compare with Equation (5.7). The solution to (5.79) can be obtained from a simple construction, known as Huygens principle in optics. Given $h_0(\mathbf{x})$, for every $\mathbf{x}$ one draws a sphere of radius λt with center $h_0(\mathbf{x})$. $h_t(\mathbf{x})$ is then the envelope function. Since the surface flattens in the course of time, the large t solution to (5.79) agrees with the one of the deterministic KPZ equation.

We now choose the initial height $h_0(\mathbf{x})$ to be a stochastic process stationary in $\mathbf{x}$ and with a finite correlation length. Then the height-height correlation function, cf. Equation (5.74), decays exponentially. Naively, this would indicate a roughness exponent $\zeta = 0$. However, the spheres which determine the surface at time t must emanate from local maxima of $h_0(\mathbf{x})$ on the appropriate scale. Therefore we *define* the roughness exponent ζ by

$$\left\langle \max_{|\mathbf{x}| \leq l} h_0(\mathbf{x}) \right\rangle \sim l^\zeta \qquad (5.80)$$

for large l. As before the dynamic exponent is then determined through the scaling relation $\zeta + z = 2$.

If $h_0(\mathbf{x})$ is a self-similar Gaussian field with asymptotics as in Equation (5.74), $\zeta > 0$, then the definitions (5.80) and (5.74) for the roughness exponent agree. If $h_0(\mathbf{x})$ is independent at different sites (we imagine here a spatial discretization with the correlation length as unit), then ζ depends on the tail of the distribution of $h_0(\mathbf{x})$. Let $P(h)$ denote this single site distribution. For $P(h) \sim \exp(-B|h|^\beta)$, $\beta > 0$, the roughness exponent $\zeta = 0$ with logarithmic corrections depending on β. In this case $z = 2$. On the other hand for an algebraic decay as $P(h) \sim h^{-\tau}$, $\tau > 1$, one finds $\zeta = d/(\tau - 1)$ and therefore $z = (2\tau - 2 - d)/(\tau - 1)$. For a single site distribution of finite support the left hand side of Equation (5.80) tends to a constant for large l with a correction $-\mathcal{O}(l^{-d})$. Thus we set $\zeta = -d$ and $z = 2 + d$. These predictions are supported by an explicit computation of the average density

63

of spheres forming the surface at time t and by numerical simulations (Kida 1979, Tang et al. 1990). For dimension $d = 1$ and a single site distribution with exponential decay Kida (1979) verifies the scaling form (5.76) and obtains the amplitude scaling function. As in other one dimensional models, his technique is to follow the dynamics of the surface cusps.

5.4.3 An exactly solved case

As an example of a deterministic growth process for which all details can be worked out, we study the one dimensional PNG model on the lattice in the limit of zero nucleation rate. As initial conditions we choose the height differences independently at each bond,

$$u_0(i) = h_0(i+1) - h_0(i) = \pm 1 \tag{5.81}$$

with equal probability, $\langle u_0(i) \rangle = 0$. The initial profile is the record of a one-dimensional random walk with unit step length, i.e. $\zeta = 1/2$. The dynamics takes the simple form (see Equation (4.3))

$$h_{t+1}(i) = \max\{h_t(i-1), h_t(i), h_t(i+1)\}. \tag{5.82}$$

Iterating this recursion t times yields the formal solution

$$h_t(i) = \max_{i-t \leq j \leq i+t} \{h_0(j)\}. \tag{5.83}$$

Hence the statistics of the surface configurations is related to the statistics of maxima of one dimensional random walks.

To see what to expect in terms of the scaling picture, we note that, since downwards (upwards) slopes propagate with velocity one (minus one), the continuum limit of (5.82) is

$$\frac{\partial}{\partial t} h_t(x) = |\frac{\partial}{\partial x} h_t(x)| \tag{5.84}$$

supplemented by the condition that $h_t(x)$ remains continuous at discontinuities of $\partial h_t / \partial x$. Thus the inclination dependent growth velocity is $v(u) = |u|$ and $\alpha = 1$ in the scaling relation (5.77), which gives the dynamic exponent $z = 1$ (fluctuations spread at a finite velocity).

64

The clue to solving the problem posed in Equations (5.81) and (5.82) is to consider the dynamics of surface steps. (This point of view will be further developed in Chapter 6.) Under (5.82) a downward step, $u_t(i) = h_t(i+1) - h_t(i) = -1$, moves one lattice spacing to the right and an upward step, $u_t(i) = 1$, moves one lattice spacing to the left. Steps of opposite sign annihilate when they collide. Hence the problem is reduced to a one dimensional gas of particles and antiparticles with velocities ± 1 which initially have an ideal gas distribution (cf. Elskens and Frisch 1985).

To illustrate the method of computation we consider the decay of the step density $\rho(t) = \langle |u_t(i)| \rangle$. This is the probability for a step to survive up to time t. Suppose the step starts from the origin at $t = 0$ and moves to the right ($u_0(0) = -1$). This step has a left-going partner which starts at a site $j > 0$ at $t = 0$. The two will annihilate at time $t_1 = j/2$, hence our chosen step survives up to time t iff $j > 2t$. Obviously the two steps have to be at the same height, i.e. j is the first site to the left of the origin for which $h_0(j) = h_0(0)$. The condition for survival is therefore

$$h_0(0) - h_0(i) > 0 \qquad \text{for} \qquad 0 \leq i \leq 2t. \tag{5.85}$$

Keeping in mind that $h_0(i)$ is the record of a random walk, it follows that $\rho(t)$ is the probability for a symmetric, one dimensional random walk not to return to its starting position in $2t$ steps. For large t (see e.g. Feller 1950)

$$\rho(t) \approx \frac{1}{\sqrt{\pi t}} \tag{5.86}$$

in accord with the scaling law (5.78) for $\zeta = 1/2$ and $z = 1$.

The same approach can be used to compute second and higher order, spatial and temporal step correlation functions (Krug and Spohn 1988, Krug 1989b). By integration this gives explicit expressions for the surface correlations. As an illustrative example we quote the result for the height-height correlation

$$\langle (h_t(0) - h_t(r))^2 \rangle \approx \begin{cases} A(r/\xi_\parallel(t))r, & r < \xi_\parallel(t) \\ r - (\frac{4}{\pi} - 1)\xi_\parallel(t), & r \geq \xi_\parallel(t) \end{cases} \tag{5.87}$$

for large r and t, with the correlation length

$$\xi_\parallel(t) = 2t \tag{5.88}$$

65

and the amplitude scaling function

$$A(y) = \frac{4}{\pi} \left(\frac{1+y}{y} \arctan \sqrt{y} - \frac{1}{\sqrt{y}} \right). \tag{5.89}$$

This confirms the scaling picture and the dynamic exponent $z = 1$: The roughness is suppressed on scales $r < \xi_\|(t), A(y) \sim \sqrt{y}$ for $y \to 0$, while on scales $r > \xi_\|(t)$ it still grows with the exponent $\zeta = \frac{1}{2}$ of the initial data, merely reduced by a constant. We note that (5.88) can be immediately read off from (5.83): For $|i - j| > 2t$, $h_t(i)$ and $h_t(j)$ depend on disjoint portions of the initial condition.

Higher order correlations contain information about the asymmetry of the growing surface with respect to the direction of growth. Specifically, we have computed the local surface skewness (cf. Wolf 1987)

$$s(r,t) = \frac{\langle \triangle(r,t)^3 \rangle}{\langle \triangle(r,t)^2 \rangle^{3/2}},$$

$$\triangle(r,t) = h_t(0) - \frac{1}{2}(h_t(r) + h_t(-r)) \tag{5.90}$$

with the result (Krug and Spohn 1988)

$$s(r,t) \approx -\tilde{s}(r/\xi_\|(t)) \tag{5.91}$$

where $\tilde{s}(y)$ is a positive, single-humped function which decays as $y^{-3/2}$ for $y \to \infty$.

It is also of interest to consider correlations between events occuring at the same site at different times. Due to the special role of $t = 0$, there is no temporal stationarity. For example, the two-point correlation of the step current $|u_t(i)|$ is given by

$$g(t,\tau) := \langle |u_t(i) u_{t+\tau}(i)| \rangle \approx \frac{1}{\pi \sqrt{t\tau}} F(t/\tau) \tag{5.92}$$

where $F(y)$ varies monotonously between $F(0) = 1$ and $F(\infty) = 1/\sqrt{2}$. For fixed t and $\tau \to \infty$ the truncated current correlation vanishes as

$$g(t,\tau) - \rho(t)\rho(t+\tau) \approx \frac{1 - 1/\sqrt{2}}{\pi \tau}. \tag{5.93}$$

The curious statistical properties of the train of steps passing a fixed site emerge more clearly from the conditional probability $C_t(\tau)$ of observing a step at time $t + \tau$, given a step at time t. From Equations (5.86) and (5.92) we have

$$C_t(\tau) = \frac{g(t,\tau)}{\rho(t)} = \frac{1}{\sqrt{\pi \tau}} F(t/\tau) \tag{5.94}$$

66

which is practically independent of t. Hence, *conditioned* on the event $\{|u_t(i)| = 1\}$ at time t, the subsequent history has the same appearance as if one had started at $t = 0$, although the *total* density of events vanishes according to (5.86). Similar behavior occurs in the context of intermittent dynamical systems with a nonnormalizable invariant measure, where it has been termed 'sporadic' (Gaspard and Wang 1988, Wang 1989). In the temporal sequences $|u_t(i)|$ this intermittency appears as a strong bunching of events, which is also implied by (5.93).

Coming back to surface properties (5.92) can be integrated to obtain the temporal fluctuations of the local height increase

$$\langle (h_t(i) - h_0(i) - \langle h_t(i) - h_0(i) \rangle)^2 \rangle \approx Dt. \qquad (5.95)$$

While the analytic expression for the diffusion constant D is difficult to evaluate, we have the bounds $\sqrt{2} - 4/\pi \leq D \leq 2 - 4/\pi$ and the numerical estimate $D \simeq 0.354$. Again, the exact result (5.95) supports the scaling theory which predicts this quantity to grow as $t^{2\zeta/z}$ in general.

6 Driven Lattice Gases

To introduce the microscopic model we imagine a hexagonal packing of discs with surface, cf. Figure 12 (Gates 1988, Gates and Westcott 1988). No overhangs are allowed. Further discs attach to the surface (respecting the hexagonal packing and no overhang rules) according to the rate α_n if the disc has n neighbors, $n = 2, 3, 4$. We also want to allow for processes where discs detach from the surface and evaporate into the ambient atmosphere (respecting the hexagonal packing and no overhang rules). The corresponding rates are γ_n if the disc has n neighbors.

For the KPZ equation we noticed already that it pays to consider the surface slope rather than the height. For our model let us follow then how the slope changes in time. We draw a line connecting the center of the discs along the top layer, such that only slopes $\pm 60°$ occur, compare with Figure 12. To the j-th line segment we assign the variable $\eta_j = 0, 1$ depending on whether the slope is $+60°$ or $-60°$. We think of η_j, $j = 0, \pm 1, \ldots$, as a lattice gas configuration. There
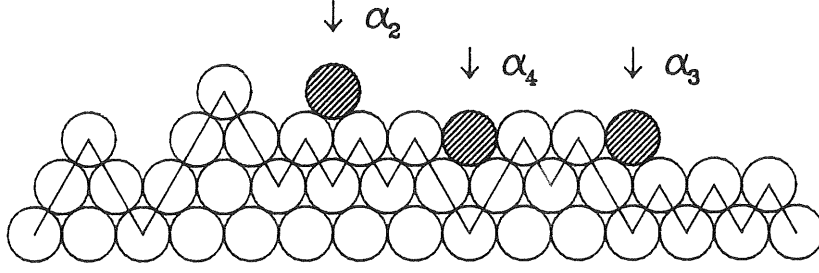
Figure 12: Edge of a two dimensional hexagonal crystal. The zig zag line is the instantaneous surface configuration. Hatched discs attach at the indicated rates.

is at most one particle per site. $\eta_j = 1$ if site j is occupied and $\eta_j = 0$ if site j is vacant. η is our short hand for a whole configuration.

The dynamics of the lattice gas is easily obtained. An attachment of a disc results in a jump to the right and a detachment in a jump to the left. The jump rates between j and $j + 1$ are given by

$$
\begin{aligned}
\eta_j = 1, \eta_{j+1} = 0 \quad &: \quad \alpha_2 \text{ for } \eta_{j-1} = 0, \eta_{j+2} = 1 \\
&\quad\ \alpha_3 \text{ for } \eta_{j-1} = 0, \eta_{j+2} = 0 \text{ and } \eta_{j-1} = 1, \eta_{j+2} = 1 \\
&\quad\ \alpha_4 \text{ for } \eta_{j-1} = 1, \eta_{j+2} = 0, \\
\eta_j = 0, \eta_{j+1} = 1 \quad &: \quad \gamma_2 \text{ for } \eta_{j-1} = 0, \eta_{j+2} = 1, \\
&\quad\ \gamma_3 \text{ for } \eta_{j-1} = 0, \eta_{j+2} = 0 \text{ and } \eta_{j-1} = 1, \eta_{j+2} = 1 \\
&\quad\ \gamma_4 \text{ for } \eta_{j-1} = 1, \eta_{j+2} = 0. \quad\quad (6.1)
\end{aligned}
$$

We denote these jump rates by $c(j, j+1, \eta)$. The probability distribution, $p_t(\eta)$, of the lattice gas at time t is then governed by the master equation

$$
\frac{d}{dt} p_t(\eta) = \sum_j [c(j, j+1, \eta^{jj+1}) p_t(\eta^{jj+1}) - c(j, j+1, \eta) p_t(\eta)]. \quad\quad (6.2)
$$

Here η^{jj+1} stands for the configuration η with the occupancies at j and $j + 1$ interchanged.

Before turning to specific properties of (6.2) let us see how the basic quantities of interest for the large scale structure of the surface are reexpressed in terms of the lattice gas.

(i) By changing the density of the lattice gas the inclination of the surface is varied. Density one corresponds to a slope of $-60°$, density zero to $60°$. Clearly, the particle number, N, is conserved. This implies that the average inclination does not change in time, as it should be.

(ii) The growth velocity is related to the average current. For given density ϱ, the lattice gas settles in a steady state which is spatially uniform. We denote this steady state, in the infinite volume limit, by $\langle \cdot \rangle_\varrho$. In principle it can be obtained as the stationary solution of (6.2) for a ring of L sites with periodic boundary conditions in the limit $N \to \infty$, $L \to \infty$, $N/L \to \varrho$. The steady state current is then given by

$$j(\varrho) = \langle c(0,1,\eta)(\eta_0 - \eta_1) \rangle_\varrho. \tag{6.3}$$

If a is the disc diameter, then the growth velocity is $v(u) = \sqrt{3/4}\, a j(\varrho)$ with slope $\frac{\partial}{\partial x} h = u = \sqrt{3}(1 - 2\varrho)$.

(iii) Surface correlations translate to density correlations. If we study the lattice gas for its own sake, then from a statistical mechanics point of view the basic quantity is the time dependent density-density correlation in the steady state. Most conveniently one defines its Fourier transform (the so called structure function or intermediate scattering function)

$$S(k,t) = \sum_j e^{ikj}(\langle \eta_{t,j}\eta_{0,0} \rangle_\varrho - \varrho^2), \tag{6.4}$$

where we used that by space-time stationarity $\langle \eta_{t,j} \rangle_\varrho = \varrho$. The term in the round brackets is the correlation of the occupation at the origin at time $t = 0$ and at the site j at time t. If $P_t(\eta, \eta')$ denotes the transition probability of the lattice gas to the configuration η' at time t given the configuration η at time $t = 0$ (in principle, computable from the master equation (6.2)), then

$$\langle \eta_{t,j}\eta_{0,0} \rangle_\varrho = \sum_\eta \sum_{\eta'} \bar{p}(\eta)\eta_0 P_t(\eta,\eta')\eta'_j \tag{6.5}$$

with $\bar{p}$ the steady state solution of (6.2) at $N/L = \varrho$. (It is understood that expectations are in the infinite volume limit at constant density.)

Since the density is the only conserved quantity, $S(k,t)$ should scale for small k and large t as

$$S(k,t) = \chi e^{ikc(\varrho)t} e^{-\nu k^2 |t|}. \tag{6.6}$$

69

χ is the compressibility of the lattice gas,

$$\chi(\varrho) = \sum_j (\langle \eta_j \eta_0 \rangle_\varrho - \varrho^2). \tag{6.7}$$

$c(\varrho)$ is the sound velocity, which is determined through

$$\frac{1}{\chi} \sum_j j (\langle \eta_{t,j} \eta_{0,0} \rangle_\varrho - \varrho^2) = t j'(\varrho) = t c(\varrho). \tag{6.8}$$

This result should be no surprise. If we consider a situation where the density varies slowly, then locally the lattice gas is stationary and its density is governed by

$$\frac{\partial}{\partial t} \varrho_t(x) + \frac{\partial}{\partial x} j(\varrho_t(x)) = 0. \tag{6.9}$$

Since correlations correspond to a small deviation from the steady state, the sound velocity is obtained by linearizing (6.9) around a uniform density. Finally, ν is the usual sound damping coefficient.

(6.6) is the result of linearized hydrodynamics, just as for fluids, only with the simplification of a single conservation law. For fluids it has been recognized for a long time that the nonlinearities in the hydrodynamic equations cannot be completely neglected (Pomeau and Résibois 1975). In three dimensions the nonlinearities give rise to a slow decay in the current-current correlations (the so called long time tails), but they do not modify the scaling form of the structure function. For a one dimensional fluid the effects are more drastic. For these we are already well prepared from our discussion of the KPZ equation. Thus (6.6) is to be replaced by the correct scaling form (van Beijeren et al. 1985)

$$S(k,t) \approx \chi e^{ikc(\varrho)t} g((\lambda^2 \chi)^{1/3} k |t|^{2/3}) \tag{6.10}$$

for small k and large t, compare with (5.29). According to (5.11) the coupling constant is

$$\lambda = v''(u) = \frac{1}{8\sqrt{3}} a j''(\varrho). \tag{6.11}$$

Of course, we assumed here that $0 < \lambda, \chi < \infty$. If $\lambda = 0$, then the linear theory of Section 5.1.1 applies and the conventional scaling form (6.6) is the correct one.

Having said all this about the structure function of the lattice gas, we still owe to the reader the link to surface fluctuations. As one relevant example we work

out how, starting from a flat substrate, the surface width increases, compare with (3.13). Let h_t be the height of the growing surface at time t and let $j_t(i, i+1)$ be the actual particle current through the bond $(i, i+1)$. Then

$$h_t(i) - h_0(i) = \sqrt{3}a \int_0^t ds j_s(i-1, i), \qquad (6.12)$$

where we used that because of the hexagonal structure the height increases in units of $\sqrt{3}a$. Therefore the average width, $W(t)$, of the surface is given by

$$\begin{aligned} W(t)^2 &= \langle [h_t(1) - h_0(1) - \langle h_t(1) - h_0(1)\rangle]^2\rangle \qquad (6.13) \\ &= 3a^2 \langle [\int_0^t ds(j_s(0,1) - \langle j_s(0,1)\rangle)]^2\rangle. \end{aligned}$$

To compute the average on the right hand side we use the conservation law,

$$\langle [\sum_{i=-l}^{l} (\eta_{t,i} - \eta_{0,i})]^2\rangle = \langle [\int_0^t ds(j_s(-l-1, -l) - j_s(l, l+1))]^2\rangle. \qquad (6.14)$$

Since t is fixed, the integrated currents through the bonds $(-l-1, -l)$ and $(l, l+1)$ are independent for sufficiently large l. Therefore, in the limit $l \to \infty$ and using translation invariance, we obtain

$$W(t)^2 = 3a^2 \frac{1}{2\pi} \int_{-\pi}^{\pi} dk (4(1 - \cos k))^{-1} \sum_j e^{ikj} \langle (\eta_{t,j} - \eta_{0,j})(\eta_{t,0} - \eta_{0,0})\rangle. \qquad (6.15)$$

At this point it may be tempting to insert the stationary structure function (6.4) in its scaling form (6.10). This would lead to a long time behavior as $3a^2[\frac{1}{2}\chi c(\varrho)t + \text{const}.t^{2/3}]$. Only for vanishing sound velocity the surface width increases as $t^{1/3}$. However, since we start from a flat substrate, the initial configuration is alternating: $\eta_j = 1$ for even j, $\eta_j = 0$ for odd j and with equal weight the same configuration shifted by one lattice unit. Therefore in (6.15) the non-stationary structure function appears. It is not quite obvious how to relate it to the scaling form (6.10). To obtain a clue we consider the KPZ equation (5.8) with nonlinearity neglected. Setting $\varrho_t = -\frac{\partial}{\partial x} h_t$ and $c = -v'(0)$ it reads

$$\frac{\partial}{\partial t}\varrho_t + c\frac{\partial}{\partial x}\varrho_t = \nu \frac{\partial^2}{\partial x^2}\varrho_t - \frac{\partial}{\partial x}\zeta_t \qquad (6.16)$$

71

with initial conditions $\varrho_0(x) = 0$. Then

$$\int dx e^{ikx} \langle (\varrho_t(x) - \varrho_0(x))(\varrho_t(0) - \varrho_0(0)) \rangle \tag{6.17}$$

$$= \int dx e^{ikx} \langle \varrho_t(x) \varrho_t(0) \rangle = \chi(1 - e^{-2\nu k^2 t}).$$

Note that the contributions from the sound velocity precisely cancel. If we assume (6.17) to continue to hold with the correct scaling form, then for large t

$$W(t)^2 = 3a^2(\lambda^{2/3}\chi^{4/3}/2\pi)t^{2/3} \int_{-\infty}^{\infty} dk \frac{1}{k^2}(1 - g(k)). \tag{6.18}$$

The surface width increases as $t^{1/3}$ with a prefactor determined by the scaling function.

6.1 Steady states

We turn to the master equation (6.2). The problem posed is to compute the structure function $S(k,t)$. Clearly this is an impossible task. More modestly we may ask for the static $(t=0)$ structure function. We have to know then first the steady state solution to (6.2). Most commonly the steady state is found by means of detailed balance. Since we assumed no particular relationship between the α's (forward jumps) and the γ's (backward jumps), in general detailed balance cannot hold. Thus we are left with guesswork. Since the jump rates depend only on the two nearest neighbors, it is natural to try the ansatz

$$\frac{1}{Z}\exp[-\beta H(\eta) + h\sum_j \eta_j] \tag{6.19}$$

with

$$H(\eta) = -\sum_j \eta_j \eta_{j+1}. \tag{6.20}$$

h just fixes the density. Inserting (6.19), (6.20) in (6.2) one has indeed a stationary solution provided

$$\alpha_2 = e^\beta \alpha_4, \quad \alpha_2 + \alpha_4 = 2\alpha_3, \tag{6.21}$$

and

$$\gamma_2 = \alpha_2 e^{-\beta} e^{-E}, \quad \gamma_3 = \alpha_3 e^{-E}, \quad \gamma_4 = \alpha_4 e^\beta e^{-E}. \tag{6.22}$$

72

Following (6.19) β is interpreted as 'inverse temperature' (times a unit binding energy). E is regarded as the external driving field causing biased jumps. Since the corresponding potential is linear, E is the energy gained in a jump to the right. Thus (6.22) can be written in the form of a local detailed balance condition,

$$c(j, j+1, \eta) = c(j, j+1, \eta^{jj+1})\exp[-\beta(H(\eta^{jj+1}) - H(\eta)) + E(\eta_j - \eta_{j+1})]. \quad (6.23)$$

Of course, there are other choices of the jump rates satisfying (6.23). We introduced the parameter E also because it regulates the growth velocity. If $E > 0$, then the attachment dominates and the surface grows. If $E < 0$, then the crystal dissolves. For $E = 0$ both processes balance and we have the model of an equilibrium interface. In equilibrium $j(\varrho) = 0$ which implies $c(\varrho) = 0$, $j''(\varrho) = 0$. The dynamic exponent is $z = 2$. The structure function is of the standard form (6.6) with ν the bulk diffusion coefficient.

Considering the local detailed balance condition (6.23) just by itself it is tempting to try the stationary solution $Z^{-1}\exp[-\beta H + h \sum_j \eta_j]$ with

$$H(\eta) = -\sum_j \eta_j \eta_{j+1} - (E/\beta) \sum_j j \eta_j. \quad (6.24)$$

Physically, this is the energy of a lattice gas in a uniform gravitational field. If $E < 0$, then particles pile up at the bottom of the 'box'. Unfortunately, the periodic boundary conditions cannot be satisfied. Of course, the infinite system does not know about boundary conditions. In fact, there are then two stationary solutions for (6.2): the homogeneous solution (6.19), (6.20) and the inhomogeneous solution (6.19), (6.24). Since for the inhomogeneous state detailed balance holds, the average current vanishes. Clearly, as applied to surfaces, (6.19),(6.20) is the state of interest.

Returning to the rates satisfying (6.21), (6.22), physically the processes of attachment are the faster the more neighbors. Therefore $\alpha_4 > \alpha_2$ and β should be negative. In terms of a spin system, the steady state is antiferromagnetic.

At least for particular rates we have found explicitely the steady state. Its two-point function $\langle \eta_0 \eta_j \rangle_\varrho - \varrho^2$ decays exponentially. Staticly, the statistics of surface configurations is an ensemble of random walks with a one-step memory and hence $\zeta = 1/2$. Furthermore the average current $j(\varrho)$ can be computed (Brandstetter
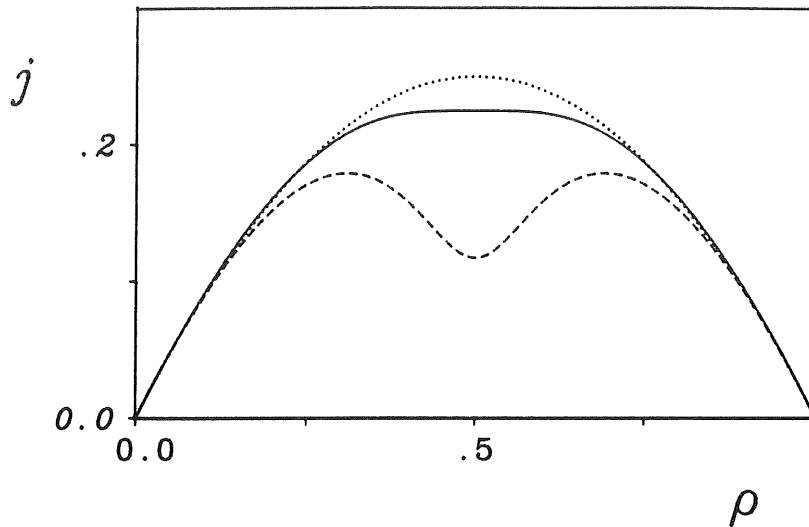
Figure 13: Average current as a function of the density for $\beta = 0$ (dotted line), $\beta = \beta_c = \frac{1}{2}\log 3$ (full line) and $\beta = -1$ (dashed line).

1990). We have then one of the few growth models for which the macroscopic inclination dependent growth velocity can be determined explicitely. In Figure 13 we show three representative examples. Note that there are exceptional densities at which $j''(\varrho) = 0$. If we adjust the average inclination to that particular value, then the surface fluctuations are governed by the linear theory, i. e. $z = 2$.

As β decreases the curvature at $\varrho = 1/2$ changes its sign. Qualitatively this can be understood as a switching between two different growth mechanisms. If β is very negative, then $\alpha_2 \ll \alpha_3$. The dominant growth is at surface steps, corresponding to a nucleation limited regime. Since a small tilt of the surface increases the step density, we expect the growth velocity to increase and hence $\lambda > 0$. On the other hand for $\beta = 0$ nucleation on flat portions of the surface and step motion occur at the same rates. The steady current of the lattice gas is proportional to $\varrho(1 - \varrho)$. Hence the growth rate is *maximal* at zero tilt and $\lambda < 0$. Such a phenomenon occurs also in higher dimensions (Amar and Family 1990a, Krug and Spohn 1990, Kim et al. 1990, Huse et al. 1990). In two dimensions the effect is even more spectacular because for vanishing λ the surface fluctuations are only logarithmic.

74

The particular role of the rates satisfying (6.21) and (6.22) has been recognized in an equilibrium context by Singer and Peschel (1980), Zwerger (1981), for driven lattice gases by Katz, Lebowitz and Spohn (1984), and for crystal growth by Gates (1988). Since the steady state is independent of the driving force, the conductivity is frequency independent. The response of the lattice gas is instantaneous. Also the bulk diffusion coefficient is given by a static average. We refer to Spohn (1990) for further details.

For general rates the steady state is not known. Monte Carlo simulations of the lattice gas indicate still a rapid decay of correlations (Katz et al. 1984). No expansion around the exactly solved cases has been tried.

Why is it so difficult to extract any kind of dynamical information from (6.2) ? After all we have something like a 1+1 dimensional field theory hence 'exactly solvable'. A way to explain the difficulty is through rewriting the generator in (6.2) as a quantum mechanical spin Hamiltonian. Rather than the general case let us consider the simplest possible case, where $\gamma_2 = \gamma_3 = \gamma_4 = 0$ ($E = \infty$, growth only) and $\alpha_2 = \alpha_3 = \alpha_4 = 1$. In particular, $\beta = 0$ which means that in the steady state all allowed configurations are equally likely. We denote the Pauli spin matrices by $\sigma = (\sigma^x, \sigma^y, \sigma^z)$. Then, identifying 1 with spin up and 0 with spin down, the generator of (6.2) reads

$$H = -\frac{1}{4}\sum_j (\sigma_j \cdot \sigma_{j+1} + i\sigma_j^x \sigma_{j+1}^y - i\sigma_j^y \sigma_{j+1}^x - 1) \tag{6.25}$$

on a ring with perodic boundary conditions. The transition probability from σ to σ' is

$$\langle \sigma | e^{-tH} | \sigma' \rangle \tag{6.26}$$

in the σ^z-representation. It is already correctly normalized as

$$\sum_{\sigma'} \langle \sigma | e^{-tH} | \sigma' \rangle = 1. \tag{6.27}$$

H is a Heisenberg Hamiltonian with complex couplings. Because of the biased jumps, H is not self-adjoint. The ground states of H (energy zero) are the same as for the ferromagnetic Heisenberg chain, namely with a factorized wave function.

Given our experience with one dimensional spin chains, it is natural to try the Bethe ansatz for the eigenfunctions of (6.25). It is claimed (Dhar 1987) that the dynamical exponent $z = 3/2$ follows from considering the low lying excitations. No details are available yet.

For the symmetric case $E = 0$ and jump rates satisfying (6.21), (6.22), the scaling form (6.6) is proved by DeMasi et al. (1986). A lower bound on $S(k,t)$ of the form $\exp[-\nu k^2 t]$ follows easily from Jensen's inequality. To establish actually the limit $k \to 0$, $t \to \infty$ with $k^2 t$ fixed is difficult.

6.2 Other one dimensional models

The mapping to driven lattice gases works also for other models. E.g. the single step model maps to a lattice gas as above with $\alpha_2 = \alpha_3 = \alpha_4 = \Gamma_+$, $\gamma_2 = \gamma_3 = \gamma_4 = \Gamma_-$. The driven lattice gas corresponding to the PNG model is a little bit more complicated (Krug and Spohn 1989). One has a collection of 'particles' (step down) and 'antiparticles' (step up). The particles move with velocity c, the antiparticles with velocity $-c$. At a collision particle and antiparticle annihilate each other. The nucleation of steps corresponds to the creation of a pair of a particle and an antiparticle with rate Γ. In the steady state particles and antiparticles have an ideal gas (uniform Poisson) distribution. The conserved quantity is $\phi = \varrho_+ - \varrho_-$, the density of particles minus the density of antiparticles. The steady state current is $j = c(\varrho_+ + \varrho_-)$. Stationarity requires $2c\varrho_+\varrho_- = \Gamma$. Thus the steady current is

$$j(\phi) = c(\phi^2 + (2\Gamma/c))^{1/2}. \tag{6.28}$$

and $j(0) = (2\Gamma c)^{1/2}$ in agreement with (4.2). As before ϕ is proportional to the average surface inclination. The corresponding growth shape is shown in Figure 3.

A further illuminating example is the Visscher-Bolsterli model for ballistic deposition of discs. The mapping to the lattice gas proceeds as for the crystal edge in Figure 12. Discs are dropped down vertically above randomly chosen positions and are allowed to roll downward along the surface until they reach

a local surface minimum. Clearly then the growth rate at a given minimum depends on its basin of attraction. In terms of the lattice gas, the jump rate of a particle at site j, which is surrounded by the local configuration

$$\eta_{j-n+1} = \eta_{j-n+2} = \ldots = \eta_j = 1,$$
$$\eta_{j+1} = \eta_{j+2} = \ldots = \eta_{j+m} = 0 \tag{6.29}$$

is given by

$$\Gamma_{nm} = \Gamma_0(m+n), \tag{6.30}$$

where Γ_0 is the number of discs deposited per unit time and unit substrate length. As shown in Chapter 4, using a more general argument, the peculiar jump rates (6.30) lead to a current (growth velocity) which is *independent* of density (inclination). To see this, we pick an arbitrary configuration η on a ring of N sites and subdivide it into $M(\eta)$ local configurations of type (6.29), containing m_j neighboring particles and n_j holes, respectively, $j = 1, \ldots, M(\eta)$. Then the total current is

$$J(\eta) = \sum_{j=1}^{M} \Gamma_0(m_j + n_j) = \Gamma_0 N \tag{6.31}$$

independent of η. The steady state corresponding to the rates (6.30) does not have a simple structure, as was erroneously claimed in Krug and Spohn (1989). Inspection of the solution for small rings ($N = 6$) indicates an effectively repulsive interaction between the lattice gas particles.

Finally, we note that the space–time histories of a particular version of an asymmetric lattice gas can be mapped onto the two dimensional six vertex model in *equilibrium* (Kandel and Domany 1990, Lebowitz 1990). Thereby one dimensional growth is related to a two dimensional equilibrium model. The dynamics is given by a parallel, discrete time algorithm. At $t = 0$ we block the particle configuration into pairs of neighboring sites. Each pair is updated independently according to the transition probabilities $T(\eta_1, \eta_2 | \eta_1', \eta_2')$. Clearly, by particle number conservation,

$$T(0,0|0,0) = T(1,1|1,1) = 1. \tag{6.32}$$

In the other cases exchanges may occur with probabilities

$$T(1,0|0,1) = p = 1 - T(1,0|1,0), \; T(0,1|1,0) = q = 1 - T(0,1|0,1), \qquad (6.33)$$

$0 < q, p < 1$. At the next time step the pairing is shifted by one lattice unit and pairs are updated according to the same rule as before. The asymmetric choice $q \neq p$ gives a growth model.

To see the connection to the six vertex model on the square lattice, we choose the diagonal as space axis and the line $x_1 = -x_2$ as time axis. The bonds carry arrows which point either right, left or up, down. Each time slice $x_2 = x_1 + t$ maps onto a lattice gas configuration: Arrows pointing up and left correspond to particles, arrows pointing down and right correspond to holes. Pairs of bonds meet at vertices in the forward time direction. Each vertex corresponds to a 'collision' event in which a particle and a hole can be exchanged. Particle number conservation leads to the ice rule for the allowed vertices: At each vertex two ingoing and two outgoing arrows have to meet. The transition matrix T translates to the Boltzmann weights of the six vertex model as $e^{-\beta \varepsilon_1} = p$, $e^{-\beta \varepsilon_2} = q$, $e^{-\beta \varepsilon_3} = 1$, $e^{-\beta \varepsilon_4} = 1$, $e^{-\beta \varepsilon_5} = 1 - q$, $e^{-\beta \varepsilon_6} = 1 - p$ (we use the standard labeling, see Lieb and Wu 1972, Baxter 1982). The symmetric choice $q = p$ lies on the boundary between the disordered and ferroelectric phase at zero electric field. The asymmetry induces an external electric field pointing along the space axis. As in the other models, one can still determine the steady state: The occupation variables at different sites are independent, but the steady state has a period of two. Only for $q = p$ the superstructure vanishes.

6.3 Higher dimensions

In $1 + 1$ dimensions we are able to obtain fairly detailed information about the steady state because surface gradients are essentially independent. As an additional bonus the dynamics of the surface gradients can be viewed as a many-particle system with a single conservation law. This certainly helps physical intuition. Although we did not present any details, it also allows one to use theoretical methods as developed in the context of kinetic theory, e.g. mode coupling

equations (van Beijeren et al. 1985, Krug 1987). Such simplifications are lost in higher dimensions. We have no theoretical result to report here, but we regard it as instructive to understand from a somewhat different perspective why higher dimensions are more difficult.

As a starting point we use the KPZ equation in the real world of $2+1$ dimensions. The surface gradient $\mathbf{u} = \nabla h$ satisfies

$$\frac{\partial}{\partial t}\mathbf{u}_t + \nabla\left(-\frac{\lambda}{2}\mathbf{u}_t^2 - \nu\nabla\cdot\mathbf{u}_t - \zeta_t\right) = 0. \tag{6.34}$$

We may regard $\mathbf{u}_t$ as the velocity field of a two dimensional fluid. Instead of the incompressibility condition $\nabla\cdot\mathbf{u}_t = 0$ it satisfies however the potential condition

$$\frac{\partial}{\partial x_1}u_{t,2} = \frac{\partial}{\partial x_2}u_{t,1}. \tag{6.35}$$

We may interpret (6.34) also as a two-component particle system where the α-current points along the α-direction. (6.35) couples then the two components. To come from a surface the gradients must satisfy an integrability condition: Line integrals over closed loops have to vanish. Even in the linear theory ($\lambda = 0$) this constraint causes a slow decay of the steady state correlations in the surface gradients. The static structure function for the surface is $(\gamma/2\nu)k^{-2}$. The gradients are then correlated in the position space as

$$\begin{aligned}\langle u_1(x_2,x_2)u_1(0,0)\rangle &= (\gamma/4\pi\nu)(x_2^2 - x_1^2)/(x_1^2 + x_2^2)^2,\\ \langle u_1(x_1,x_2)u_2(0,0)\rangle &= (\gamma/2\pi\nu)x_1x_2/(x_1^2 + x_2^2)^2.\end{aligned} \tag{6.36}$$

The correlations decay as $|\mathbf{x}|^{-2}$ without definite sign.

To illustrate the microscopic gradient dynamics we consider the two–dimensional single step model (Meakin et al. 1986b). The height variables $h_t(\mathbf{x})$ at sites $\mathbf{x} = (i,j)$ take only integer values, which are even/odd for $i+j$ even/odd. They also satisfy the single step condition $|h_t(\mathbf{x}) - h_t(\mathbf{y})| = 1$ for $|\mathbf{x} - \mathbf{y}| = 1$. As in one dimension each allowed height configuration can be mapped onto a spin configuration (van Beijeren 1977). To each bond in the dual lattice we give a direction (arrow) in such a way that looking along the arrow the higher point of the surface is to the right. The continuum integrability condition (6.35) translates to the ice rule. There can be only closed loops, i.e. no sinks and sources. Thus

79

at each site of the dual lattice there must be two incoming and two outgoing arrows. The allowed vertices are those of the six vertex model.

The surface grows by filling up local minima with the rate Γ_+ : If $h_t(i+1,j) + h_t(i,j+1) + h_t(i-1,j) + h_t(i,j-1) - 4h_t(i,j) = 4$ (local minimum), then $h_t(i,j)$ increases to $h_t(i,j) + 2$ with rate Γ_+. Correspondingly, we also introduce evaporation processes: If $h_t(i+1,j) + h_t(i,j+1) + h_t(i-1,j) + h_t(i,j-1) - 4h_t(i,j) = -4$ (local maximum), then $h_t(i,j)$ decreases to $h_t(i,j) - 2$ with rate Γ_-. The translation to the six vertex model is straightforward. A local minimum corresponds to a closed four loop (plaquette) oriented counter clockwise. As the height increases, it changes its orientation (with rate Γ_+). The reverse process (with rate Γ_-) corresponds to a height decrease.

If $\Gamma_+ = \Gamma_-$, then in the steady state all allowed configurations are equally likely. This is the situation of an equilibrium surface above the roughening transition. Sutherland (1968) computed the arrow-arrow correlations. Their large distance behavior is as in (6.36). (For the finite temperature six vertex model we refer to Lieb and Wu (1972). It models ferroelectrics and the equilibrium roughening transition, cf. van Beijeren and Nolden (1987).) For the growing surface one has $\Gamma_+ > \Gamma_-$. At present no theoretical method is available for the prediction of steady state correlations. Numerically one finds $\zeta \simeq 0.37$ (Meakin et al. 1986b, Liu and Plischke 1988), corresponding to a static height structure function $S(k) \sim |k|^{-2.74}$ for small k and hence a decay of the arrow-arrow correlation as $|x|^{-1.26}$. Thus, in contrast to the driven one dimensional lattice gases, the steady state correlations depend on the bias. The steady states for $\Gamma_+ \neq \Gamma_-$ should all be in the same universality class with a crossover to the equilibrium behavior as $\Gamma_+ \to \Gamma_-$.

The difference between the one dimensional and the two (and higher) dimensional case can be traced back to a basic topological property: In one dimension the number of local maxima is equal to the number of local minima for *any* surface configuration. This property, which is no longer true for higher dimensions, is the reason for the simplicity of the steady states in $d = 1$.

6.4 Shock fluctuations

Shock formation and shock propagation are a traditional subject of fluid dynamics. As in growth processes there is a traveling front. We may ask then for fluctuations in the position of the front. Properly speaking, our investigation should be carried out in the context of nonlinear hydrodynamics with fluctuating currents. To our knowledge, such a program has not been achieved. Instead we discuss a simplified model. Our main aim is yet another illustration of the theory developed.

As in the previous sections we consider driven lattice gases, for simplicity the infinite temperature case. The lattice gas is now in d dimensions and the driving force points along the positive 1-axis. Subject to the constraint of single occupancy, the jump rates are $1 \pm \alpha$ along the ± 1-axis, $0 < \alpha \leq 1$, and 1 along all other directions. Before we were in $d = 1$ with a uniform density of particles. For a shock we need an inhomogeneous density distribution. We impose therefore an average density, ϱ, where $\varrho(x) = \varrho_-$ for $x_1 < 0$ and $\varrho(x) = \varrho_+$ for $x_1 \geq 0$, $\varrho_- < \varrho_+$. For visualization, the extreme case $\varrho_+ = 1$ is helpful. Since the particles in the right half space are stuck, the particles in the left half space are pushed against a solid and pile up. With fluctuations the front moves to the left. Our usual picture of a stable phase growing at the expense of an unstable phase is not applicable here. Rather we have two stable, spatially homogeneous steady states separated by a front moving through external driving.

Without further information, we would expect naively the front to smear out diffusively. Certainly this happens when particles jump independently. However, the interaction due to the single occupancy constraint stabilizes the front. We will argue that the shock fluctuations are governed by the linear ($\lambda = 0$) KPZ equation. In particular, in three dimensions this implies that the front has only logarithmic fluctuations.

The steady state current of the lattice gas is

$$\mathbf{j}(\varrho) = 2\alpha\varrho(1 - \varrho)\mathbf{e_1}. \tag{6.37}$$

If we assume local equilibrium, then the Euler equation for the density reads

$$\frac{\partial}{\partial t}\varrho_t + \frac{\partial}{\partial x_1}[2\alpha\varrho_t(1-\varrho_t)] = 0. \tag{6.38}$$

(Note that the density is the only locally conserved field.) Equation (6.38) is a text book example of a nonlinear hyperbolic equation leading to shock formation: Even if the initial data are smooth, the solution of (6.38) may develop discontinuities. To determine the location of the shock (6.38) has to be supplemented then by the entropy condition (for an introduction see Chorin and Marsden (1979)). For the inital condition from above the solution to (6.38) is a sharp shock which travels with velocity

$$v_s = 2\alpha(1-\varrho_+ - \varrho_-). \tag{6.39}$$

If $\varrho_- + \varrho_+ > 1$, then particles pile up and the shock moves to the left, whereas for $\varrho_+ + \varrho_- < 1$ the shock travels to the right. Phenomenologically it is natural to add a viscosity term, as $\nu\Delta\varrho_t$, to (6.38). This smears out the shock over a length $\sqrt{\nu/\alpha}$. The shock velocity remains unchanged.

Since the dynamics is local, we can use the KPZ equation as large scale theory. To determine λ the inclination dependent growth velocity is then needed. If one solves (6.38) with an initial step along a plane tilted relative to the $\{x_1 = 0\}$ plane, then the growth velocity along the 1-axis is again v_s, also if the viscosity term $\nu\Delta\varrho_t$ is added. Even without computation, this result follows from mass conservation together with the fact that the densities away from the shock are determined by the initial conditions and do not change in time. We conclude that $\lambda = 0$ and that the linear theory governs the shock fluctuations. (The one-dimensional problem is studied by Boldrighini et al. (1989), Gärtner and Presutti (1990), Ferrari et al. (1990).)

7 Growth and Percolation

7.1 First passage percolation

The connection between growth processes and percolation has been cultivated mostly in the probabilistic camp. Besides proving some basic properties, like the

existence of an asymptotic shape, this approach could deepen our understanding since growth is viewed as a sort of optimization problem. Somewhat unexpected, we will find a close relation to directed polymers.

In standard percolation on the simple hypercubic lattice $\mathbb{Z}^d$ a bond is open (occupied, present) with probability p and closed (vacant, absent) with probability $1 - p$. (We restrict our attention to bond percolation with independent bond probabilities. There is also the essentially equivalent site percolation.) One investigates such problems as the size of a connected cluster containing the origin, the probability for the origin to be connected to infinity, etc. To a large extent the interest in percolation stems from the theory of second order phase transitions (Stauffer 1985).

The name 'percolation' signals the picture of a fluid being pushed into solid material (like a filter or a rock). The fluid crosses a given bond if open. With this background it is natural to assume that it takes some time for the fluid to spread across a bond. To model such a physical situation we assign, independently, to each bond b, $b = \{\mathbf{x},\mathbf{y}\}$, $|\mathbf{x} - \mathbf{y}| = 1$, a random variable, τ_b, $\tau_b \geq 0$. τ_b is the amount of time the fluid needs to cross b. A path, w, in our lattice is a sequence of connected bonds. The *passage time* from $\mathbf{x}$ to $\mathbf{y}$ along the path w, w starts at $\mathbf{x}$ and ends at $\mathbf{y}$, is then given by

$$\tau_{\mathbf{x}\mathbf{y}}(w) = \sum_{b \in w} \tau_b. \tag{7.1}$$

The fluid is injected at the origin. One would like to know the time a certain site is first reached by the fluid. Therefore we define the *first passage time* from $\mathbf{0}$ to $\mathbf{x}$ by

$$\tau_{\mathbf{x}} = \min\{\tau_{\mathbf{0}\mathbf{x}}(w) \mid w \text{ is a path from } \mathbf{0} \text{ to } \mathbf{x}\}. \tag{7.2}$$

First passage percolation studies the asymptotics of the first passage times. Besides the point to point first passage also the point to line first passage is of interest. We characterize a hyperplane, $H(\mathbf{r})$, through a vector $\mathbf{r}$: The plane is orthogonal to $\mathbf{r}$ and its smallest distance from the origin is $r = |\mathbf{r}|$. The first passage time from the origin to the hyperplane $H(\mathbf{r})$ is then

$$\tau_{\mathbf{r}} = \min\{\tau_{\mathbf{x}} \mid \mathbf{x} \text{ lies beyond } H(\mathbf{r}) \text{ as seen from the origin }\}. \tag{7.3}$$

Standard percolation can be understood as the particular case where $\tau_b = 1$ with probability p and $\tau_b = \infty$ with probability $1 - p$.

The connection to growth is immediate. We simply ask for the set of sites which are reached by the fluid at time t. This is a random set $A_t \subset \mathbb{Z}^d$ with $A_0 = \{0\}$. Clearly A_t is defined by

$$A_t = \{\mathbf{x} \,|\, \tau_\mathbf{x} \leq t\}. \tag{7.4}$$

A_t is a cluster growing from a single seed.

It may help to illustrate the connection of first passage percolation and growth through a simple example. Let us consider a random walk, on a one dimensional lattice, starting at the origin. We may study then the transition probability, $p_t(j)$ to find the walker at site j at time t. This corresponds to growth. On the other side we may introduce a boundary at L and ask for the time the walker first hits the boundary. This is the first passage problem. To amplify even further: For the one dimensional lattice let τ_b have an exponential distribution with mean α. A_t is then simply an interval expanding at both ends. The probability for the edge to be at site j at time t is $p_t(j) = \frac{1}{j!}(t/\alpha)^j e^{-t/\alpha}$. In particular the growth velocity is $1/\alpha$. On the other hand the first passage time to the site j has the distribution $(j/\alpha)e^{-jt/\alpha}$, because the minimum of a sum of independent exponentials is again exponential. As a consequence, $\frac{1}{j}\tau_j \to \alpha$ as $j \to \infty$.

Actually, we introduced already two growth models defined through first passage percolation.

(i) Let τ_b have an exponential distribution with mean 1. This gives the bond version of the Eden model of the Introduction: A perimeter site becomes part of the growing cluster with a rate equal to the number of nearest neighbor sites already belonging to the cluster.

(ii) Let τ_b have the discrete distribution $\sum_{n=1}^{\infty} p(1-p)^{n-1}\delta(t-n)$. This is the Richardson model (discrete time version of the Eden model). In one time step (here set equal to one) an already infected site infects a neighboring site with probability p and does not infect it with probability $1 - p$.

Some rigorous results

It is impossible to pay justice to a beautiful probabilistic development. Good reviews are available (Smythe and Wierman 1978, Kesten 1986, Durrett 1988). We 'explain' only a few results of relevance in our context.

The most basic result is the existence of an asymptotic cluster shape, in the sense that the scaled down random set $\frac{1}{t}A_t = \{\frac{1}{t}\mathbf{x} \mid \mathbf{x} \in A_t\}$ tends to a deterministic limit, $\overline{A}$, with probability one as $t \to \infty$. Of course, $\overline{A}$ is the macroscopic form discussed in Chapter 2. Let p_c be the critical bond percolation probability. If $\mathrm{Prob}(\{\tau_b = 0\}) < p_c$, then $\overline{A}$ is a compact and convex subset of $\mathbb{R}^d$. (Otherwise $\overline{A}$ would be all of $\mathbb{R}^d$. For the behavior close to p_c cf. Chayes et al. (1986).) One also knows that $\overline{A}$ depends continuously on τ_b. This means the following: Let $F(t)$ be the distribution function for τ_b, $F(t) = \mathrm{Prob}(\{\tau_b \leq t\})$. The first passage percolation with distribution $F(t)$ defines a macroscopic shape $\overline{A}$. If $F_n(t) \to F(t)$ as $n \to \infty$ with the exception of the jump points of F, then also the corresponding shapes converge. Note that no recipe to compute $\overline{A}$ is given.

The strategy of the proof is similar to the existence of the free energy for systems in equilibrium. The first passage time from the origin to a plane is subadditive, which ensures the existence of the limit

$$\lim_{\lambda \to \infty} \frac{1}{\lambda r} \tau_{\lambda \mathbf{r}} = c(\mathbf{r}/r) \tag{7.5}$$

with probability one. Thus the first passage time scales linearly with the distance of the plane from the origin. $c(\mathbf{r}/r)$ is called the time constant. It depends on the orientation of the plane. As in our one dimensional example above, the time constant is inverse to the growth velocity,

$$c(\mathbf{r}/r)v(\mathbf{r}/r) = 1. \tag{7.6}$$

Using (7.5) the macroscopic shape $\overline{A}$ is then built up from planes.

Very little is known about the shape on a rigorous level. One has conditions on the distribution of τ_b, which imply that the form has flat pieces (Kesten 1986). One example is the Richardson model, which will be discussed in detail below. Another result concerns the asymptotics in large dimensions. For the continuous time Eden model we consider the growth along one of the lattice axis,

say $e_1 = (1, 0, \ldots, 0)$. Lower and upper bounds on the growth velocity imply

$$v(e_1) \approx 2d/\log d \qquad (7.7)$$

for large d (Dhar 1988).

Fluctuations

For first passage percolation the macroscopic object is the time constant $c(\mathbf{r}/r)$ of (7.5) and associated with it the Wulff constructed shape $\overline{A}$. Two fluctuating quantities are of obvious interest. (1) $c(\mathbf{r}/r)$ gives the mean first passage time, $\langle \tau_\mathbf{r} \rangle \approx r c(\mathbf{r}/r)$ for large r. What is then the typical width of the first passage time distribution? (2) Instead of the time we may also consider the *location* of the first passage in the plane $H(\mathbf{r})$. Denoting this location by $\mathbf{x}(\mathbf{r}) \in H(\mathbf{r})$, how does $\mathbf{x}(\mathbf{r})$ then scatter typically around its average?

We blow up $\overline{A}$ self similarly as $t\overline{A}$. Let $\mathbf{x_0}$ be the point of first contact with $H(\mathbf{r})$ and let t_0 be the time of contact. Then $\langle \tau_\mathbf{r} \rangle \simeq t_0$ and $\langle \mathbf{x}(\mathbf{r}) \rangle \simeq \mathbf{x_0}$ for sufficiently large r. We consider the surface of the cluster A_t at times slightly less than t_0 and close to $\mathbf{x_0}$. Let h_t be the height of the surface measured relative to the hyperplane $H(\mathbf{r})$. We decompose h_t into a deterministic part and a fluctuating part, denoted by $\tilde{h}_t$. Then $h_t(\mathbf{x}) = v(\mathbf{r}/r)(t - t_0) - \lambda(\mathbf{x} - \mathbf{x_0})^2/2t + \tilde{h}_t(\mathbf{x})$, where we assumed that $\overline{A}$ has a nonvanishing curvature λ at $\mathbf{x_0}/t_0$. From the general scaling theory we know that $\langle \tilde{h}_t(\mathbf{x})^2 \rangle^{1/2}$ grows as $t^{\zeta/z}$. The cluster surface crosses the plane $H(\mathbf{r})$ with a finite velocity. Therefore the fluctuations in $\tilde{h}_t(\mathbf{x})$ translate linearly to fluctuations in $\tau_\mathbf{r}$ and

$$\langle (\tau_\mathbf{r} - \langle \tau_\mathbf{r} \rangle)^2 \rangle^{1/2} \sim r^{\zeta/z}. \qquad (7.8)$$

Typical scatters of $\mathbf{x}(\mathbf{r})$ originate in the events where the fluctuations in the surface just reach $H(\mathbf{r})$. Thus

$$\langle (\mathbf{x}(\mathbf{r}) - \langle \mathbf{x}(\mathbf{r}) \rangle)^2 \rangle \sim t \langle \tilde{h}_t(\mathbf{x})^2 \rangle^{1/2} \sim t^{1+\zeta/z} = t^{2/z}, \qquad (7.9)$$

where in the last step we used the scaling relation (3.18). For example in two dimensions the first passage time distribution has a width of the order $r^{1/3}$ whereas the first passage location scatters as $r^{2/3}$.

86

Directed first passage percolation

In directed first passage percolation the fluid spreads across a bond only along a preassigned direction. Again for simplicity, let us only consider the two dimensional case. In the first quadrant all bonds are positively oriented. We study the first passage from the origin to the line $\{x_1 + x_2 = n\}$. The reader will have noticed immediately that we have described nothing else than the ground state problem of a directed polymer. The walks are directed along the (1,1) direction. Each walk has n steps. Adding the passage times, τ_b, along the walk corresponds to adding up the random potentials V_b. The minimal energy is the first passage time. The time constant is the ground state energy per length. As for undirected first passage percolation the growing cluster is the set of sites reached by the fluid at time t. This cluster is described by the standard theory. No surprise then, the fluctuations of directed first passage percolation are again governed by (7.8), (7.9), which of course coincide with (5.45) and (5.47). (Large d bounds for the time constant are proved by Cox and Durrett (1983).)

7.2 Facets and directed percolation

We noted in Chapter 4 that several synchronous growth models exhibit a faceting transition. Here we study this transition in more detail, using as an example the two dimensional Richardson model (Richardson 1973). Time runs in discrete steps, $t = 0, 1, 2, \ldots$. Initially the cluster consists only of the origin. A perimeter site at time t becomes part of the cluster at time $t + 1$ with probability p. By symmetry it suffices to consider only the cluster in the upper right quadrant of the square lattice. Clearly the growth velocity v_1 along the diagonal cannot exceed $v_{\max} = 1/\sqrt{2}$ in units of the lattice spacing. For small p $v_1(p)$ is linear in p. At some critical value p_c, $v_1(p_c) = v_{\max}$ and remains constant up to $p = 1$. For $p > p_c$ there is a sector enclosing the diagonal in which the cluster edge is faceted and propagates at the maximal speed $1/\sqrt{2}$. At $p = 1$ the sector contains the whole quadrant and the cluster forms a diamond. The surprise is to have facets already at values of p with $p_c < p < 1$.

This can be understood through a mapping to directed percolation (Durrett and Liggett 1981, Savit and Ziff 1985, Kertész and Wolf 1989, Krug et al. 1990). We draw the line $x_1 + x_2 = t$ which marks the range of influence of the origin. The cluster at time t cannot extend beyond this line. We record all sites of the cluster located on the line at time t and call this set B_t. B_t is determined through a graphical rule: Each site of the quadrant is open with probability p and closed with probability $1 - p$, just as in ordinary (site) percolation. However, we orient the bonds positively in the direction of the diagonal. A site x in $\{x_1 + x_2 = t\}$ belongs to B_t if x is connected to the origin by a path of adjacent open sites and bonds respecting the orientation. This is the so called directed percolation problem, in our case the symmetric site version (for an introduction see Kinzel 1983). For $p < p_c$, there are too many closed sites and the set B_t will be empty for large t. The infection spreading from the origin dies out. This means that $v_1 < 1/\sqrt{2}$. However, for $p > p_c$ the infection survives and B_t is a set expanding linearly, of course with some holes. Close to the diagonal the surface sticks then to the line $\{x_1 + x_2 = t\}$ with random excursions of a few lattice spacings. The surface width is $\mathcal{O}(1)$ and purely intrinsic, cf. Section 3.2. In two dimensions the percolation threshold is at $p_c \simeq 0.705489$ (Essam et al. 1988).

To proceed we need some concepts from directed percolation theory. We focus first on the *subcritical case*, $p < p_c$. The infected set B_t has a typical survival time ξ_t and a typical (maximal) spatial extension ξ_r. Both lengths diverge as $p \to p_c$, defining the correlation length exponents ν_t and ν_r,

$$\xi_t \sim |p - p_c|^{-\nu_t} \ , \ \xi_r \sim |p - p_c|^{-\nu_r} \tag{7.10}$$

with $\nu_t > \nu_r$. In two dimensions $\nu_t \simeq 1.733$ and $\nu_r \simeq 1.097$ (Essam et al. 1988). When viewed as a cluster on the square lattice, the infection history is club-shaped with an extension ξ_t along the diagonal and ξ_r perpendicular to it. As $p \to p_c$ typical clusters become increasingly elongated with an opening angle φ_0 relative to the diagonal, $\varphi_0 \sim \xi_r/\xi_t \sim |p - p_c|^{\nu_t - \nu_r}$. Let us now choose a ray forming some angle φ with the diagonal and ask for the typical extension $\xi(\varphi)$ of the directed percolation cluster along that ray. Obviously $\xi(\varphi) = 0$ for $\varphi > \varphi_0$ and

$\xi(0) = \xi_t$. This suggests the scaling form

$$\xi(\varphi) = \xi_t f(\varphi/\varphi_0), \qquad (7.11)$$

where $f(x) = 0$ for $x > 1$, $f(0) = 1$, and $f(x)$ has a quadratic maximum at $x = 0$, $\xi(\varphi) \approx \xi_t(1 - a(\xi_t/\xi_r)^2 \varphi^2)$ for $\varphi \ll \varphi_0$.

To see how (7.11) relates to the growth shape of the Richardson cluster (not to be confused with the directed percolation clusters), we put a coordinate axis through the origin perpendicular to the diagonal and consider the scaled shape function $g(y)$ relative to this axis ($g(y)$ was defined in Equation (2.3)). Close to $\varphi = 0$ we have $y \approx g(0)\varphi$ ($g(0) = v_1$). For a fixed angle φ, the distance between the cluster edge and the line $\{x_1 + x_2 = t\}$ is $t(v_{\max} - g(y))$ at time t. This distance becomes observable (of the order of a few lattice spacings) after a time of the order $\xi(\varphi)$, hence

$$v_{\max} - g(y) \sim \xi(\varphi)^{-1}. \qquad (7.12)$$

Inserting the expansion of (7.11) for $\varphi \ll \varphi_0$ it follows that $v_{\max} - v_1 \sim \xi_t^{-1}$ and that the curvature of the cluster edge vanishes as

$$g''(0) \sim -\xi_t/\xi_r^2 \sim -(p_c - p)^{2\nu_r - \nu_t}. \qquad (7.13)$$

At the critical point $p = p_c$, $\xi(\varphi)$ is finite for any $\varphi \neq 0$. The scaling form (7.11) then requires $\xi(\varphi)$ to diverge for $\varphi \to 0$ as $\xi(\varphi) \sim \varphi^{-\nu_t/(\nu_t - \nu_r)}$, and therefore using (7.12) we obtain the singular growth shape

$$g(0) - g(y) \sim |y|^{\nu_t/(\nu_t - \nu_r)}, \quad p = p_c. \qquad (7.14)$$

The above considerations apply equally well to d-dimensional surfaces, corresponding to $(d+1)$-dimensional directed percolation, although the exponents ν_t and ν_r depend on dimension of course. The upper critical dimension of directed percolation is $d_c + 1 = 5$. For $d \geq 4$, $\nu_t = 1$ and $\nu_r = 1/2$ independent of d, while $\nu_t/\nu_r < 2$ for $d < 4$ (Kinzel 1983). In the mean field regime $d > 4$ the power law (7.13) is replaced by a logarithmic behavior, $g''(0) \sim 1/\log(p_c - p)$, as will be shown explicitly in Chapter 8.

The critical behavior of the inclination dependent growth velocity $v(u)$ is obtained by simply inverting the Legendre transform (2.6). From (2.7) we conclude

that the curvature (and hence the coupling constant λ in the KPZ equation, cf. (5.11)) diverges for $p \to p_c$ as $v''(0) \sim (p_c - p)^{\nu_t - 2\nu_r}$, and logarithmically for $d > 4$. At criticality $v(u)$ is of the singular form (2.12), $v(u) - v(0) \sim |u|^\alpha$ with

$$\alpha = \nu_t / \nu_r. \tag{7.15}$$

Via (3.20) this determines the relation between the exponents ζ and z of the shape fluctuations. The dynamic exponent z can be obtained by noting that at p_c the spatial spread of the infection (conditioned on survival) grows with time as $\xi_r(t) \sim t^{\nu_r/\nu_t}$. This is identified with the surface correlation length $\xi_\parallel(t)$ in Equation (3.6) and leads to (Kertész and Wolf 1989)

$$z = \nu_t / \nu_r. \tag{7.16}$$

From (7.15) and (7.16) we conclude, using (3.20), that

$$\zeta = 0 \tag{7.17}$$

independent of the surface dimension. Numerical simulations at p_c indicate that the surface width increases logarithmically, $W(t) \sim (\log t)^{\zeta'}$, where $\zeta' \simeq 0.4 - 0.5$ in two dimensions (Kertész and Wolf 1989, Krug and Meakin 1990).

In the *supercritical regime* $(p > p_c)$ the set B_t of infected sites spreads linearly at some speed $c(p)$. The size of the facet of the Richardson cluster is $2ct$ at time t, so the leading behavior of the growth velocity is $v(u) \approx v_{\max} + c|u|$ (see Equation (2.10)). The exponent in (2.12) is $\alpha = 1$, hence the scaling relation (3.20) predicts that fluctuations spread at a finite velocity, $z = 1$ (Krug and Spohn 1988). As $p \to p_c$ from above, c vanishes as $(p - p_c)^{\nu_t - \nu_r}$ (Kinzel 1983). The directed percolation clusters extend to infinity within the angle $\varphi_c(p) = \arctan(c(p))$ from the diagonal (the 'percolation cone'). Thus the direction dependent correlation length $\xi(\varphi)$ is infinite for $\varphi < \varphi_c$ and finite for $\varphi > \varphi_c$. The behavior of the shape function $g(y)$ close to the facet can be obtained from (7.12), once we know how $\xi(\varphi)$ diverges as $\varphi \to \varphi_c$ from above. We define the *supercritical correlation length exponent* ν through

$$\xi(\varphi) \sim (\varphi - \varphi_c)^{-\nu}. \tag{7.18}$$

90

This exponent is related to the fuzziness of the boundary of the set B_t (Krug et al. 1990). We pick a ray at an angle $\varphi = \varphi_c + \triangle\varphi$ outside the percolation cone. At time t the distance between the ray and the cone boundary is $t\triangle\varphi$. For $t \sim \xi(\varphi)$ this distance is comparable to the width $W_B(t)$ of the boundary. To determine $W_B(t)$, we note that the growth of the supercritical cluster B_t is yet another example of local growth. Hence its edge fluctuations are governed by the general theory of a $(d-1)$-dimensional growing surface (recall that d is the surface dimension of the Richardson cluster) and $W_B(t) \sim t^{\zeta_{d-1}/z_{d-1}}$. We conclude then that

$$\nu_d = \frac{z_{d-1}}{z_{d-1} - \zeta_{d-1}}. \tag{7.19}$$

In particular, $\nu_1 = 2$ and $\nu_2 = 3/2$. The result for $d = 1$ has been noted previously (Grassberger and de la Torre 1979, Domany and Kinzel 1981, Harms and Straley 1982). It should be emphasized that the exponent ν arises from purely kinetic considerations and is in no way related to the critical point of directed percolation.

Using (7.12), Equation (7.18) is rewritten in terms of the shape function $g(y)$ as

$$g(c) - g(c + \epsilon) \sim \epsilon^\nu \tag{7.20}$$

(recall that the infection speed c determines the location of the facet). Comparing to (2.10) we obtain the exponent δ of the next to leading term of the growth velocity $v(u) = v_{\max} + c|u| + \mathcal{O}(|u|^\delta)$,

$$\delta = \nu/(\nu - 1) = z_{d-1}/\zeta_{d-1}. \tag{7.21}$$

There are several surprising features to (7.20) and (7.21). Firstly, the shape fluctuations of a $(d-1)$-dimensional surface show up in the d-dimensional macroscopic cluster shape. Secondly, the result $\nu = 3/2$ for a three dimensional cluster $(d = 2)$ happens to coincide with the behavior of equilibrium crystals below the roughening temperature (van Beijeren and Nolden 1987). Needless to say, the 3/2-power law has a totally different origin in that case. Thirdly, the correction exponent δ takes integer values ($\delta = 2$ and 3 resp.) in the exactly solved cases $d = 1$ and 2. If one could show generally that only integer powers of $|u|$ appear in the expansion of $v(u)$, this would lend support to the conjecture that z/ζ is

91

an integer for any d (Wolf and Kertész 1987, Kim and Kosterlitz 1989, Zhang 1989). Finally we note that in high dimensions one expects $\zeta \to 0$, $z \to 2$ and hence $\delta \to \infty$, $\nu \to 1$. This is supported by the mean field calculation in Chapter 8, but it contradicts the Cayley tree result of Harms and Straley (1982), who find $\nu = 2$.

8 An Approximation of Mean Field Type

One of the most useful concepts in equilibrium statistical mechanics is the mean field approximation. Of course, we now understand that fine details, as the critical exponents at a second order phase transition, cannot be correctly predicted by this method. But the overall phase diagram, the free energy and susceptibilities are reproduced qualitatively by mean field theory, if applied with the appropriate caution.

We want to explain that for growth processes there is an approximation in a similar spirit. Mean field type approaches have repeatedly appeared in the literature, both in discrete (Bensimon et al. 1984b, Savit and Ziff 1985, Cheng et al. 1987) and continuum (Nauenberg 1983, Nauenberg et al. 1983, Ball et al. 1984, Parisi and Zhang 1985) formulations. However it has not been commonly recognized what kind of useful information these theories contain, and how it can be extracted. Here we give a general treatment and apply our method to the problem of growth shapes in the Eden and Richardson models. No information about kinetic roughening is obtained, since the exponent ζ/z always takes its $d \to \infty$ value of zero. The mean field approach to ballistic deposition (Bensimon et al. 1984b) is discussed in detail elsewhere (Krug and Meakin 1990).

As explanatory example we choose the continuous time Eden model in its bond version. This time we need a little bit of notation. We let $\eta_{\mathbf{x}}$ be the occupation variable at the site $\mathbf{x} \in \mathbb{Z}^d$, $\eta_{\mathbf{x}} = 0$ if site $\mathbf{x}$ is vacant and $\eta_{\mathbf{x}} = 1$ if site $\mathbf{x}$ is occupied. In the course of time $\eta_{\mathbf{x}}$ will change from zero to one (the reverse process is forbidden). Such an event happens with rate $c_{\mathbf{x}}(\eta)$, which is

proportional to the number of 'infected' neighbors, i.e.

$$c_{\mathbf{x}}(\eta) = (1 - \eta_{\mathbf{x}}) \sum_{\mathbf{e}, |\mathbf{e}|=1} \eta_{\mathbf{x}+\mathbf{e}}, \qquad (8.1)$$

where for simplicity we fixed the time scale. The master equation reads then

$$\frac{d}{dt} f_t(\eta) = L f_t(\eta) \qquad (8.2)$$

with

$$Lf(\eta) = \sum_{\mathbf{x}} c_{\mathbf{x}}(\eta)[f(\eta^{\mathbf{x}}) - f(\eta)]. \qquad (8.3)$$

Here $\eta^{\mathbf{x}}$ is the configuration η with the occupancy at $\mathbf{x}$ changed from zero to one. The formal solution to (8.2), $e^{Lt}(\eta, \eta')$, is the probability to have the configuration η' at time t given the initial configuration η. Now the average occupation is governed by

$$\begin{aligned} \frac{d}{dt} \langle \eta_{\mathbf{x}} \rangle_t &= \langle L\eta_{\mathbf{x}} \rangle_t \qquad (8.4) \\ &= \langle (1 - \eta_{\mathbf{x}}) \sum_{\mathbf{e}, |\mathbf{e}|=1} \eta_{\mathbf{x}+\mathbf{e}} \rangle_t. \end{aligned}$$

The mean field approximation consists in neglecting correlations on the right hand side. If we define $\tilde{\varrho}_t(\mathbf{x}) = \langle \eta_{\mathbf{x}} \rangle_t$, then, in this approximation,

$$\frac{\partial}{\partial t} \tilde{\varrho}_t(\mathbf{x}) = (1 - \tilde{\varrho}_t(\mathbf{x})) \sum_{\mathbf{e}, |\mathbf{e}|=1} \tilde{\varrho}_t(\mathbf{x}+\mathbf{e}). \qquad (8.5)$$

A representative initial condition for (8.5) is $\tilde{\varrho}_0(\mathbf{0}) = 1$ and $\tilde{\varrho}_0(\mathbf{x}) = 0$ for $\mathbf{x} \neq 0$. We are interested in the macroscopic shape. There is no easy way to solve the nonlinear equation (8.5). However, we really need only the inclination dependent macroscopic growth velocity. If the growth direction is characterized by the unit vector $\mathbf{n}$, then the appropriate initial condition for (8.5) is $\tilde{\varrho}_0(\mathbf{x}) = 1$ for $\mathbf{n} \cdot \mathbf{x} < 0$ and $\tilde{\varrho}_0(\mathbf{x}) = 0$ for $\mathbf{n} \cdot \mathbf{x} > 0$. With the solution ansatz $\tilde{\varrho}_t(\mathbf{x}) = \varrho_t(\mathbf{n} \cdot \mathbf{x})$, Equation (8.5) reduces to the *one dimensional* equation

$$\frac{\partial}{\partial t} \varrho_t(x) = (1 - \varrho_t(x)) \sum_{\mathbf{e}, |\mathbf{e}|=1} \varrho_t(x + \mathbf{n} \cdot \mathbf{e}). \qquad (8.6)$$

(Properly speaking, we should take for $\mathbf{n}$ a vector with integer entries and produce the general case through approximation.) We have to solve (8.6) with the

93

initial condition $\varrho_0(x) = 1$ for $x < 0$, $\varrho_0(x) = 0$ for $x \geq 0$. Physically we expect as solution a front traveling with velocity $v(\mathbf{n})$ for large t. This leads to a

Digression on traveling fronts and minimal speed

The simplest and best understood equation with a traveling front is the Fisher-Kolmogorov equation (Fisher 1937, Kolmogorov et al. 1937). One version of it reads

$$\frac{\partial}{\partial t}\varrho_t = \frac{\partial^2}{\partial x^2}\varrho_t + \varrho_t(1 - \varrho_t) \tag{8.7}$$

with initial condition $\varrho_0(x) = 1$ for $x \leq 0$ and $\varrho_0(x) \to 0$ for $x \to \infty$. To obtain a traveling front we make the ansatz

$$\varrho_t(x) = w(x - ct). \tag{8.8}$$

w satisfies then

$$w'' + cw' + w(1 - w) = 0. \tag{8.9}$$

We interpret (8.9) as the equation of motion of a mechanical particle with friction coefficient c rolling down the potential hill $\frac{1}{2}w^2(1 - \frac{2}{3}w)$. The boundary conditions are $w(-\infty) = 1$ and $w(\infty) = 0$. Clearly (8.9) does not fix c. If we assume an exponential decay as e^{-qx} for $x \to \infty$, then the corresponding velocity is

$$c(q) = q + \frac{1}{q}. \tag{8.10}$$

Thus any $c(q) \geq 2$ is allowed. For $c < 2$ the solution to (8.9) overshoots at $w = 0$ and becomes negative, which is not admissable. Note that the front is exponentially sharp, i.e. $\zeta/z = 0$. A more careful analysis of the Fisher-Kolmogorov equation (Aronson and Weinberger 1978, Bramson 1983, 1987) shows that if the initial density $\varrho_0(x)$ decays as e^{-qx} for large x, then it travels with speed $c(q)$ for large t provided $q \leq 1$. For $q > 1$ the speed is always the minimal speed

$$c^* = \min_q c(q). \tag{8.11}$$

In particular, an initial step travels with speed c^*. The mechanism behind is not difficult to unterstand. $\varrho_t = 0$ is an unstable solution of Equation (8.7), $\varrho_t = 1$ is

94

stable. The slower the decay at infinity, the more effectively $\varrho_t(x)$ is broken away from zero and the faster the solution travels.

We have to issue one word of caution. Let us consider the Fisher-Kolmogorov equation with some different nonlinearity, say

$$\frac{\partial}{\partial t}\varrho_t = \frac{\partial^2}{\partial x^2}\varrho_t + (\lambda\varrho_t + \varrho_t^2)(1-\varrho_t) \qquad (8.12)$$

with step initial conditions. From the large x decay, as above, the minimal speed is $c^*(\lambda) = 2\sqrt{\lambda}$. This result is valid however only for $\lambda \geq \lambda_c = \frac{1}{2}$. For $\lambda < \lambda_c$ the asymptotic velocity depends on the full steady solution. It no longer suffices to consider only the right tail. For our particular example $c^*(\lambda) = \sqrt{2}(\lambda + \frac{1}{2})$ for $0 \leq \lambda \leq \lambda_c$ (Ben-Jacob et al. 1985, van Saarloos 1989). To deal with such kind of situation the authors propose a principle of marginal stability (see also Dee and Langer 1983, Langer 1987, van Saarloos 1988, 1989).

Let us return to (8.6). Assuming a traveling front solution $w(x - c(q)t)$ with exponential decay e^{-qx} as $x \to \infty$ gives the direction dependent growth velocity

$$v(\mathbf{n}) = \min_q \left\{ \frac{1}{q} \sum_{\mathbf{e},|\mathbf{e}|=1} e^{-q\mathbf{n}\cdot\mathbf{e}} \right\}. \qquad (8.13)$$

We arrived at the following recipe: Ignoring correlations one writes down the evolution equation for the average density. This could also be a discrete time iteration. The exponential ansatz yields then the direction dependent growth as the solution of a variational problem. As in Equation (8.12) it may happen however that the variational ansatz is valid only in a restricted range of parameters.

8.1 Shape anisotropy for the Eden model

As a first application of (8.13) we wish to compare the growth velocity along the lattice axis $(\mathbf{n} = (1,0,\ldots,0))$ and along the diagonal $(\mathbf{n} = \frac{1}{\sqrt{d}}(1,1,\ldots,1))$ for the Eden model on a d-dimensional hypercubic lattice. The velocity is given by

$$v_0(d) = \min_{q>0} \frac{2}{q}(\cosh q + d - 1) \qquad (8.14)$$

for the lattice axis, and by

$$v_1(d) = \min_{q>0} \frac{2\sqrt{d}}{q}\cosh q \qquad (8.15)$$

for the diagonal. In arriving at (8.15) we have made the substitution $q \to q\sqrt{d}$ in (8.13). It follows from (8.15) that the d-dependence of v_1 is trivial, $v_1 = \text{const.}\sqrt{d}$. Taking the derivative of the right hand sides of (8.14) and (8.15) with respect to q we obtain the implicit equations

$$f(v_0) = 2d - 2 \tag{8.16}$$

and

$$f(v_1/\sqrt{d}) = 0, \tag{8.17}$$

where

$$f(x) := x\,\text{arsinh}(x/2) - \sqrt{x^2 + 4}. \tag{8.18}$$

The solution of (8.17) is

$$v_1 \simeq 3.0177591\sqrt{d}. \tag{8.19}$$

(8.16) can be solved analytically in the limit of large d. Using the asymptotics of (8.18), $f(x) \sim x\log x - x - x^{-1}$, we obtain

$$v_0(d) \approx \frac{2d}{\log d}\left\{1 + \frac{\log(\log d)}{\log d} + \mathcal{O}(1/\log d)\right\}. \tag{8.20}$$

The large d behavior coincides with the rigorous result (7.7) due to Dhar (1988). This is not completely surprising, as one would naively expect a mean field type approximation to become more accurate in high dimensions. As we go along we will encounter more situations in which our mean field theory appears to give a consistent description of the high dimensionality behavior. However we are not aware of any serious argument for why this should always be the case.

Together (8.19) and (8.20) imply that the shape anisotropy $a := v_0/v_1$ diverges as $a \approx 0.66\sqrt{d}/\log d$ for large d. However due to the large correction terms in (8.20) the asymptotics is approached very slowly. In Table 4 we show values of v_0 and a for small d. For $d = 2$ the anisotropy is 4.67% and it increases monotonously with d.

For comparison with numerical simulations we first point out that our mean field approach makes no difference (with respect to the cluster shape) between

the site and bond versions of the Eden model. For the site version the equation of motion corresponding to (8.5) reads

$$\frac{\partial}{\partial t}\tilde{\varrho}(\mathbf{x}) = (1 - \tilde{\varrho}_t(\mathbf{x}))(1 - \prod_{\mathbf{e}, |\mathbf{e}|=1} (1 - \tilde{\varrho}_t(\mathbf{x}+\mathbf{e}))). \qquad (8.21)$$

Since our working assumption states that the growth velocity is determined only by the exponential tail of the density profile, we may linearize (8.21) and obtain the same expression (8.13) as for the bond version.

Hirsch and Wolf (1986) determine the shape anisotropy for the site version of the Eden model on the square lattice, finding $a \simeq 1.020$. Meakin et al. (1986a) use a bond version (version C in the notation of Jullien and Botet (1985)) and obtain $a \simeq 1.025$ in $d = 2$. The mean field approach thus strongly overestimates the shape anisotropy, but it gives the correct order of magnitude. The numerical results published by Hirsch and Wolf (1986) for $d = 3$ indicate that the anisotropy is about twice as large than for $d = 2$ (we infer $a \simeq 1.043$ from their data) in accordance with the trend of Table 4. A systematic numerical study of the shape anisotropy in higher dimensions is so far lacking.

d	v_0	a
2	4.46685	1.0467
3	5.67295	1.0853
4	6.75370	1.1190
5	7.75405	1.1491
10	12.1058	1.2686
100	62.9996	2.0876

Table 4: Mean field estimates for the growth velocity v_0 and the shape anisotropy $a = v_0/v_1$ of Eden clusters on a d-dimensional hypercubic lattice.

Let us finally note that our mean field estimates for v_0 and v_1 are in fact upper bounds to the true growth velocities. This can be seen by comparing Equations (8.16) and (8.17) to rigorous bounds derived by Dhar (1986,1988). For the lattice axis Dhar (1988) proves that $v_0 \leq v_0^+$ where

$$f(v_0^+) = 2d - 3 \qquad (8.22)$$

and $f(x)$ is given by (8.18), while for the diagonal it is shown that $v_1 \leq v_1^+$ with (Dhar 1986)

$$f(v_1^+/\sqrt{d}) = -1/d. \qquad (8.23)$$

These bounds are derived assuming that all infection paths from the origin to a given hyperplane are independent (Dhar 1986). Since $f(x)$ is a monotonously increasing function for $x > 0$, the solution to (8.22) is smaller than that to (8.16), and the solution to (8.23) is smaller than that to (8.17). Hence the mean field estimates are upper bounds also.

8.2 The faceting transition in the Richardson model

In this Section we will use the mean field approach to explicitly check several of the scaling assumptions made in the treatment of the faceting transiton in Section 7.2. Moreover we will gain some insight into the surprisingly rich structure hidden in simple equations like (8.13). Since faceting occurs in the diagonal direction, our starting point is the discrete time analogue of (8.6) with $\mathbf{n} = \frac{1}{\sqrt{d}}(1,\ldots,1)$,

$$\varrho_{t+1}(z) - \varrho_t(z) = p(1 - \varrho_t(z))[1 - (1 - \varrho_t(z-1))^d(1 - \varrho_t(z+1))^d], \qquad (8.24)$$

where p is the growth probability parameter (the Richardson model is described in Sections 4.1 and 7.2) and distances are measured in units of $1/\sqrt{d}$, $z = x\sqrt{d}$. We know already that faceting is related to an infection process which lives on the hyperplane $x_1 + \ldots + x_d = t$, i.e. $z = t$ in (8.24). The occupation density $\sigma(t) := \varrho_t(t)$ of the facet plane evolves according to

$$\sigma(t+1) = p(1 - (1 - \sigma(t))^d) \qquad (8.25)$$

(note that $\varrho_t(z) = 0$ for $z > t$). This is simply the mean field version of directed percolation (Kinzel 1983): For $p < p_c = 1/d$ the only fixed point of (8.25) is at $\sigma = 0$, and it is approached exponentially fast in time, $\sigma(t) \sim e^{-t/\xi_t}$ with the temporal correlation length $\xi_t = -1/\log(pd) \sim (1 - p/p_c)^{-1}$ for $p \rightarrow p_c$. Hence the corresponding exponent is

$$\nu_t^{\mathrm{MF}} = 1. \qquad (8.26)$$

For $p > p_c$ a nontrivial fixed point $\sigma^* > 0$ appears. For p close to p_c, $\sigma^* \sim p - p_c$, leading to the order parameter exponent

$$\beta^{\mathrm{MF}} = 1. \tag{8.27}$$

At $p = p_c$ $\sigma(t)$ relaxes according to a power law, $\sigma(t) \sim 1/t$ which is consistent with the general scaling law $\sigma(t) \sim t^{-\beta/\nu_t}$. We remark that the mean field value $p_c = 1/d$ is the leading term in the $1/d$-expansion for p_c as carried out by Blease (1977).

For $p > p_c$ the density profile $\varrho_t(z)$ has a jump of size σ^* at $z = t$. Hence the assumption of an exponential tail $\varrho_t(z) \sim e^{-qz}$ for $z \to \infty$ must break down as one passes p_c. To see what happens we derive the growth velocity v_1 along the diagonal from (8.24) in the manner described above. We obtain

$$v_1(p,d) = \min_q \tilde{v}_q(p,d), \tag{8.28}$$

$$\tilde{v}_q(p,d) = \frac{1}{q}\log(1 + 2pd\cosh q).$$

For large q, $\tilde{v}_q \approx 1 + \log(pd)/q$. The limiting value $\tilde{v}_\infty = 1$ is approached from below for $p < p_c$ ($pd < 1$), but from above for $p > p_c$. Hence for $p > p_c$ the minimum in (8.28) is located at $q^* = \infty$, which corresponds formally to a step profile. We shall see later that $1/q^*$ is in fact proportional to the growth shape curvature.

The divergence of the minimal value q^* in (8.28) for $p \to p_c$ is linked to the approach of the growth velocity $v_1 \to 1$. Indeed, for $p < p_c$ we have $\sigma(t) = \varrho_t(t) \sim e^{-q^*(t - v_1 t)} \sim e^{-t/\xi_t}$ and therefore

$$(1 - v_1)q^* \sim \xi_t^{-1}. \tag{8.29}$$

As q^* diverges for $p \to p_c$, we may determine the critical behavior of v_1 from (8.28) by expanding $\tilde{v}_q$ for large q,

$$\tilde{v}_q \approx 1 + \frac{\log pd}{q} + \frac{e^{-q}}{pdq}. \tag{8.30}$$

Taking the derivative with repect to q we obtain, with $\epsilon = 1 - p/p_c$,

$$(1 - v_1)(1 - \log(1 - v_1)) \sim \epsilon \tag{8.31}$$

which yields the critical behavior

$$1 - v_1 \sim \epsilon / \log(1/\epsilon) \tag{8.32}$$

and from (8.29) and (8.26)

$$q^* \sim \log(1/\epsilon). \tag{8.33}$$

The scaling theory of Kertész and Wolf (1989) predicts $1 - v_1$ and ξ_t^{-1} to vanish with the same exponent ν_t as $\epsilon \to 0$. Here we see that this is true up to logarithmic corrections. We also note that the derivative of v_1 with repect to p vanishes continuously at the transition.

To discuss the growth shape singularities we must determine the inclination dependence of the growth velocity close to the diagonal direction. As usual in mean field theory, the critical behavior is independent of dimension. Hence we may restrict ourselves to $d = 2$. We want to compute

$$
\begin{aligned}
v(u) &= \min_q \tilde{v}_q(u) \tag{8.34} \\
\tilde{v}_q(u) &= \frac{1}{q} \log[1 + 2p(\cosh q(1 + u) + \cosh q(1 - u))].
\end{aligned}
$$

Note that here the growth velocity is measured in the direction of the diagonal rather than normal to the front as in (8.13). The two velocities differ by a factor of $\sqrt{1 + u^2}$ (cf. Chapter 2). As we are interested in situations where the minimum in (8.34) is located at a value $q^* \gg 1$ (close to p_c or close to $u = 0$ for $p > p_c$) the cosh's can be replaced by exponentials, whence

$$\tilde{v}_q(u) \approx 1 + \frac{1}{q} \log(2p \cosh qu + e^{-q}). \tag{8.35}$$

In fact this amounts to considering a directed version of the Richardson model, in which infection propagates in the forward direction only.

We consider first the supercritical case, $p > p_c$. We know that $q^* = \infty$ for $u = 0$, thus $q^*(u)$ must diverge as $u \to 0$ (note that a front growing in a direction different from the diagonal, $u \neq 0$, is never faceted). Using (8.35) we find that $q^* \approx \lambda/|u|$ for $u \to 0$, where $\lambda = \lambda(p)$ is determined by

$$\lambda \tanh \lambda = \log(2p \cosh \lambda) \tag{8.36}$$

100

which has a solution only for $p > p_c = \frac{1}{2}$. For $p \to p_c$ from above λ vanishes as

$$\lambda \approx (2(p - p_c))^{1/2}. \tag{8.37}$$

Setting $q = q^* = \lambda/|u|$ in (8.35) we obtain for $|u| \ll \lambda$

$$v(u) \approx 1 + |u|\tanh\lambda + \frac{|u|e^{-\lambda/|u|}}{2p\lambda\cosh\lambda} \quad (p > p_c). \tag{8.38}$$

The facet size is $c = \tanh\lambda$ and it vanishes for $p \to p_c^+$ as $(p - p_c)^{1/2}$. Comparing this with the generally expected behavior $c \sim (p - p_c)^{\nu_t - \nu_r}$, we conclude (using (8.26)) that

$$\nu_r^{MF} = 1/2 \tag{8.39}$$

as is well known from other approaches (Harms and Straley 1982, Kinzel 1983). The surprising feature in (8.38) is the essential singularity in the next to leading term. It was shown in Chapter 2 that this term describes the growth shape close to the facet. We argued in Section 7.2 that it should be proportional to $|u|^{z_d - 1/\zeta_d - 1}$ in d dimensions. Thus the essential singularity reflects the fact that $\zeta/z = 0$ in our mean field theory. The corresponding growth shape is

$$g(c) - g(c + \triangle) \approx \frac{\lambda\triangle}{\log(1/\triangle)} \tag{8.40}$$

where $\triangle > 0$ and the facet boundary is located at $y = c$. Up to a logarithmic factor, the curved surface joins the facet linearly.

In the subcritical regime $(p < p_c)$ q^* is finite for $u = 0$, hence $q^*u \to 0$ for $u \to 0$. The $\cosh qu$ in (8.35) may then be expanded, and we obtain

$$\tilde{v}_q(u) \approx 1 - \frac{\epsilon - e^{-q}}{q} + \frac{1}{2}qu^2 \tag{8.41}$$

for $\epsilon = 1 - p/p_c \ll 1$ and $|u| \ll 1$. Minimizing this relative to q we find the position $q^*(u)$ of the minimum as

$$q^*(u) \approx q^*(0)(1 - \frac{1}{2}e^{q^*(0)}u^2). \tag{8.42}$$

Inserting this into (8.41) it follows that the second derivative of $v(u)$ diverges on approaching the transition as

$$v''(0) \approx q^*(0) \sim \log(1/\epsilon) \quad (p < p_c) \tag{8.43}$$

101

according to (8.33), and hence the curvature of the growth shape vanishes logarithmically, $g''(0) = -1/v''(0) \sim -1/\log(1/\epsilon)$. This is consistent with the scaling prediction (7.13), since $\nu_t^{MF} - 2\nu_r^{MF} = 0$.

At the transition point $p = p_c$ $q^*(u)$ diverges as $u \to 0$, however q^*u still vanishes and (8.41) with $\epsilon = 0$ can be used to determine the divergence. To leading order we find $q^*(u) \approx 2\log(1/u)$. Inserting into (8.41) we obtain the anomalous small u behavior of $v(u)$,

$$v(u) \approx 1 + u^2 \log(1/|u|) \quad (p = p_c) \tag{8.44}$$

and the corresponding growth shape $g(y) \approx 1 - y^2/\log(1/|y|)$. Again, this is consistent with (7.14) and (7.15), since $\nu_t^{MF}/\nu_r^{MF} = 2$.

Acknowledgements

References

Amar J G and Family F (1990a), Phys. Rev. Lett. **64**, 543.

Amar J G and Family F (1990b), Phys. Rev. **A** (in press).

Andreev A F (1982), Sov. Phys. JETP **53**, 1063.

Aronson D G and Weinberger H F (1978), Adv. Math. **30**, 33.

Baiod R, Kessler D, Ramanlal P, Sander L and Savit R (1988), Phys. Rev. **A38**, 3672.

Ball R, Nauenberg M and Witten T A (1984), Phys. Rev. **A29**, 2017.

Bausch R, Dohm V, Janssen H K and Zia R K P (1981), Phys. Rev. Lett. **47**,

1837.

Baxter R J (1982), *Exactly Solved Models in Statistical Mechanics* (Academic Press,London).

van Beijeren H (1977), Phys. Rev. Lett. **38**, 993.

van Beijeren H, Kutner R and Spohn H (1985), Phys. Rev. Lett. **54**, 2026.

van Beijeren H and Nolden I (1987), in *Structure and Dynamics of Surfaces II*, ed. by W. Schommers and P. von Blanckenhagen, Topics in Current Physics **43** (Springer, Berlin).

Ben-Jacob E, Brand H, Dee G, Kramer L and Langer J S (1985), Physica **14D**, 348.

Bensimon D, Shraiman B and Liang S (1984a), Phys. Lett. **102A**, 238.

Bensimon D, Shraiman B and Kadanoff L P (1984b), in *Kinetics of Aggregation and Gelation*, ed. by F. Family and D. P. Landau (Elsevier, Amsterdam).

Berker A N and Ostlund S (1979), J. Phys. **C12**, 4961.

Blease J (1977), J. Phys. **C10**, 925.

Blöte H W J and Hilhorst H J (1982), J. Phys. **A15**, L631.

Boldrighini C, Cosimi G, Frigio S and Grasso Nuñes M (1989), J. Stat. Phys. **55**, 611.

Bolthausen E (1989), Commun. Math. Phys. **123**, 529.

Botet R (1986), J. Phys. **A19**, 2233.

Bovier A, Fröhlich J and Glaus U (1986), Phys. Rev. **B34**, 6409.

Bradley R M and Strenski P N (1985), Phys. Rev. **B31**, 4319.

Bramson M (1983), Mem. Am. Math. Soc. **285**.

Bramson M (1987), Lectures at Paris, unpublished.

Bramson M and Griffeath D (1980), Math. Proc. Camb. Phil. Soc. **88**, 339.

Bramson M and Griffeath D (1981), Ann. Prob. **9**, 173.

Brandstetter H (1990), Diplomarbeit, Universität München (in preparation).

Buff F P, Lovett R A and Stillinger F H (1965), Phys. Rev. Lett. **15**, 621.

Burgers J M (1974), *The Nonlinear Diffusion Equation* (Riedel, Boston).

Burkhardt T W (1987), Phys. Rev. Lett. **59**, 1058.

Cardy J L (1983), J. Phys. **A16**, L709.

Chakrabarti A and Toral R (1989), Phys. Rev. **A40**, 11419.

Chayes J T, Chayes L and Durrett (1986), J. Stat. Phys. **45**, 933.

Cheng Z, Baiod R and Savit R (1987), Phys. Rev. **A35**, 313.

Chernoutsan A and Milošević S (1985), J. Phys. **A18**, L 449.

Chernov A A (1963), Sov. Phys. Cryst. **7**, 728.

Chernov A A (1984), *Modern Crystallography III: Crystal Growth*, Springer Series in Solid State Sciences **36** (Springer,Berlin).

Chorin A J and Marsden J E (1979), *A Mathematical Introduction to Fluid Mechanics* (Springer, Berlin).

Cole J D (1951), Quart. Appl. Math **9**, 225.

Cook J and Derrida B (1989a), J. Stat. Phys. **57**, 89.

Cook J and Derrida B (1989b), Europhys. Lett. **10**, 195.

Cook J and Derrida B (1990), J. Phys. **A** (in press).

Cox J T and Durrett R (1983), Math. Proc. Camb. Phil. Soc. **93**, 151.

Dee G and Langer J S (1983), Phys. Rev. Lett. **50**, 383.

DeMasi A, Presutti E, Spohn H and Wick D (1986), Ann. Prob. **14**, 409.

Derrida B (1990), Physica **A** (in press).

Derrida B and Griffiths R B (1989), Europhys. Lett. **8**, 111.

Derrida B and Spohn H (1988), J. Stat. Phys. **51**, 817.

Devillard D and Stanley H E (1989), Physica **A160**, 298.

Dhar D (1986), in *On Growth and Form*, ed. by H. E. Stanley and N. Ostrowsky (Martinus Nijhoff, Dordrecht), p. 288.

Dhar D (1987), Phase Transitions **9**, 51.

Dhar D (1988), Phys. Lett. **A130**, 308.

Diehl H W, Kroll D M and Wagner H (1980), Z. Phys. **B36**, 329.

Domany E and Kinzel W (1981), Phys. Rev. Lett. **47**, 5.

Durrett R (1988), Mathematical Intelligencer **10**, 37.

Durrett R and Liggett T M (1981), Ann. Prob. **9**, 186.

Eden M (1958), in *Symposium on Information Theory in Biology*, ed. by H.P. Yockey (Pergamon Press, New York).

Eden M (1961), in *Proceedings of the Fourth Berkeley Symposium on Mathematical Statistics and Probability*, ed. by F. Neyman, Vol. IV (University of California Press, Berkeley).

Edwards S F and Wilkinson D R (1982), Proc. Roy. Soc. London **A381**, 17.

Elskens Y and Frisch H L (1985), Phys. Rev. **A31**, 3812.

Essam J W, Guttmann A J and De Bell K (1988), J. Phys. **A21**, 3815.

Family F (1986), J. Phys. **A19**, L 441.

Family F (1990), Physica **A** (in press).

Family F and Vicsek T (1985), J. Phys. **A18**, L75.

Feller W (1950), *An Introduction to Probability Theory and its Applications* (John Wiley, New York).

Ferrari P A, Kipnis C and Saada E (1990), to be published.

Fisher D S (1986), Phys. Rev. Lett. **56**, 1964.

Fisher M E (1986), J. Chem. Soc. Faraday Trans. 2, **82**, 1569.

Fisher R A (1937), Ann. Eugenics **7**, 355.

Forrest B M and Tang L-H (1990), Phys. Rev. Lett. **64**, 1405.

Forster D, Nelson D R and Stephen M J (1977), Phys. Rev. **A16**, 732.

Frank F C (1974), J. Cryst. Growth **22**, 233.

Freche P, Stauffer D and Stanley H E (1985), J. Phys. **A18**, L1163.

Friedberg R (1986), Ann. Phys. **171**, 321

Gärtner J and Presutti E (1990), to be published.

Garmer M (1989), Diplomarbeit, Universität München (unpublished).

Gaspard P and Wang X-J (1988), Proc. Nat. Acad. Sci. U. S. A., **85**, 4591.

Gates D J (1988), J. Stat. Phys. **52**, 245.

Gates D J and Westcott M (1988), Proc. Roy. Soc. London **A416**, 443, 463.

Gilmer G H (1980), J. Cryst. Growth **49**, 465.

Goldenfeld N (1984), J. Phys. **A17**, 2807.

Grassberger P and de la Torre A (1979), Ann. Phys. **122**, 373.

Griffiths R B and Kaufman M (1982), Phys. Rev. **B26**, 5022.

Gross R (1918), Abhandl. math. phys. Klasse der Kgl. sächs. Ges. der Wiss. Leipzig, Bd. 35, Heft 4, 135.

Guo H, Grossmann B and Grant M (1990), Phys. Rev. Lett. **64**, 1262.

Halpin-Healy T (1989a), Phys. Rev. Lett. **62**, 442.

Halpin-Healy T (1989b), Phys. Rev. Lett. **63**, 917.

Halpin-Healy T (1990a), Phys. Rev. Lett. **64**, 109 (E).

Halpin-Healy T (1990b), Phys. Rev. **A** (in press).

Harms B C and Straley J P (1982), J. Phys. **A15**, 1865.

Henderson D, Brodsky M H and Chaudhari P (1974), Appl. Phys. Lett. **25**, 641.

Hirsch R and Wolf D E (1986), J. Phys. **A19**, L251.

Hopf E (1950), Comm. Pure Appl. Math. **3**, 201.

Huse D A and Henley C L (1985), Phys. Rev. Lett. **54**, 2708.

Huse D A, Henley C L and Fisher D A (1985), Phys. Rev. Lett. **55**, 2924.

Huse D A, van Saarloos W and Weeks J D (1985), Phys. Rev. **B32**, 233.

Huse D A, Amar J G and Family F (1990), preprint.

Hyman J M, Nicolaenko B and Zaleski S (1986), Physica **D23**, 265.

Imbrie J Z and Spencer T (1988), J. Stat. Phys. **52**, 609.

Janssen H K and Schmittmann B (1986), Z. Phys. **B63**, 517.

Jullien R and Botet R (1985), J. Phys. **A18**, 2279.

Jullien R, Kolb M and Botet R (1984), J. Physique **45**, 395.

Jullien R and Meakin P (1987), Europhys. Lett. **4**, 1385.

Jullien R and Meakin P (1989), J. Phys. **A22**, L219; ibd. L1115.

Kandel D and Domany E (1990), J. Stat. Phys. **58**, 685.

Kardar M (1985), Phys. Rev. Lett. **55**, 2923.

Kardar M (1987), Nucl. Phys. **B290**, 582.

Kardar M, Parisi G and Zhang Y C (1986), Phys. Rev. Lett. **56**, 889.

Kardar M and Zhang Y C (1987), Phys. Rev. Lett. **58**, 2087.

Katz S, Lebowitz J L and Spohn H (1984), J. Stat. Phys. **34**, 497.

Kaufman M and Griffiths R B (1984), Phys. Rev. **B30**, 244.

Kawasaki K and Ohta T (1982), Progr. Theor. Phys. **67**, 147; ibd. **68**, 129.

Kesten H (1986), Lecture Notes in Mathematics **1180** (Springer, Berlin).

Kertész J and Wolf D E (1988), J. Phys. **A21**, 747.

Kertész J and Wolf D E (1989), Phys. Rev. Lett. **62**, 2571.

Kida S (1979), J. Fluid Mech. **93**, 337.

Kim J M and Kosterlitz J M (1989), Phys. Rev. Lett. **62**, 2289.

Kim J M, Ala-Nissilä T and Kosterlitz J M (1990), preprint.

Kinzel W (1983), in *Percolation Structures and Processes*, ed. by G. Deutscher,

R. Zallen and J. Adler, Ann. Isr. Phys. Soc. **5**, 425.

Kolmogorov A, Petrovsky I and Piskunov N (1937), Bull. Univ. Moskou, Ser. Internat., Sec. **A1**, 1.

Krug J (1987), Phys. Rev. **A36**, 5465.

Krug J (1988), J. Phys. **A21**, 4637.

Krug J (1989a), J. Phys. **A22**, L769.

Krug J (1989b), PhD dissertation, Universität München (unpublished).

Krug J and Meakin P (1989), Phys. Rev. **A40**, 2064.

Krug J and Meakin P (1990), in preparation.

Krug J and Spohn H (1988), Phys. Rev. **A38**, 4271.

Krug J and Spohn H (1989), Europhys. Lett. **8**, 219.

Krug J and Spohn H (1990), preprint.

Krug J, Kertész J and Wolf D E (1990), Europhys. Lett. (in press).

Kuramoto Y and Yamada T (1976), Progr. Theor. Phys. **56**, 724.

Langer J S (1987), in *Chance and Matter*, ed. by J. Souletie, J. Vannimenus and R. Stora (North Holland, Amsterdam).

Leamy H J, Gilmer G H and Dirks A G (1980), in *Current Topics in Materials Science*, Vol. 6, ed. by E. Kaldis (North-Holland, Amsterdam).

Lebowitz J L (1990), private communication.

Liang S and Kadanoff L P (1985), Phys. Rev. **A31**, 2628.

Lieb E H and Liniger W (1963), Phys. Rev. **130**, 1605.

Lieb E H and Wu F Y (1972), in *Phase Transitions and Critical Phenomena*, Vol. 1, ed. by C. Domb and M. S. Green (Academic Press, London).

Limaye A V and Amritkar R E (1986), Phys. Rev. **A34**, 5085.

Lipowsky R (1988), in *Random Fluctuations and Pattern Growth*, ed. by H. E. Stanley and N. Ostrowsky, NATO ASI Series **E157** (Kluwer Academic, Dordrecht).

Lipowsky R (1989), in *Fundamental Problems in Statistical Mechanics VII* (in preparation).

Liu D and Plischke M (1988), Phys. Rev. **B38**, 4781.

Mandelbrot B B (1982), *The Fractal Geometry of Nature* (W. H. Freeman, San Francisco).

Mandelbrot B B (1986), in *Fractals in Physics*, ed. by L. Pietronero and E. Tosatti (North-Holland, Amsterdam).

Marchand J-P and Martin Ph A (1986), J. Stat. Phys. **44**, 491.

McKane A J and Moore M A (1988), Phys. Rev. Lett. **60**, 527.

Meakin P (1983), Phys. Rev. **B28**, 5221.

Meakin P (1986), in *On Growth and Form*, ed. by H. E. Stanley and N. Ostrowsky (Martinus Nijhoff, Dordrecht).

Meakin P (1987a), CRC Crit. Rev. Solid State Mat. Sci. **13**, 143.

Meakin P (1987b), J. Phys. **A20**, L1113.

Meakin P (1988a), in *Phase Transitions and Critical Phenomena*, Vol. 12, ed. by C. Domb and J. L. Lebowitz (Academic Press, London).

Meakin P (1988b), Phys. Rev. **A38**, 418.

Meakin P (1988c), in *Random Fluctuations and Pattern Growth*, ed. by H. E. Stanley and N. Ostrowsky, NATO ASI Series **E157** (Kluwer Academic, Dordrecht).

Meakin P (1988d), Phys. Rev. **A38**, 994.

Meakin P and Deutch J M (1986), J. Chem. Phys. **85**, 2320.

Meakin P and Jullien R (1987), J. Physique **48**, 1651.

Meakin P and Jullien R (1989), Europhys. Lett. **9**, 71.

Meakin P and Jullien R (1990), Phys. Rev. **A41**, 983.

Meakin P and Krug J (1990), Europhys. Lett. **11**, 13.

Meakin P, Jullien R and Botet R (1986a), Europhys. Lett. **1**, 609.

Meakin P, Ramanlal P, Sander L M and Ball R C (1986b), Phys. Rev. **A34**, 5091.

Medina E, Hwa T, Kardar M and Zhang Y C (1989), Phys. Rev. **A39**, 3053.

Melrose J R (1983), J. Phys. **A16**, 3077.

Métois J J, Spiller G D T and Venables J A (1982), Phil. Mag. **A46**, 1015.

Mollison D (1972), Nature **240**, 467.

Mullins W W (1959), J. Appl. Phys. **30**, 77.

Nadal J P, Derrida B and Vannimenus J (1984), Phys. Rev. **B30**, 376.

Nattermann T (1989), KFA Jülich preprint.

Nattermann T and Renz W (1988), Phys. Rev. **B38**, 5184.

Nauenberg M (1983), Phys. Rev. **B28**, 449.

Nauenberg M, Richter R and Sander L M (1983), Phys. Rev. **B28**, 1649.

Nieuwenhuizen J M and Haanstra H B (1966), Philips Technische Rundschau **27**, 177.

Nieuwenhuizen T (1989), private communication.

Parisi G and Zhang Y C (1984), Phys. Rev. Lett. **53**, 1791.

Parisi G and Zhang Y C (1985), J. Stat. Phys. **41**, 1.

Plischke M and Rácz Z (1985), Phys. Rev. **A32**, 3825.

Plischke M, Rácz Z and Liu D (1987), Phys. Rev. **B35**, 3485.

Pomeau Y and Résibois P (1975), Phys. Rep. **19**, 63.

Renz W (1990), KFA Jülich preprint.

Richardson D (1973), Proc. Camb. Phil. Soc. **74**, 515.

Rost H (1981), Z. Wahrsch. verw. Geb. **58**, 41.

Rottman C and Wortis M (1984), Phys. Rep. **103**, 59.

van Saarloos W (1988), Phys. Rev. **A37**, 211.

van Saarloos W (1989), Phys. Rev. **A39**, 6367.

van Saarloos W and Gilmer G H (1986), Phys. Rev. **B33**, 4927.

Saito Y and Ueta T (1989), Phys. Rev. **A40**, 3408.

Savit R and Ziff R (1985), Phys. Rev. Lett. **55**, 2515.

Sawada Y, Ohta S, Yamazaki M and Honjo H (1982), Phys. Rev. **A26**, 3557.

Simon B (1976), Ann. Phys. **97**, 279.

Singer H and Peschel I (1980), Z. Phys. **B39**, 333.

Sivashinsky G I (1977), Acta Astronautica **4**, 1177.

Smythe R T and Wierman J C (1978), *First Passage Percolation on the Square Lattice*, Lecture Notes in Mathematics **671** (Springer, Berlin).

Spohn H (1990), *Large Scale Dynamics of Interacting Particles*, Texts and Monographs in Physics (Springer, Berlin), to appear.

Stauffer D (1985), *Introduction to Percolation Theory* (Taylor and Francis, London).

Sutherland B (1968), Phys. Lett. **26A**, 532.

Szép J, Cserti J and Kertész J (1985), J. Phys. **A18**, L 413.

Tang C, Alexander S and Bruinsma R (1990), Phys. Rev. Lett. **64**, 772.

Vannimenus J, Nickel B and Hakim V (1984), Phys. Rev. **B30**, 391.

Visscher W M and Bolsterli M (1972), Nature **239**, 504.

Vold M J (1959), J. Colloid Sci. **14**, 168.

Vold M J (1963), J. Colloid Sci. **18**, 684.

Wang X-J (1989), Phys. Rev. **A40**, 6647.

Williams T and Bjerknes R (1972), Nature **236**, 19.

Witten T A and Sander L M (1981), Phys. Rev. Lett. **47**, 1400.

Wolf D E (1987), J. Phys. **A20**, 1251.

Wolf D E and Kertész J (1987a), J. Phys. **A20**, L257.

Wolf D E and Kertész J (1987b), Europhys. Lett. **4**, 651.

Wolf D E and Kertész J (1989), Phys. Rev. Lett. **63**, 1191.

Wong P-Z and Bray A J (1987), Phys. Rev. Lett. **59**, 1057.

Wulff G (1901), Z. Kristallogr. Mineral. **34**, 449.

Yakhot V (1981), Phys. Rev. **A24**, 642.

Yakhot V and She Z-S (1988), Phys. Rev. Lett. **60**, 1840.

Yamada T and Kuramoto Y (1976), Progr. Theor. Phys. **56**, 681.

Zabolitzky J G and Stauffer D (1986), Phys. Rev. **A34**, 1523.

Zaleski S (1989), Physica **D34**, 427.

Zhang Y C (1989), J. Stat. Phys. **57**, 1123.

Zwerger W (1981), Z. Phys. **B42**, 333.